PHILOSOPHICAL TRANSACTIONS OF THE ROYAL SOCIETY A
MATHEMATICAL, PHYSICAL & ENGINEERING SCIENCES

Analysis of Developable Shells with Special Reference to the Finite Element Method and Circular Cylinders

L. S. D. Morley

Phil. Trans. R. Soc. Lond. A 1976 **281**, 113-170
doi: 10.1098/rsta.1976.0023

Phil. Trans. R. Soc. Lond. A. **281**, 113–170 (1976) [113]
Printed in Great Britain

ANALYSIS OF DEVELOPABLE SHELLS WITH SPECIAL REFERENCE TO THE FINITE ELEMENT METHOD AND CIRCULAR CYLINDERS

By L. S. D. MORLEY
Royal Aircraft Establishment

(*Communicated by E. H. Mansfield, F.R.S. – Received* 8 *January* 1975)

CONTENTS

The paper begins by noting that the practical and efficient numerical analysis of thin walled shells is far from a reality.

Groundwork for the investigation starts with an examination of existing sufficiency conditions for convergence of the finite element method of analysis with refinement of mesh size; new and more practical conditions are then given specifically for shells. Working formulae of a suitable first approximation theory for the linear small deflexion behaviour are then given for arbitrary shells in lines of curvature and in geodesic coordinates. A variational principle is introduced which is more general than that for the well known assumed stress hybrid finite element model; its purpose is to provide a means to overcome the excessive rank deficiency which is sometimes encountered in the derived element stiffness matrix.

The formulae are next specialized to general developable shells for they are the simplest to analyse and frequently occur in technology. Emphasis is given to the derivation of general formulae governing inextensional deformation, membrane action and rigid body movement because these constitute important factors in any adequate numerical analysis.

Specific application is made to circular cylindrical shells by first considering the interpolation of the kinematic continuity conditions along an arbitrary geodesic line. Details and numerical examples are provided for the first known fully compatible lines of curvature rectangular finite element which directly recovers arbitrary rigid body movements as well as inextensional deformations and membrane actions.

The paper concludes with details and numerical examples of an arbitrarily shaped triangular finite element which employs the above mentioned variational principle in conjunction with linearly varying stress fields. All the rigid body movements are directly recovered as well as inextensional deformations and membrane actions. It is anticipated that this finite element and its derivatives will find widespread application.

1. Introduction

It can hardly escape the notice of the most casual observer that shells, i.e. thin curved plates, are commonplace in almost every aspect of modern day life. We fully sympathize, therefore, with the more discriminating individual who is perplexed when he discovers that serious difficulty is still experienced by designers in calculating the behaviour of the shell even for some apparently simple static situations. This fact must cause surprise also among fellow engineers, scientists and mathematicians who work in other fields because they are aware that the finite element method, the brainchild of the structural analyst and conceived just at the right time in the dawn of the computer age, has grown up in so many other respects to be such an astonishing success. Where and what is the root cause of the difficulty? The answer to this question is by no means straightforward for it lies partly in the nature of the underlying shell theory and partly in a deficiency, or perhaps it is a lack of understanding, of the present character of the finite element method.

Let us very quickly trace the development of linear shell theory the first treatment of which, from the point of view of the general equations of elasticity, is credited to H. Aron in 1874 (see the treatise by Love 1927). Much of the early work was directed towards an understanding of the vibrations of shells so as to predict the tones of bells. Lord Rayleigh (1881) deduced from physical reasoning that the middle surface to the vibrating shell remains unstretched and accordingly derived a theory of inextensional deformation. A first complete theory, based upon the now well known Love–Kirchhoff assumptions, was given by Love (1890). This theory is often referred to as 'Love's first approximation theory' and, despite certain shortcomings, has occupied a position of prominence ever since. It led to equations of motion and boundary conditions which were difficult to reconcile with Lord Rayleigh's theory. Later investigations showed, however, that the extensional strain which had been proved to be a necessary concomitant of the vibrations was practically confined to a narrow region near the edge of the shell. This rapidly decaying edge effect can be adjusted so as to secure the satisfaction of the proper boundary conditions while the greater part of the shell vibrates in an inextensional manner according to Lord Rayleigh's original conjecture. The main shortcomings in Love's first approximation theory are the lack of symmetry in the expression for the change of twist and the assumption of a symmetric shear stress resultant. The challenge proffered by these shortcomings incited, in more recent times, a tremendous effort into further development of shell theory, there being considerable rivalry between authors to achieve higher accuracy for their equations on account of more rigorous derivation from the basic assumptions. It was left to Koiter (1960) to point out, in view of the approximate character of the Love–Kirchhoff assumptions, that many of these claims for higher accuracy must be open to doubt, Koiter showed that in most cases the further developments involved refinements which are of the same order of magnitude as the errors which remain on account of the basic assumptions. Such refinements are, of course, meaningless in a general theory. Thus, the lavish effort spent on the further development of linear first approximation shell theory in the present century did not lead, after the initial corrections had been made, to any significant improvement of Love's general equations, although it is true that there is now a much better understanding of the nature of the approximations.

At first sight, it may seem incongruous that the attention paid to these versions of the theory was matched with marked reluctance to become involved with numerical applications of any of the versions. This is understandable, however, when it is realized that the degree of algebraic complexity which builds up during numerical solution by continuous function processes (say) is such that it soon becomes quite overwhelming. This complexity led to the separate development of approximate methods, notably the membrane theory where the stress resultants are calculated from purely statical considerations; the deflected shape is calculated from particular integrals of the stress resultants of membrane theory supplemented with complementary function solutions derived from inextensional theory. Membrane theory has valid application only to those problems where the proper boundary conditions can be satisfied and where the stresses from bending are insignificant in comparison with those from stretching as a membrane; problems which involve rapidly decaying edge effects are therefore specifically excluded. These restrictions are sufficient to severely limit the practical usefulness of membrane theory to a relatively small number of situations. Another approximate method known as shallow shell theory provided an alternative approach towards obtaining numerical results, it is associated with many names of which some of the best known are Donnell (1933), Marguerre (1938) and Vlasov (1958). Unfortunately, shallow shell theory rests on a number of simplifying assumptions with reference to the deformation pattern and these are not generally applicable. Approximate methods of calculation have a much more secure foundation in the special although technically important circular cylindrical shell. Here, simplified but adequate governing equations are available which are completely consistent within the basic assumptions of first approximation shell theory; one of the best known is that presented by Morley (1959) and later justified by Simmonds (1966), Koiter (1968) and Morley (1972).

About a decade ago, after the finite element method of analysis for planar and solid continua was reasonably well consolidated with the facilities afforded by the high speed digital computer, the time seemed ripe to engage with detailed numerical analysis of the general shell problem. In early work, the shape of the actual shell reference surface was approximated as a polyhedral surface formed from an assembly of flat facet elements, usually triangular in shape, in which the bending and stretching behaviours are separately represented, see, for example, Clough & Johnson (1968). Flat facet elements are known to suffer kinematic discontinuity at the inter-element boundaries but, nonetheless, it is on record that they provide reasonable results for some problems. They do not, however, constitute a general means of solution because there is no assurance that the results of first approximation shell theory are reproduced in the limit of refinement of the facet representation.† Recognizing the limitations, many authors have since given attention to the development of curved finite elements so that the shape of the shell surface is accurately represented, see the reviews by Gallagher (1969, 1974) and Dawe (1971). Nevertheless, the practical and efficient numerical analysis of shells is still far from a reality.

The finite element method is identified as a Rayleigh–Ritz process and its success in the analysis of planar continua is in no small part attributable to the fact that it is a simple matter to select trial functions for the displacements which reproduce independent distributions of constant (or nearly constant) strain for each component ϵ_{11}, ϵ_{22}, ϵ_{12} or, as the case may be, for each curvature change component κ_{11}, κ_{22}, κ_{12}.‡ This is, indeed, central to the sufficiency conditions for convergence of the finite element displacement method as discussed by Melosh (1963) and Tong & Pian (1967). Correspondingly, sufficiency in the finite element analysis of shells would require trial functions for the displacements which reproduce constant, or nearly constant, values for all six components ϵ_{11}, ϵ_{22}, ϵ_{12}, κ_{11}, κ_{22}, $\bar{\kappa}_{12}$. This is, however, quite impossible to achieve because of the nature of the compatibility equations for shells; in particular when $\epsilon_{11} = \epsilon_{22} = \epsilon_{12} = 0$ these equations require that

$$\frac{\kappa_{11}}{R_2} + \frac{\kappa_{22}}{R_1} = 0$$

for lines of curvature coordinates with R_1 and R_2 the principal radii. At most, therefore, only two independent distributions of constant curvature change are admissible and these refer to $\bar{\kappa}_{12}$ and a combination between κ_{11}, κ_{22}. There are other kinds of difficulties and, to reveal these, it is necessary to examine the character of symbolic strain and curvature change components ϵ and κ in relation to trial functions for the out of surface displacement W; the two insurface displacements can be ignored for this purpose. Symbolically,

$$\epsilon = W/R, \quad \kappa = -\partial^2 W/\partial \xi^2,$$

where R is a radius of curvature of the middle surface and ξ measures arc length on the surface. Consider polynomial trial functions

$$W = \alpha_1 + \alpha_2 \xi + \alpha_3 \xi^2,$$

where α_1, α_2, α_3 are constants. This gives

$$\epsilon = (\alpha_1 + \alpha_2 \xi + \alpha_3 \xi^2)/R, \quad \kappa = -2\alpha_3.$$

The trial function in α_1 is seen to provide an independent and constant strain ϵ, but the trial function in α_3 contributes to both ϵ and κ. Let us examine whether it is practicable to limit the size of the finite element so that the contribution from ϵ is negligible in comparison with the outer fibre strain from κ. Now, it is fundamental to first approximation shell theory that the relative error is $O(h/R)$ so that the strain ϵ is negligible if

$$\epsilon/R = O(\kappa h^2/12R^2),$$

where h is wall thickness and the symbol O is read as 'a term of order most...'. Thus, to secure a (virtually) independent and constant distribution of curvature change κ requires the size of the finite element to be limited by the condition

$$\xi = O(h).$$

† This remark applies equally to the more recently developed isoparametric finite element, see, for example, Zienkiewicz, Taylor & Too (1971).

‡ A list of the principal symbols appears at the end of the paper (pp. 167–9).

The severity of this limitation remains undiminished when trial functions like those in α_1 and α_2 provide compensating adjustment, it is such as to preclude a satisfactory basis for practical calculation. All this applies equally when the outer fibre strain $\frac{1}{2}\kappa h$ is of the same order of magnitude as that from ϵ, this state occurs in Gol'denveizer's (1961) 'simple edge effect'. There are as many different types of edge effect, all of which decay rapidly in intensity with distance away from the edge, as there are types of stress and strain distribution in the shell interior. The simple edge effect, however, assumes importance in finite element philosophy because the intensity of its components of stress and strain is constant, or nearly constant, along the edge. Symbolically, the solving equation of simple edge effect is

$$\frac{\partial^4 W}{\partial \xi^4} + \frac{\lambda^4}{R^2 h^2} W = 0,$$

where λ is of order unity so that we identify

$$W = \alpha(\xi) \exp\left(-\lambda\xi/\sqrt{(Rh)}\right),$$

where $\alpha(\xi)$ is smoothly varying and the origin of ξ is on the edge with positive direction towards the interior.

In view of these remarks, there must be reservation in subscribing to the body of opinion as expressed by Strang & Fix (1973) that '... the (finite element shell) problem is in every essential respect like any other problem in the plane'. It seems to us that existing sufficiency conditions for convergence, directly extrapolated from those for planar continua, are not really applicable and therefore provide inadequate guidance to the selection of trial functions in the practical finite element analysis of shells. Moreover, some rather special analytical techniques remain to be evolved. Our earlier discussion points towards four quite sharply defined states of static response, they may be summarized as

(I) membrane actions where the outer fibre stresses/strains from bending vanish or are insignificant in comparison with those from stretching;

(II) inextensional deformations where the middle surface of the shell remains unstretched. The stresses/strains from stretching vanish or are insignificant in comparison with those from bending;

(III) rigid body movements which contribute nothing to the stresses/strains;

(IV) edge effects where the stress/strain intensities from stretching and bending may be of the same order of magnitude, they decay rapidly with increase in distance away from the edge or discontinuity.

Practical conditions for convergence in the finite element analysis of shells require the trial functions to have capability to reproduce, in a general but piecewise smoothly varying way, each of these four states of static response. (Simple edge effects are regarded as smoothly varying.) Thus

(i) arbitrary choice of low degree polynomial displacement trial functions has already been demonstrated to lead to significant membrane actions where the curvature changes κ_{11}, κ_{22}, $\bar{\kappa}_{12}$ are negligible. Particularized responses are required for each of the three strain components ϵ_{11}, ϵ_{22}, ϵ_{12};

(ii) trial functions which reproduce inextensional deformation have to be selected from the set of complementary function solutions to the partial differential equations in the displacements which govern $\epsilon_{11} = \epsilon_{22} = \epsilon_{12} = 0$. Particularized responses are required for a curvature change combination κ_{11} with κ_{22}, and, separately, for $\bar{\kappa}_{12}$. Note here the relation $\kappa_{11}/R_2 + \kappa_{22}/R_1 = 0$;

(iii) trial functions for rigid body displacements satisfy the partial differential equations of (ii) as well as those which govern $\kappa_{11} = \kappa_{22} = \bar{\kappa}_{12} = 0$;

(iv) trial functions which reproduce simple edge effects require to be of the type

$$W = \alpha(\xi) \exp(-\lambda\, \xi/\surd(Rh)).$$

While it is true that awareness of the existence of these response states dates back to the early work of Love, it is equally true that the essentially more recent literature contains no record of premeditated finite element development to recover, in a practical and efficient manner, each of these four states of response. It is daunting, indeed, to reflect upon the hard won progress when it is realized that we are not yet sensibly poised to deal with the finite element analysis of Lord Rayleigh's problem of predicting the tones of bells.

Acknowledging all this, we feel constrained to confine the objective of the present investigation to a cautious re-examination and development of finite element technique towards the solution of a special class of shell which has developable middle surface. Developable surfaces have considerable advantage in that they are relatively simple to analyse and this constitutes the prime motive in so specializing the investigation from the arbitrary shell; they do, however, embrace the most frequently occurring shapes in technology and include the especially important circular cylindrical shell which we select as the vehicle for numerical demonstration. The objective is further moderated so as to exclude questions of edge effect. This must not be construed, however, as a statement that strong coupling rarely occurs between all aforementioned states (I)–(IV) of static response, if this were true then the practical usefulness of membrane theory would have been more widely extended a long time ago. Finally, the technique does not admit capability to deal with highly localized effects such as those caused by concentrated loads or discontinuous boundary conditions, these require further and specialized attention such as in the manner described by Morley (1973).

Mr B. C. Merrifield was responsible for major contributions to the computations. It is a pleasure to acknowledge his invaluable assistance.

2. Selected results from first approximation shell theory and variational principles

In surveying sources of error in the analysis of shells by the finite element method, Morris (1974) points out that the most rigorous considerations should govern the selection of the underlying shell theory so as to be certain that any errors which do arise come from the numerical approximation technique and not from an unsuitable shell theory. It is unnecessarily perilous to ignore the intent of this advice but it need not hinder a more relaxed attitude, identified with the name of Koiter, as to what constitutes a satisfactory first approximation shell theory.

Shell theory sets out to provide a two dimensional representation of an essentially three dimensional problem by dealing with variables defined only on a reference surface, usually the middle surface. An important identifying feature is the wall thickness h, measured as the distance between the bounding surfaces of the shell along a normal to the reference surface. This wall thickness, taken relative to a radius R of curvature or of torsion of the reference surface is a crucial parameter h/R governing the response to external loads. Neither the wall thickness nor material properties need be uniform although they are in a large number of practical cases.

Although the expectancy is that the thinner the shell the more accurately the actual three dimensional stress and displacement field can be inferred from a two dimensional solution (except in regions of highly concentrated loading, discontinuities and, possibly, close to the edges), it is wise to accept at the outset that shell theory is approximate and that extreme rigour in its development is hardly desirable. In no sense, however, does this justify free licence for arbitrary approximation. Thus, in Koiter's (1960) very careful examination of the character of two dimensional shell theory he commences by establishing that Love's (1927) so called first approximation for the strain energy, as the sum of the bending and stretching energies, is indeed a consistent first approximation. An evaluation of the differences which arise between this and the strain energy from a rigorous evaluation of the Love–Kirchhoff assumptions shows that the differences are of the same order of magnitude as those due to the inherently neglected effects of transverse normal and shearing stresses. An important observation is that these differences are of the same order of magnitude as those caused by replacing κ with $\kappa+\lambda\epsilon/R$ where κ is any physical curvature change component, λ is non-dimensional $O(1)$ and ϵ is any physical surface strain component. With a reservation concerning the shear stress resultants and twisting couples, this means that changes may be made in the strain energy expression which are equivalent to adjusting the constitutive relations of first approximation theory by replacing not only κ with $\kappa+\lambda\epsilon/R$ but also ϵ/R with $\epsilon/R+\lambda\kappa h^2/12R^2$. In other words, theories which differ only by terms of this type are said to be equivalent within first approximation theory. This latitude has led to the situation where, as commented by Budiansky & Sanders (1963), it is only a slight exaggeration to say that each investigator favours a different theory.

It is by no means the present purpose to provide just one more version of a first approximation shell theory, it is more a matter that because there are so many feasible alternatives it seems prudent to assemble in the required detail all the working formulae of that theory which we find most suitable for the finite element analysis of linear small deflexion behaviour. This makes reference convenient, unambiguous and consistent. The given formulae essentially agree with those developed by Sanders (1959) and by Koiter (1960) but the outline vector derivation given here follows a different emphasis, it owes rather more to the work of Gol'denveizer (1961). It provides a simple apparatus for systematic manipulation of the formulae into the form most suitable for the actual application. The kinematics of bending and stretching of the reference surface are treated in some detail because, as has already been pointed out in §1, the often neglected inextensional deformations† of the shell play a special and important role in finite element analysis by the displacement method. Formulae for the statics of stress resultants and stress couples are then written down with the aid of Gol'denveizer's static-geometric analogy. Convention is followed by using lines of curvature coordinates although there are subsequent transformations along arbitrary orthogonal directions to facilitate the introduction of geodesic coordinates. The formalism of tensor algebra is avoided, this kind of abstraction does not seem appropriate to the applications which are considered in the sequel.

The section concludes by introducing a new variational principle. In a finite element analysis, major difficulties can be experienced in finding suitable Rayleigh–Ritz trial functions for displacements which permit direct application of the principle of minimum total potential energy.

† The smoothest distributions of displacements which produce inextensional deformation are called 'sensitive solutions' by Morley (1972) and by Morris (1974). The description is apt because many finite element analyses produce extraordinarily inaccurate results when they are set the task of recovering these simple and very basic solutions.

Consequently, many authors give attention to alternative finite element approaches and these are characterized by several different variational principles. The text by Washizu (1968) contains an account of basic variational principles while Pian & Tong (1969) and Tong (1970) describe modified principles which are designed specifically for finite element analysis and allow various relaxations of the inter-element continuity requirements. In the course of the present treatment of the shell problem, however, we encounter further difficulties, specifically in excessive rank deficiency of the stiffness matrix. The new variational principle provides a relatively simple means to overcome these difficulties.

2.1. *Geometry and kinematics*

Let z_1, z_2, z_3 refer to a fixed right-handed orthogonal cartesian coordinate system and denote by $\boldsymbol{r}$ the position vector of a generic point so that

$$\boldsymbol{r} = z_1\boldsymbol{e}_1+z_2\boldsymbol{e}_2+z_3\boldsymbol{e}_3 \tag{2.1}$$

where the $\boldsymbol{e}_i$ are unit vectors in the z_i directions. Let the lines of curvature on the reference surface of the shell be used as an orthogonal coordinate net with ξ_1 and ξ_2 the coordinates, see figure 1, as in Reissner (1941) and Sanders (1959) so that

$$z_i = z_i(\xi_1, \xi_2) \quad (i = 1, 2, 3), \tag{2.2}$$

and

$$\boldsymbol{r} = \boldsymbol{r}(\xi_1, \xi_2). \tag{2.3}$$

An infinitesimal increment of the vector $\boldsymbol{r}$ is given by

$$\begin{aligned} \mathrm{d}\boldsymbol{r} &= \frac{\partial \boldsymbol{r}}{\partial \xi_1}\mathrm{d}\xi_1+\frac{\partial \boldsymbol{r}}{\partial \xi_2}\mathrm{d}\xi_2 \\ &= \alpha_1\boldsymbol{t}_1\,\mathrm{d}\xi_1+\alpha_2\boldsymbol{t}_2\,\mathrm{d}\xi_2, \end{aligned} \tag{2.4}$$

where $\boldsymbol{t}_1$ and $\boldsymbol{t}_2$ are defined as unit tangent vectors in the ξ_1 and ξ_2 directions respectively with

$$\boldsymbol{t}_1 = \frac{1}{\alpha_1}\frac{\partial \boldsymbol{r}}{\partial \xi_1}, \quad \boldsymbol{t}_2 = \frac{1}{\alpha_2}\frac{\partial \boldsymbol{r}}{\partial \xi_2} \tag{2.5}$$

where the coefficients of the first fundamental form are given by

$$\alpha_1 = \left|\frac{\partial \boldsymbol{r}}{\partial \xi_1}\right|, \quad \alpha_2 = \left|\frac{\partial \boldsymbol{r}}{\partial \xi_2}\right|. \tag{2.6}$$

The orthogonality of the coordinates ξ_1 and ξ_2 requires that

$$\boldsymbol{t}_1\cdot\boldsymbol{t}_2 = 0, \tag{2.7}$$

so that the square of a linear element on the reference surface is given by

$$\mathrm{d}\boldsymbol{r}\cdot\mathrm{d}\boldsymbol{r} = \alpha_1^2\,\mathrm{d}\xi_1^2+\alpha_2^2\,\mathrm{d}\xi_2^2. \tag{2.8}$$

If $\boldsymbol{n}$ is the unit normal vector which acts in the z direction, see figure 1, and is defined by

$$\boldsymbol{n} = \boldsymbol{t}_1\times\boldsymbol{t}_2 \tag{2.9}$$

then we can write down the following well known equations for the derivatives of $\boldsymbol{t}_1$, $\boldsymbol{t}_2$ and $\boldsymbol{n}$ with respect to ξ_1 and ξ_2,

$$\left.\begin{aligned}\frac{\partial \boldsymbol{t}_1}{\partial \xi_1} &= -\frac{1}{\alpha_2}\frac{\partial \alpha_1}{\partial \xi_2}\boldsymbol{t}_2 - \frac{\alpha_1}{R_1}\boldsymbol{n}, & \frac{\partial \boldsymbol{t}_1}{\partial \xi_2} &= \frac{1}{\alpha_1}\frac{\partial \alpha_2}{\partial \xi_1}\boldsymbol{t}_2,\\ \frac{\partial \boldsymbol{t}_2}{\partial \xi_1} &= \frac{1}{\alpha_2}\frac{\partial \alpha_1}{\partial \xi_2}\boldsymbol{t}_1, & \frac{\partial \boldsymbol{t}_2}{\partial \xi_2} &= -\frac{1}{\alpha_1}\frac{\partial \alpha_2}{\partial \xi_1}\boldsymbol{t}_1 - \frac{\alpha_2}{R_2}\boldsymbol{n},\\ \frac{\partial \boldsymbol{n}}{\partial \xi_1} &= \frac{\alpha_1}{R_1}\boldsymbol{t}_1, & \frac{\partial \boldsymbol{n}}{\partial \xi_2} &= \frac{\alpha_2}{R_2}\boldsymbol{t}_2,\end{aligned}\right\} \tag{2.10}$$

where R_1 and R_2 are the principal radii of curvature in the ξ_1, ξ_2 directions respectively. The identity

$$\frac{\partial^2 \boldsymbol{n}}{\partial \xi_1 \partial \xi_2} = \frac{\partial^2 \boldsymbol{n}}{\partial \xi_2 \partial \xi_1}$$

provides the Codazzi relations

$$\frac{\partial}{\partial \xi_2}\left(\frac{\alpha_1}{R_1}\right) = \frac{1}{R_2}\frac{\partial \alpha_1}{\partial \xi_2}, \quad \frac{\partial}{\partial \xi_1}\left(\frac{\alpha_2}{R_2}\right) = \frac{1}{R_1}\frac{\partial \alpha_2}{\partial \xi_1}, \tag{2.11}$$

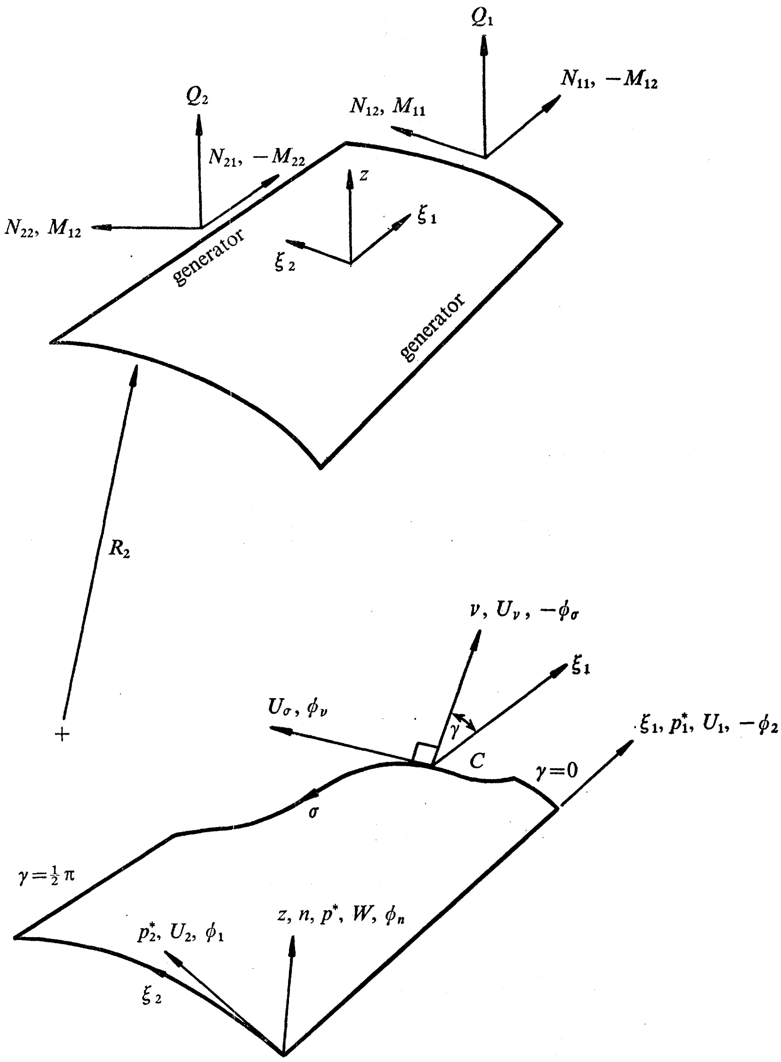

FIGURE 1. Notation for the developable surface.

while the identity

$$\frac{\partial^2 \boldsymbol{t}_1}{\partial \xi_1 \partial \xi_2} = \frac{\partial^2 \boldsymbol{t}_1}{\partial \xi_2 \partial \xi_1}$$

provides the Gauss relation

$$\frac{\partial}{\partial \xi_1}\left(\frac{1}{\alpha_1}\frac{\partial \alpha_2}{\partial \xi_1}\right) + \frac{\partial}{\partial \xi_2}\left(\frac{1}{\alpha_2}\frac{\partial \alpha_1}{\partial \xi_2}\right) = -\frac{\alpha_1 \alpha_2}{R_1 R_2}. \tag{2.12}$$

In the sequel it is convenient to re-express the position vector $\boldsymbol{r}$ of equation (2.3) in the alternative form

$$\boldsymbol{r}(\xi_1, \xi_2) = \rho_1 \boldsymbol{t}_1 + \rho_2 \boldsymbol{t}_2 + \rho_n \boldsymbol{n} \tag{2.13}$$

where, in the usual way,

$$\rho_1 = \boldsymbol{r}\cdot\boldsymbol{t}_1, \quad \rho_2 = \boldsymbol{r}\cdot\boldsymbol{t}_2, \quad \rho_n = \boldsymbol{r}\cdot\boldsymbol{n}. \tag{2.14}$$

The displacement vector $\boldsymbol{U}$ of a point lying on the reference surface may be written in the form

$$\boldsymbol{U} = U_1 \boldsymbol{t}_1 + U_2 \boldsymbol{t}_2 + W\boldsymbol{n} \tag{2.15}$$

where the components U_1, U_2 and W have the directions as shown in figure 1. The accompanying rotation of the point is given by the vector $\boldsymbol{\Phi}$ where

$$\boldsymbol{\Phi} = -\phi_2 \boldsymbol{t}_1 + \phi_1 \boldsymbol{t}_2 + \phi_n \boldsymbol{n} \tag{2.16}$$

and this is related to the displacement vector by the equations

$$\left.\begin{aligned}
\phi_1 &= -\frac{1}{\alpha_1}\frac{\partial \boldsymbol{U}}{\partial \xi_1}\cdot\boldsymbol{n} = \frac{U_1}{R_1} - \frac{1}{\alpha_1}\frac{\partial W}{\partial \xi_1},\\
\phi_2 &= -\frac{1}{\alpha_2}\frac{\partial \boldsymbol{U}}{\partial \xi_2}\cdot\boldsymbol{n} = \frac{U_2}{R_2} - \frac{1}{\alpha_2}\frac{\partial W}{\partial \xi_2},\\
\phi_n &= \frac{1}{2}\left(\frac{1}{\alpha_1}\frac{\partial \boldsymbol{U}}{\partial \xi_1}\cdot\boldsymbol{t}_2 - \frac{1}{\alpha_2}\frac{\partial \boldsymbol{U}}{\partial \xi_2}\cdot\boldsymbol{t}_1\right) = \frac{1}{2\alpha_1\alpha_2}\left(\frac{\partial \alpha_2 U_2}{\partial \xi_1} - \frac{\partial \alpha_1 U_1}{\partial \xi_2}\right).
\end{aligned}\right\} \tag{2.17}$$

The (small) strains are given by

$$\left.\begin{aligned}
\epsilon_{11} &= \frac{1}{\alpha_1}\frac{\partial \boldsymbol{U}}{\partial \xi_1}\cdot\boldsymbol{t}_1 = \frac{1}{\alpha_1}\frac{\partial U_1}{\partial \xi_1} + \frac{1}{\alpha_1\alpha_2}\frac{\partial \alpha_1}{\partial \xi_2}U_2 + \frac{W}{R_1},\\
\epsilon_{22} &= \frac{1}{\alpha_2}\frac{\partial \boldsymbol{U}}{\partial \xi_2}\cdot\boldsymbol{t}_2 = \frac{1}{\alpha_2}\frac{\partial U_2}{\partial \xi_2} + \frac{1}{\alpha_1\alpha_2}\frac{\partial \alpha_2}{\partial \xi_1}U_1 + \frac{W}{R_2},\\
\epsilon_{12} = \epsilon_{21} &= \frac{1}{2}\left(\frac{1}{\alpha_1}\frac{\partial \boldsymbol{U}}{\partial \xi_1}\cdot\boldsymbol{t}_2 + \frac{1}{\alpha_2}\frac{\partial \boldsymbol{U}}{\partial \xi_2}\cdot\boldsymbol{t}_1\right)\\
&= \frac{1}{2}\left(\frac{1}{\alpha_1}\frac{\partial U_2}{\partial \xi_1} - \frac{1}{\alpha_1\alpha_2}\frac{\partial \alpha_1}{\partial \xi_2}U_1 + \frac{1}{\alpha_2}\frac{\partial U_1}{\partial \xi_2} - \frac{1}{\alpha_1\alpha_2}\frac{\partial \alpha_2}{\partial \xi_1}U_2\right),
\end{aligned}\right\} \tag{2.18}$$

while the (small) curvature changes are given by

$$\left.\begin{aligned}
\kappa_{11} &= \frac{1}{\alpha_1}\frac{\partial \boldsymbol{\Phi}}{\partial \xi_1}\cdot\boldsymbol{t}_2 = \frac{1}{\alpha_1}\frac{\partial \phi_1}{\partial \xi_1} + \frac{1}{\alpha_1\alpha_2}\frac{\partial \alpha_1}{\partial \xi_2}\phi_2,\\
\kappa_{22} &= -\frac{1}{\alpha_2}\frac{\partial \boldsymbol{\Phi}}{\partial \xi_2}\cdot\boldsymbol{t}_1 = \frac{1}{\alpha_2}\frac{\partial \phi_2}{\partial \xi_2} + \frac{1}{\alpha_1\alpha_2}\frac{\partial \alpha_2}{\partial \xi_1}\phi_1,\\
\kappa_{12} &= -\frac{1}{\alpha_1}\frac{\partial \boldsymbol{\Phi}}{\partial \xi_1}\cdot\boldsymbol{t}_1 = \frac{1}{\alpha_1}\frac{\partial \phi_2}{\partial \xi_1} - \frac{1}{\alpha_1\alpha_2}\frac{\partial \alpha_1}{\partial \xi_2}\phi_1 - \frac{\phi_n}{R_1},\\
\kappa_{21} &= \frac{1}{\alpha_2}\frac{\partial \boldsymbol{\Phi}}{\partial \xi_2}\cdot\boldsymbol{t}_2 = \frac{1}{\alpha_2}\frac{\partial \phi_1}{\partial \xi_2} - \frac{1}{\alpha_1\alpha_2}\frac{\partial \alpha_2}{\partial \xi_1}\phi_2 + \frac{\phi_n}{R_2}.
\end{aligned}\right\} \tag{2.19}$$

The definitions which are given above for ϵ_{12}, κ_{12} and κ_{21} yield the identity

$$\kappa_{12}-\kappa_{21} = -\left(\frac{1}{R_1}-\frac{1}{R_2}\right)\epsilon_{12} \tag{2.20}$$

and, in view of this, we may reduce the number of strain and curvature change measures to six through the substitution

$$\bar{\kappa}_{12} = \tfrac{1}{2}(\kappa_{12}+\kappa_{21}). \tag{2.21}$$

It follows that

$$\left.\begin{aligned}\kappa_{12} &= \bar{\kappa}_{12}-\frac{1}{2}\left(\frac{1}{R_1}-\frac{1}{R_2}\right)\epsilon_{12},\\ \kappa_{21} &= \bar{\kappa}_{12}+\frac{1}{2}\left(\frac{1}{R_1}-\frac{1}{R_2}\right)\epsilon_{12}.\end{aligned}\right\} \tag{2.22}$$

In the finite element analysis in the sequel there is need to consider behaviour along contours which do not coincide with the ξ_1, ξ_2 lines of curvature coordinate system. On these occasions it is convenient to introduce additional orthogonal curvilinear coordinates ν and σ lying on the reference surface and orientated in the positive sense as shown in figure 1. An infinitesimal increment of the position vector $\boldsymbol{r}$, see equation (2.4), is now given by

$$\mathrm{d}\boldsymbol{r} = \alpha_\nu \boldsymbol{t}_\nu \mathrm{d}\nu + \alpha_\sigma \boldsymbol{t}_\sigma \mathrm{d}\sigma, \tag{2.23}$$

where the unit tangent vectors $\boldsymbol{t}_\nu$, $\boldsymbol{t}_\sigma$ are related to those of the ξ_1, ξ_2 coordinate system by

$$\left.\begin{aligned}\boldsymbol{t}_\nu &= \boldsymbol{t}_1\cos\gamma+\boldsymbol{t}_2\sin\gamma,\\ \boldsymbol{t}_\sigma &= -\boldsymbol{t}_1\sin\gamma+\boldsymbol{t}_2\cos\gamma,\end{aligned}\right\} \tag{2.24}$$

where γ is the included angle between tangent vectors $\boldsymbol{t}_\nu$ and $\boldsymbol{t}_1$. On substituting equations (2.24) into (2.23) and then comparing with equation (2.4) we find

$$\left.\begin{aligned}\alpha_\nu \mathrm{d}\nu &= \alpha_1 \mathrm{d}\xi_1\cos\gamma+\alpha_2\mathrm{d}\xi_2\sin\gamma = \alpha_\nu\left(\frac{\partial\nu}{\partial\xi_1}\mathrm{d}\xi_1+\frac{\partial\nu}{\partial\xi_2}\mathrm{d}\xi_2\right),\\ \alpha_\sigma\mathrm{d}\sigma &= -\alpha_1\mathrm{d}\xi_1\sin\gamma+\alpha_2\mathrm{d}\xi_2\cos\gamma = \alpha_\sigma\left(\frac{\partial\sigma}{\partial\xi_1}\mathrm{d}\xi_1+\frac{\partial\sigma}{\partial\xi_2}\mathrm{d}\xi_2\right).\end{aligned}\right\} \tag{2.25}$$

From this it follows that

$$\left.\begin{aligned}\frac{1}{\alpha_1}\frac{\partial}{\partial\xi_1} &= \frac{\partial\nu}{\partial\xi_1}\frac{\partial}{\partial\nu}+\frac{\partial\sigma}{\partial\xi_1}\frac{\partial}{\partial\sigma} = \cos\gamma\frac{1}{\alpha_\nu}\frac{\partial}{\partial\nu}-\sin\gamma\frac{1}{\alpha_\sigma}\frac{\partial}{\partial\sigma},\\ \frac{1}{\alpha_2}\frac{\partial}{\partial\xi_2} &= \frac{\partial\nu}{\partial\xi_2}\frac{\partial}{\partial\nu}+\frac{\partial\sigma}{\partial\xi_2}\frac{\partial}{\partial\sigma} = \sin\gamma\frac{1}{\alpha_\nu}\frac{\partial}{\partial\nu}+\cos\gamma\frac{1}{\alpha_\sigma}\frac{\partial}{\partial\sigma},\end{aligned}\right\} \tag{2.26}$$

or, alternatively,

$$\left.\begin{aligned}\frac{1}{\alpha_\nu}\frac{\partial}{\partial\nu} &= \cos\gamma\frac{1}{\alpha_1}\frac{\partial}{\partial\xi_1}+\sin\gamma\frac{1}{\alpha_2}\frac{\partial}{\partial\xi_2},\\ \frac{1}{\alpha_\sigma}\frac{\partial}{\partial\sigma} &= -\sin\gamma\frac{1}{\alpha_1}\frac{\partial}{\partial\xi_1}+\cos\gamma\frac{1}{\alpha_2}\frac{\partial}{\partial\xi_2}.\end{aligned}\right\} \tag{2.27}$$

Aided by equations (2.10), the derivatives of $\boldsymbol{t}_\nu$, $\boldsymbol{t}_\sigma$ and $\boldsymbol{n}$ with respect to ν and σ are soon established as

$$\left.\begin{aligned}\frac{\partial\boldsymbol{t}_\nu}{\partial\nu} &= -\alpha_\nu k_\nu \boldsymbol{t}_\sigma-\frac{\alpha_\nu}{R_\nu}\boldsymbol{n}, & \frac{\partial\boldsymbol{t}_\nu}{\partial\sigma} &= \alpha_\sigma k_\sigma\boldsymbol{t}_\sigma+\frac{\alpha_\sigma}{R_{\nu\sigma}}\boldsymbol{n},\\ \frac{\partial\boldsymbol{t}_\sigma}{\partial\nu} &= \alpha_\nu k_\nu\boldsymbol{t}_\nu+\frac{\alpha_\nu}{R_{\nu\sigma}}\boldsymbol{n}, & \frac{\partial\boldsymbol{t}_\sigma}{\partial\sigma} &= -\alpha_\sigma k_\sigma\boldsymbol{t}_\nu-\frac{\alpha_\sigma}{R_\sigma}\boldsymbol{n},\\ \frac{\partial\boldsymbol{n}}{\partial\nu} &= \frac{\alpha_\nu}{R_\nu}\boldsymbol{t}_\nu-\frac{\alpha_\nu}{R_{\nu\sigma}}\boldsymbol{t}_\sigma, & \frac{\partial\boldsymbol{n}}{\partial\sigma} &= \frac{\alpha_\sigma}{R_\sigma}\boldsymbol{t}_\sigma-\frac{\alpha_\sigma}{R_{\nu\sigma}}\boldsymbol{t}_\nu,\end{aligned}\right\} \tag{2.28}$$

where $-k_\nu$ and k_σ are respectively the geodesic curvatures of the curves σ = constant and ν = constant

$$\left.\begin{aligned} k_\nu &= -\boldsymbol{t}_\nu \times \frac{1}{\alpha_\nu}\frac{\partial \boldsymbol{t}_\nu}{\partial \nu}\cdot\boldsymbol{n} = \frac{1}{\alpha_\nu\alpha_\sigma}\frac{\partial \alpha_\nu}{\partial \sigma} \\ &= \frac{1}{\alpha_1\alpha_2}\left\{\frac{\partial}{\partial \xi_2}(\alpha_1\cos\gamma) - \frac{\partial}{\partial \xi_1}(\alpha_2\sin\gamma)\right\}, \\ k_\sigma &= \boldsymbol{t}_\sigma \times \frac{1}{\alpha_\sigma}\frac{\partial \boldsymbol{t}_\sigma}{\partial \sigma}\cdot\boldsymbol{n} = \frac{1}{\alpha_\nu\alpha_\sigma}\frac{\partial \alpha_\sigma}{\partial \nu} \\ &= \frac{1}{\alpha_1\alpha_2}\left\{\frac{\partial}{\partial \xi_2}(\alpha_1\sin\gamma) + \frac{\partial}{\partial \xi_1}(\alpha_2\cos\gamma)\right\}, \end{aligned}\right\} \tag{2.29}$$

and R_ν, R_σ and $R_{\nu\sigma}$ are defined by

$$\left.\begin{aligned} \frac{1}{R_\nu} = \frac{\cos^2\gamma}{R_1} + \frac{\sin^2\gamma}{R_2}, \quad \frac{1}{R_\sigma} = \frac{\sin^2\gamma}{R_1} + \frac{\cos^2\gamma}{R_2}, \\ \frac{1}{R_{\nu\sigma}} = \left(\frac{1}{R_1} - \frac{1}{R_2}\right)\sin\gamma\,\cos\gamma. \end{aligned}\right\} \tag{2.30}$$

The displacement vector $\boldsymbol{U}$ of equation (2.15) for points on the reference surface can now be expressed alternatively by

$$\boldsymbol{U} = U_\nu \boldsymbol{t}_\nu + U_\sigma \boldsymbol{t}_\sigma + W\boldsymbol{n} \tag{2.31}$$

where U_ν and U_σ are respectively the components of displacement in the ν and σ directions and

$$\left.\begin{aligned} U_\nu &= U_1\cos\gamma + U_2\sin\gamma, \\ U_\sigma &= -U_1\sin\gamma + U_2\cos\gamma. \end{aligned}\right\} \tag{2.32}$$

Similarly, the rotation vector $\boldsymbol{\Phi}$ of equation (2.16) can be expressed by

$$\boldsymbol{\Phi} = -\phi_\sigma \boldsymbol{t}_\nu + \phi_\nu \boldsymbol{t}_\sigma + \phi_n \boldsymbol{n}, \tag{2.33}$$

where

$$\left.\begin{aligned} \phi_\nu &= -\frac{1}{\alpha_\nu}\frac{\partial \boldsymbol{U}}{\partial \nu}\cdot\boldsymbol{n} = \phi_1\cos\gamma + \phi_2\sin\gamma = \frac{U_\nu}{R_\nu} - \frac{U_\sigma}{R_{\nu\sigma}} - \frac{1}{\alpha_\nu}\frac{\partial W}{\partial \nu}, \\ \phi_\sigma &= -\frac{1}{\alpha_\sigma}\frac{\partial \boldsymbol{U}}{\partial \sigma}\cdot\boldsymbol{n} = -\phi_1\sin\gamma + \phi_2\cos\gamma = \frac{U_\sigma}{R_\sigma} - \frac{U_\nu}{R_{\nu\sigma}} - \frac{1}{\alpha_\sigma}\frac{\partial W}{\partial \sigma}, \\ \phi_n &= \frac{1}{2}\left(\frac{1}{\alpha_\nu}\frac{\partial \boldsymbol{U}}{\partial \nu}\cdot\boldsymbol{t}_\sigma - \frac{1}{\alpha_\sigma}\frac{\partial \boldsymbol{U}}{\partial \sigma}\cdot\boldsymbol{t}_\nu\right) = \frac{1}{2}\left(\frac{1}{\alpha_\nu}\frac{\partial U_\sigma}{\partial \nu} + k_\sigma U_\sigma - \frac{1}{\alpha_\sigma}\frac{\partial U_\nu}{\partial \sigma} - k_\nu U_\nu\right). \end{aligned}\right\} \tag{2.34}$$

Analogously to equations (2.18), the expressions for the strains as referred to the new coordinate system are given by

$$\left.\begin{aligned} \epsilon_{\nu\nu} &= \frac{1}{\alpha_\nu}\frac{\partial \boldsymbol{U}}{\partial \nu}\cdot\boldsymbol{t}_\nu = \epsilon_{11}\cos^2\gamma + \epsilon_{22}\sin^2\gamma + 2\epsilon_{12}\sin\gamma\cos\gamma = \frac{1}{\alpha_\nu}\frac{\partial U_\nu}{\partial \nu} + k_\nu U_\sigma + \frac{W}{R_\nu}, \\ \epsilon_{\sigma\sigma} &= \frac{1}{\alpha_\sigma}\frac{\partial \boldsymbol{U}}{\partial \sigma}\cdot\boldsymbol{t}_\sigma = \epsilon_{11}\sin^2\gamma + \epsilon_{22}\cos^2\gamma - 2\epsilon_{12}\sin\gamma\cos\gamma = \frac{1}{\alpha_\sigma}\frac{\partial U_\sigma}{\partial \sigma} + k_\sigma U_\nu + \frac{W}{R_\sigma}, \\ \epsilon_{\nu\sigma} = \epsilon_{\sigma\nu} &= \frac{1}{2}\left(\frac{1}{\alpha_\nu}\frac{\partial \boldsymbol{U}}{\partial \nu}\cdot\boldsymbol{t}_\sigma + \frac{1}{\alpha_\sigma}\frac{\partial \boldsymbol{U}}{\partial \sigma}\cdot\boldsymbol{t}_\nu\right) = -(\epsilon_{11} - \epsilon_{22})\sin\gamma\cos\gamma + \epsilon_{12}(\cos^2\gamma - \sin^2\gamma) \\ &= \frac{1}{2}\left(\frac{1}{\alpha_\nu}\frac{\partial U_\sigma}{\partial \nu} - k_\nu U_\nu + \frac{1}{\alpha_\sigma}\frac{\partial U_\nu}{\partial \sigma} - k_\sigma U_\sigma - \frac{2W}{R_{\nu\sigma}}\right). \end{aligned}\right\} \tag{2.35}$$

The analysis in the sequel does not require expressions for the curvature changes in the new coordinate system although reference is made to quasi measures $\kappa_{\nu\nu}$, $\kappa_{\sigma\sigma}$, $\kappa_{\nu\sigma}$, $\kappa_{\sigma\nu}$ as given by

$$\left.\begin{aligned}
\kappa_{\nu\nu} &= \frac{1}{\alpha_\nu}\frac{\partial \boldsymbol{\Phi}}{\partial \nu}\cdot \boldsymbol{t}_\sigma = \kappa_{11}\cos^2\gamma + \kappa_{22}\sin^2\gamma + (\kappa_{12}+\kappa_{21})\sin\gamma\cos\gamma \\
&= \frac{1}{\alpha_\nu}\frac{\partial \phi_\nu}{\partial \nu} + k_\nu \phi_\sigma - \frac{\phi_n}{R_{\nu\sigma}}, \\
\kappa_{\sigma\sigma} &= -\frac{1}{\alpha_\sigma}\frac{\partial \boldsymbol{\Phi}}{\partial \sigma}\cdot \boldsymbol{t}_\nu = \kappa_{11}\sin^2\gamma + \kappa_{22}\cos^2\gamma - (\kappa_{12}+\kappa_{21})\sin\gamma\cos\gamma \\
&= \frac{1}{\alpha_\sigma}\frac{\partial \phi_\sigma}{\partial \sigma} + k_\sigma \phi_\nu + \frac{\phi_n}{R_{\nu\sigma}}, \\
\kappa_{\nu\sigma} &= -\frac{1}{\alpha_\nu}\frac{\partial \boldsymbol{\Phi}}{\partial \nu}\cdot \boldsymbol{t}_\nu = -(\kappa_{11}-\kappa_{22})\sin\gamma\cos\gamma + \kappa_{12}\cos^2\gamma - \kappa_{21}\sin^2\gamma \\
&= \frac{1}{\alpha_\nu}\frac{\partial \phi_\sigma}{\partial \nu} - k_\nu \phi_\nu - \frac{\phi_n}{R_\nu}, \\
\kappa_{\sigma\nu} &= \frac{1}{\alpha_\sigma}\frac{\partial \boldsymbol{\Phi}}{\partial \sigma}\cdot \boldsymbol{t}_\sigma = -(\kappa_{11}-\kappa_{22})\sin\gamma\cos\gamma - \kappa_{12}\sin^2\gamma + \kappa_{21}\cos^2\gamma \\
&= \frac{1}{\alpha_\sigma}\frac{\partial \phi_\nu}{\partial \sigma} - k_\sigma \phi_\sigma + \frac{\phi_n}{R_\sigma}.
\end{aligned}\right\} \tag{2.36}$$

Equations (2.36) with (2.20) provide the identity

$$\kappa_{\nu\sigma} - \kappa_{\sigma\nu} = \kappa_{12} - \kappa_{21} = -\left(\frac{1}{R_1} - \frac{1}{R_2}\right)\epsilon_{12}, \tag{2.37}$$

and, in view of equations (2.21), the last two equations in (2.36) may be combined as

$$\bar{\kappa}_{\nu\sigma} = \tfrac{1}{2}(\kappa_{\nu\sigma}+\kappa_{\sigma\nu}) = -(\kappa_{11}-\kappa_{22})\sin\gamma\cos\gamma + \bar{\kappa}_{12}(\cos^2\gamma - \sin^2\gamma). \tag{2.38}$$

(Note that the above quasi measures are the static geometric analogue to equations (2.58) in the sequel.)

2.2. *Static-geometric analogy*

The derivatives of the vectors $\boldsymbol{U}$ and $\boldsymbol{\Phi}$ are expressed in equations (2.17)–(2.19) in terms of the rotation, strain and curvature change measures and, indeed,

$$\left.\begin{aligned}
\frac{\partial \boldsymbol{U}}{\partial \xi_1} &= \alpha_1\{\epsilon_{11}\boldsymbol{t}_1 + (\epsilon_{12}+\phi_n)\boldsymbol{t}_2 - \phi_1 \boldsymbol{n}\}, \\
\frac{\partial \boldsymbol{U}}{\partial \xi_2} &= \alpha_2\{(\epsilon_{12}-\phi_n)\boldsymbol{t}_1 + \epsilon_{22}\boldsymbol{t}_2 - \phi_2 \boldsymbol{n}\}, \\
\frac{\partial \boldsymbol{\Phi}}{\partial \xi_1} &= \alpha_1(-\kappa_{12}\boldsymbol{t}_1 + \kappa_{11}\boldsymbol{t}_2 + \zeta_1 \boldsymbol{n}), \\
\frac{\partial \boldsymbol{\Phi}}{\partial \xi_2} &= \alpha_2(-\kappa_{22}\boldsymbol{t}_1 + \kappa_{21}\boldsymbol{t}_2 + \zeta_2 \boldsymbol{n}),
\end{aligned}\right\} \tag{2.39}$$

where it is convenient to introduce, temporarily, the quantities ζ_1 and ζ_2 as defined by

$$\zeta_1 = \frac{1}{\alpha_1}\frac{\partial \boldsymbol{\Phi}}{\partial \xi_1}\cdot \boldsymbol{n}, \quad \zeta_2 = \frac{1}{\alpha_2}\frac{\partial \boldsymbol{\Phi}}{\partial \xi_2}\cdot \boldsymbol{n}. \tag{2.40}$$

If equations (2.39) are regarded as differential equations to determine $\boldsymbol{U}$ and $\boldsymbol{\Phi}$ from known ϵ_{11}, ϵ_{22}, ϵ_{12}, ϕ_1, etc. then the requirements for integrability–compatibility are

$$\frac{\partial}{\partial \xi_1}\left(\frac{\partial \boldsymbol{U}}{\partial \xi_2}\right) = \frac{\partial}{\partial \xi_2}\left(\frac{\partial \boldsymbol{U}}{\partial \xi_1}\right), \quad \frac{\partial}{\partial \xi_1}\left(\frac{\partial \boldsymbol{\Phi}}{\partial \xi_2}\right) = \frac{\partial}{\partial \xi_2}\left(\frac{\partial \boldsymbol{\Phi}}{\partial \xi_1}\right). \tag{2.41}$$

Now, instead of writing down the resulting equations of compatibility, it is more appropriate to our needs to make immediate resort to the static-geometric analogy due to Gol'denveizer (1961), that is to make the following correspondence of variables

$$\left.\begin{array}{lll} \epsilon_{11} \to -M_{22}, & \kappa_{11} \to N_{22}, & \zeta_1 \to Q_2, \\ \epsilon_{22} \to -M_{11}, & \kappa_{22} \to N_{11}, & \zeta_2 \to -Q_1, \\ \epsilon_{12} = \epsilon_{21} \to M_{12} = M_{21}, & \kappa_{12} \to -N_{21}, & \\ & \kappa_{21} \to -N_{12}, & \end{array}\right\} \tag{2.42}$$

and so derive the equilibrium equations. The complete set of equations may be written

$$\left.\begin{array}{r} \dfrac{\partial \alpha_2 N_{11}}{\partial \xi_1} + \dfrac{\partial \alpha_1 N_{21}}{\partial \xi_2} + \dfrac{\partial \alpha_1}{\partial \xi_2} N_{12} - \dfrac{\partial \alpha_2}{\partial \xi_1} N_{22} + \dfrac{\alpha_1 \alpha_2}{R_1} Q_1 = -\alpha_1 \alpha_2 p_1^*, \\ \dfrac{\partial \alpha_2 N_{12}}{\partial \xi_1} + \dfrac{\partial \alpha_1 N_{22}}{\partial \xi_2} + \dfrac{\partial \alpha_2}{\partial \xi_1} N_{21} - \dfrac{\partial \alpha_1}{\partial \xi_2} N_{11} + \dfrac{\alpha_1 \alpha_2}{R_2} Q_2 = -\alpha_1 \alpha_2 p_2^*, \\ \dfrac{\partial \alpha_2 Q_1}{\partial \xi_1} + \dfrac{\partial \alpha_1 Q_2}{\partial \xi_2} - \alpha_1 \alpha_2 \left(\dfrac{N_{11}}{R_1} + \dfrac{N_{22}}{R_2}\right) = -\alpha_1 \alpha_2 p^*, \\ \dfrac{\partial \alpha_2 M_{11}}{\partial \xi_1} + \dfrac{\partial \alpha_1 M_{12}}{\partial \xi_2} + \dfrac{\partial \alpha_1}{\partial \xi_2} M_{12} - \dfrac{\partial \alpha_2}{\partial \xi_1} M_{22} - \alpha_1 \alpha_2 Q_1 = 0, \\ \dfrac{\partial \alpha_2 M_{12}}{\partial \xi_1} + \dfrac{\partial \alpha_1 M_{22}}{\partial \xi_2} + \dfrac{\partial \alpha_2}{\partial \xi_1} M_{12} - \dfrac{\partial \alpha_1}{\partial \xi_2} M_{11} - \alpha_1 \alpha_2 Q_2 = 0, \\ N_{12} - N_{21} + \left(\dfrac{1}{R_1} - \dfrac{1}{R_2}\right) M_{12} = 0, \end{array}\right\} \tag{2.43}$$

which agree with those of Sanders (1959) when $M_{12} = M_{21}$. The right hand sides of these equations provide the contributions from the distributed surface forces p_1^*, p_2^* and p^* (see figure 1). The first three of these are the equations of equilibrium in small deflexion first approximation shell theory, the fourth and fifth equations serve to define the normal shearing forces Q_1 and Q_2, while the sixth equation relates to moment equilibrium about the normal to the reference surface and is the analogue of the identity which is given in equation (2.20).

If the following additional correspondence of variables is made,

$$U_1 \to -\chi_1, \quad U_2 \to -\chi_2, \quad W \to -\psi \tag{2.44}$$

then χ_1, χ_2 and ψ are stress functions such that equations (2.17)–(2.19) with (2.42) provide stress resultants N_{11}, N_{22}, N_{12}, N_{21} and stress couples M_{11}, M_{22}, $M_{12} = M_{21}$ which satisfy the equations of equilibrium with $p_1^* = p_2^* = p^* = 0$.

The static-geometric analogy is completed by introducing the quantity $\bar{N}_{12}$ by

$$\bar{N}_{12} = \tfrac{1}{2}(N_{12} + N_{21}), \tag{2.45}$$

and noting from equations (2.21) and (2.42) the correspondence of variables

$$\bar{\kappa}_{12} \to -\bar{N}_{12}. \tag{2.46}$$

Equations (2.22), or the last of equations (2.43), then provide the relations

$$\left.\begin{aligned} N_{12} &= \bar{N}_{12} - \frac{1}{2}\left(\frac{1}{R_1} - \frac{1}{R_2}\right) M_{12}, \\ N_{21} &= \bar{N}_{12} + \frac{1}{2}\left(\frac{1}{R_1} - \frac{1}{R_2}\right) M_{12}. \end{aligned}\right\} \tag{2.47}$$

2.3. *Constitutive relations and accuracy of results*

Attention is now confined to the important case where the shell is constructed from an isotropic elastic material for which the constitutive relations may be taken to be the same as in Love's first approximation,

$$\left.\begin{aligned} N_{11} &= \frac{12D}{h^2}(\epsilon_{11} + \nu\epsilon_{22}), & M_{11} &= D(\kappa_{11} + \nu\kappa_{22}), \\ N_{22} &= \frac{12D}{h^2}(\epsilon_{22} + \nu\epsilon_{11}), & M_{22} &= D(\kappa_{22} + \nu\kappa_{11}), \\ \bar{N}_{12} &= \frac{12D}{h^2}(1-\nu)\,\epsilon_{12}, & M_{12} &= D(1-\nu)\,\bar{\kappa}_{12}, \end{aligned}\right\} \tag{2.48}$$

where h is the wall thickness, D is the flexural rigidity

$$D = \frac{Eh^3}{12(1-\nu^2)}, \tag{2.49}$$

where E is the Young modulus and ν the Poisson ratio.

Koiter (1960) has already pointed out that it is useless to attempt to achieve greater accuracy in first approximation theory by refinements to the constitutive relations. The magnitude of any such 'improvements' can only be of the same order as that of the errors which are anyways inherent because of the approximate character of the underlying Love–Kirchhoff assumptions. Indeed, the shell problems which are most suitable for analysis by the finite element method are concerned with stress and deformation patterns where the wavelength is many times the wall thickness h.† In these circumstances, the relative error in an analysis by first approximation shell theory is $O(h/R)$ where R is any radius of curvature or torsion of the reference surface. Thus, since a typical stress resultant N produces a stress intensity of N/h, while a typical stress couple produces a maximum stress intensity of $6M/h^2$, it follows that

$$\left.\begin{array}{ll} \text{(i)} & \text{if } RN = O(M) \text{ then } N \text{ contributes negligibly to the significant fibre stress,} \\ \text{(ii)} & \text{if } M = O(kRN) \text{ then } M \text{ contributes negligibly to the significant fibre stress,} \\ \text{(iii)} & k = h^2/12R^2 \text{ may be ignored in comparison with unity.} \end{array}\right\} \tag{2.50}$$

Consequently, if a comparison of results from a numerical method, like the finite element method, is made with those from an explicit solution to a first approximation theory, then one must be prepared to accept large relative differences in the magnitude of stress resultants N or stress couples M which contribute negligibly to the significant fibre stress.

Similar conclusions can be drawn about the strain and curvature change components by making use of the static-geometric analogy.

† The wavelength of simple edge effect is $> \surd(Rh)$.

2.4. *Energy, boundary conditions and variational principles*

The strain energy is the sum of the uncoupled bending and stretching energies, as in Love's (1927) theory. It is supplemented here with expressions for the work done by the surface loads and by the edge tractions, this latter provides a means of deriving boundary conditions appropriate to the first approximation shell theory.

A brief statement of the principle of minimum total potential energy is then given before deriving a variational principle from a finite element version of the Hellinger–Reissner (1914, 1950) principle. The new principle requires trial functions to interpolate, along the finite element boundaries, the complete kinematic conditions which maintain inter-element compatibility. The behaviour over the element is then partially described in terms of trial functions for stress resultants and stress couples and partially in terms of trial functions for displacements. The combination is such as to achieve rank sufficiency in the derived element stiffness matrix together with a 'best' satisfaction of compatibility at the element boundary. The variational principle separates naturally into two successively applied principles. The first principle operates at element level and is concerned with minimization of complementary energy, while the second applies at global level and is implicitly concerned with minimization of the total potential energy estimate. For the purpose of practical computation, however, there is advantage in simplifying the strictly derived second principle so that it is explicitly concerned with minimization of the total potential energy estimate. The new variational principle has versatile application, it is recognized as a generalization of the assumed stress hybrid model introduced by Pian (1964), see also Pian & Tong (1969), it provides a means to rectify the inadequacies of some existing non-compatible displacement finite element models.

It is convenient to introduce special notation, freely used in the sequel, so that displacements, strains and curvature changes, stress resultants and stress couples together with surface forces may be expressed as column matrices. Thus,

$$\left.\begin{aligned}
\mathsf{U} &= (U_1\,U_2\,W)^{\mathrm{T}}, & \bar{\mathsf{N}} &= (N_{11}\,N_{22}\,\bar{N}_{12}\,M_{11}\,M_{22}\,2M_{12})^{\mathrm{T}},\\
\mathsf{U}_C &= (U_\nu\,U_\sigma\,\phi_\nu\,W)^{\mathrm{T}}, & \bar{\mathsf{N}}_p &= (N_{11p}\,N_{22p}\,\bar{N}_{12p}\,M_{11p}\,M_{22p}\,2M_{12p})^{\mathrm{T}},\\
\mathsf{U}_C^* &= (U_\nu^*\,U_\sigma^*\,\phi_\nu^*\,W^*)^{\mathrm{T}}, & \mathsf{N}_C &= (N_{\nu\nu}\,N_{\nu\sigma}\,M_{\nu\nu}\,V_\nu)^{\mathrm{T}},\\
\mathsf{U}_C' &= (U_\nu\,U_\sigma\,\phi_\nu\,\phi_\sigma\,W)^{\mathrm{T}}, & \mathsf{N}_C^* &= (N_{\nu\nu}^*\,N_{\nu\sigma}^*\,M_{\nu\nu}^*\,V_\nu^*)^{\mathrm{T}},\\
\boldsymbol{\varepsilon} &= (\epsilon_{11}\,\epsilon_{22}\,\epsilon_{12}\,\epsilon_{21}\,\kappa_{11}\,\kappa_{22}\,\kappa_{12}\,\kappa_{21})^{\mathrm{T}}, & \mathsf{N}_{pC} &= (N_{\nu\nu p}\,N_{\nu\sigma p}\,M_{\nu\nu p}\,V_{\nu p})^{\mathrm{T}},\\
\bar{\boldsymbol{\varepsilon}} &= (\epsilon_{11}\,\epsilon_{22}\,2\epsilon_{12}\,\kappa_{11}\,\kappa_{22}\,\bar{\kappa}_{12})^{\mathrm{T}}, & \mathsf{N}_C' &= (N_{\nu\nu}\,N_{\nu\sigma}\,M_{\nu\nu}\,M_{\nu\sigma}\,Q_\nu)^{\mathrm{T}},\\
\mathsf{N} &= (N_{11}\,N_{22}\,N_{12}\,N_{21}\,M_{11}\,M_{22}\,M_{12}\,M_{21})^{\mathrm{T}}, & \mathsf{p}^* &= (p_1^*\,p_2^*\,p^*)^{\mathrm{T}}.
\end{aligned}\right\} \quad (2.51)$$

The suffix C is used to identify values at the boundary, while the asterisk signifies a prescribed quantity. Note that the boundary conditions of the shell problem may be expressed by components from

$$\mathsf{U}_C = \mathsf{U}_C^* \text{ and } \mathsf{N}_C = \mathsf{N}_C^* \quad (2.52)$$

where U_C is related to U by equations (2.32) and the first of equations (2.34), while N_C is later shown to be related to N by substituting equations (2.58) into (2.60).

The strain energy $\frac{1}{2}\iint \mathsf{N}^{\mathrm{T}}\varepsilon\,\mathrm{d}A$ which is stored in the thin walled shell is calculated by

$$\iint \mathsf{N}^{\mathrm{T}}\varepsilon\,\mathrm{d}A = \iint_A (N_{11}\epsilon_{11}+N_{22}\epsilon_{22}+N_{12}\epsilon_{12}+N_{21}\epsilon_{21} + M_{11}\kappa_{11}+M_{22}\kappa_{22}+M_{12}\kappa_{12}+M_{21}\kappa_{21})\,\alpha_1\alpha_2\,\mathrm{d}\xi_1\,\mathrm{d}\xi_2; \tag{2.53}$$

substitutions from equations (2.18), (2.22), (2.42) and (2.47) show that this may be simplified to

$$\iint \overline{\mathsf{N}}^{\mathrm{T}}\bar{\varepsilon}\,\mathrm{d}A = \iint_A (N_{11}\epsilon_{11}+N_{22}\epsilon_{22}+2\overline{N}_{12}\epsilon_{12}+M_{11}\kappa_{11}+M_{22}\kappa_{22}+2M_{12}\bar{\kappa}_{12})\,\alpha_1\alpha_2\,\mathrm{d}\xi_1\,\mathrm{d}\xi_2. \tag{2.54}$$

The external work $\iint \mathsf{p}^{*\mathrm{T}}\mathsf{U}\,\mathrm{d}A$ of the prescribed distributed surface loads p_1^*, p_2^* and p^* is given by

$$\iint \mathsf{p}^{*\mathrm{T}}\mathsf{U}\,\mathrm{d}A = \iint_A (p_1^*U_1+p_2^*U_2+p^*W)\,\alpha_1\alpha_2\,\mathrm{d}\xi_1\,\mathrm{d}\xi_2 \tag{2.55}$$

while the external work $\int \mathsf{N}_C^{*\mathrm{T}}\mathsf{U}_C\,\mathrm{d}C$ of prescribed tractions $N_{\nu\nu}^*$, $N_{\nu\sigma}^*$, $M_{\nu\nu}^*$ and V_ν^* applied at the boundary C is

$$\iint \mathsf{N}_C^{*\mathrm{T}}\mathsf{U}_C\,\mathrm{d}C = \int_C (N_{\nu\nu}^*U_\nu+N_{\nu\sigma}^*U_\sigma+M_{\nu\nu}^*\phi_\nu+V_\nu^*W)\,\alpha_\sigma\,\mathrm{d}\sigma. \tag{2.56}$$

The correct boundary conditions of the shell problem may be derived by equating $\int \mathsf{N}_C^{*\mathrm{T}}\mathsf{U}_C\,\mathrm{d}C$ with the work of the internal stress resultants and stress couples acting at the boundary C. Thus

$$\int \mathsf{N}_C'^{\mathrm{T}}\mathsf{U}_C'\,\mathrm{d}C = \int_C (N_{\nu\nu}U_\nu+N_{\nu\sigma}U_\sigma+M_{\nu\nu}\phi_\nu+M_{\nu\sigma}\phi_\sigma+Q_\nu W)\,\alpha_\sigma\,\mathrm{d}\sigma \tag{2.57}$$

where, on making use of the equations (2.42) of the static-geometric analogy and the strain and quasi measures of equations (2.35), (2.36), (2.38) together with equation (2.47), we have

$$\left.\begin{aligned}
N_{\nu\nu} &= N_{11}\cos^2\gamma+N_{22}\sin^2\gamma+2\overline{N}_{12}\sin\gamma\cos\gamma,\\
N_{\nu\sigma} &= -(N_{11}-N_{22})\sin\gamma\cos\gamma+\overline{N}_{12}(\cos^2\gamma-\sin^2\gamma)-\frac{1}{2}\left(\frac{1}{R_1}-\frac{1}{R_2}\right)M_{12},\\
M_{\nu\nu} &= M_{11}\cos^2\gamma+M_{22}\sin^2\gamma+2M_{12}\sin\gamma\cos\gamma,\\
M_{\nu\sigma} &= -(M_{11}-M_{22})\sin\gamma\cos\gamma+M_{12}(\cos^2\gamma-\sin^2\gamma),\\
Q_\nu &= Q_1\cos\gamma+Q_2\sin\gamma.
\end{aligned}\right\} \tag{2.58}$$

(Note that equations (2.57), (2.58) can be derived from equation (2.54) by substituting for the strain and curvature changes in terms of the displacements, equations (2.17)–(2.22), and then integrating by Green's formula.) A substitution for the rotation ϕ_σ is now made from equations (2.34) so that a partial integration of equation (2.57), when equated with equation (2.56) thus

$$\int \mathsf{N}_C'^{\mathrm{T}}\mathsf{U}_C'\,\mathrm{d}C = \int \mathsf{N}_C^{*\mathrm{T}}\mathsf{U}_C\,\mathrm{d}C, \tag{2.59}$$

shows that the following conditions have to be satisfied on the boundary C, see equations (2.52),

$$\left.\begin{aligned}
N_{\nu\nu}-\frac{M_{\nu\sigma}}{R_{\nu\sigma}} &= N_{\nu\nu}^* \quad\text{or}\quad U_\nu = U_\nu^*,\\
N_{\nu\sigma}+\frac{M_{\nu\sigma}}{R_\sigma} &= N_{\nu\sigma}^* \quad\text{or}\quad U_\sigma = U_\sigma^*,\\
M_{\nu\nu} &= M_{\nu\nu}^* \quad\text{or}\quad \phi_\nu = \phi_\nu^*,\\
Q_\nu+\frac{1}{\alpha_\sigma}\frac{\partial M_{\nu\sigma}}{\partial\sigma} &= V_\nu^* \quad\text{or}\quad W = W^*,
\end{aligned}\right\} \tag{2.60}$$

where U_ν^*, U_σ^*, ϕ_ν^* and W^* are prescribed kinematic conditions. For concentrated loads V_ν^* acting in the direction of the normal n at the boundary C, it is necessary to satisfy pointwise conditions

$$[M_{\nu\sigma}]_{\sigma-}^{\sigma+} = V_\nu^*. \tag{2.61}$$

Turning to the question of variational principles suppose first, and ideally, that a set of suitable Rayleigh–Ritz trial functions is available for displacements in U_i over the whole of the ith finite element so that it is feasible to proceed by straightforward minimization of the global total potential energy. Denote the area of the ith finite element by A_i, its boundary by C_i, etc. The solution then follows by minimizing the functional Π,

$$\Pi = \sum_i \left\{\frac{1}{2}\iint \overline{N}_i^{\mathrm{T}}\bar{\varepsilon}_i \,\mathrm{d}A_i - \iint p^{*\mathrm{T}} U_i \,\mathrm{d}A_i - \int_{N_C^*} N_C^{*\mathrm{T}} U_{Ci}\,\mathrm{d}C_i\right\}, \tag{2.62}$$

where the line integral is taken only over the portion of C_i where tractions N_C^* are prescribed. The trial functions in U_i necessarily satisfy kinematic subsidiary conditions, see equations (2.60),

$$\left.\begin{aligned} U_{Ci+} - U_{Ci-} &= 0, \\ U_{Ci} &= U^* \quad \text{if} \quad U^* \text{ is prescribed,}\end{aligned}\right\} \tag{2.63}$$

the subscripts + and − referring here to the two sides of C_i. In equation (2.62) it is understood that the strain and curvature changes $\bar{\varepsilon}_i$ correspond with U_i by using displacement-strain equations of the type (2.17) to (2.22) and, moreover, that the stress resultants and stress couples $\overline{N}_i$ correspond in their turn with $\bar{\varepsilon}_i$ in virtue of constitutive relations of the type given in equations (2.48). The displacements U_i are thus the only quantities which are subject to arbitrary variation.

As already indicated, however, it is usually impracticable in shell problems to satisfy all the subsidiary conditions of equations (2.63) and it is, indeed, rather easier to widen the search for trial functions to quantities other than just displacements and then to resort to some weaker functional. Accordingly, let U_{Ci} now denote a set of trial functions which interpolate the kinematic conditions along the boundary C_i and let $U_{\alpha i}$ denote trial functions which partially describe the displacements over the element. Also, let $\overline{N}_{\beta i}$ denote supplementary trial functions for stress resultants and stress couples over this ith finite element. The functional Π_R which is associated with this wide choice of trial functions may then be derived from that which is used in the Hellinger–Reissner principle, thus

$$\begin{aligned}\Pi_R = \sum_i \Bigg\{\frac{1}{2}\iint (\overline{N}_{\alpha i}^{\mathrm{T}} + \overline{N}_{\beta i}^{\mathrm{T}})\,(\bar{\varepsilon}_{\alpha i} + \bar{\varepsilon}_{\beta i})\,\mathrm{d}A_i - \iint p^{*\mathrm{T}} U_{\alpha i}\,\mathrm{d}A_i \\ - \int_{N_C^*} N_C^{*\mathrm{T}} U_{Ci}\,\mathrm{d}C_i - \iint (\overline{N}_{\alpha i}^{\mathrm{T}} + \overline{N}_{\beta i}^{\mathrm{T}})\,\bar{\varepsilon}_{\beta i}\,\mathrm{d}A_i + \int (N_{\alpha Ci}^{\mathrm{T}} + N_{\beta Ci}^{\mathrm{T}})\,(U_{Ci} - U_{\alpha Ci})\,\mathrm{d}C_i\Bigg\},\end{aligned} \tag{2.64}$$

where the kinematic subsidiary conditions on $U_{\alpha i}$ are relaxed so that it is linearly related in some (best) way with U_{Ci}, e.g. through†

$$\left.\begin{aligned} U_{\alpha Ci} &= U_{Ci} \quad \text{at points on } C_i, \\ U_{Ci} &= U^* \quad \text{where } U^* \text{ is prescribed,}\end{aligned}\right\} \tag{2.65}$$

† The variational adjunct derived from Π_R is

$$\delta\left\{\frac{1}{2}\iint \overline{N}_{\alpha i}^{\mathrm{T}}\bar{\varepsilon}_{\alpha i}\,\mathrm{d}A_i - \iint p^{*\mathrm{T}} U_{\alpha i}\,\mathrm{d}A_i + \int N_{\alpha Ci}^{\mathrm{T}}(U_{Ci} - U_{\alpha Ci})\,\mathrm{d}C_i\right\} = 0$$

for arbitrary variations in $U_{\alpha i}$. This adjunct can be used to satisfy the subsidiary conditions in a best sense once the rigid body components in $U_{\alpha i}$ are equated at points on C_i.

such that $U_{\alpha Ci}$ (and therefore also $U_{\alpha i}$) is completely determined in terms of U_{Ci}; the subsidiary conditions on the stress resultants and stress couples in $\overline{N}_{\beta i}$ are that they satisfy the partial differential equations of homogeneous equilibrium (see equations (2.43) and (2.47)),

$$\left.\begin{array}{l}\frac{\partial \alpha_2 N_{11\beta i}}{\partial \xi_1}+\frac{\partial \alpha_1 N_{21\beta i}}{\partial \xi_2}+\frac{\partial \alpha_1}{\partial \xi_2} N_{12\beta i}-\frac{\partial \alpha_2}{\partial \xi_1} N_{22\beta i}+\frac{\alpha_1 \alpha_2}{R_1} Q_{1\beta i}=0, \\ \ldots\ldots\ldots\ldots\ldots\ldots\ldots\ldots\ldots\ldots\ldots\ldots\ldots\ldots\ldots\ldots\ldots\end{array}\right\} \tag{2.66}$$

over A_i. It is understood, moreover, that the strain and curvature changes $\bar{\boldsymbol{\varepsilon}}_{\alpha i}$ correspond with the $U_{\alpha i}$ by using displacement-strain equations of the type (2.17)–(2.21) and that the stress resultants and stress couples $\overline{N}_{\alpha i}$ correspond with $\bar{\boldsymbol{\varepsilon}}_{\alpha i}$ in virtue of constitutive relations of the type given in equations (2.48). Also, it is understood that the strains and curvature changes $\bar{\boldsymbol{\varepsilon}}_{\beta i}$ correspond with $\overline{N}_{\beta i}$ in virtue of their constitutive relations. The quantities which remain subject to arbitrary variation in equation (2.64) are thus $\overline{N}_{\beta i}$ and U_{Ci}. The functional Π_R becomes identical with Π for the global total potential energy, see equation (2.62), in the limiting case where $\overline{N}_{\beta i}=0$ and where the subsidiary conditions on the $U_{\alpha Ci}$ of equations (2.65) are satisfied everywhere on C_i. In another limiting case where both $U_{\alpha i}$ and $p^*=0$ then Π_R agrees with the functional introduced by Pian (1964) in his assumed stress hybrid finite element model; this same model is successfully employed by Allman (1970) in deriving a triangularly shaped finite element to solve problems in the bending of flat plates.

The principles follow by rendering $\delta \Pi_R=0$. Consider initially the consequences of arbitrary variations $\delta\overline{N}_{\beta i}$ over A_i, this leads to the principle

$$\iint \delta\overline{N}_{\beta i}^{\mathrm{T}} \bar{\boldsymbol{\varepsilon}}_{\beta i}\,\mathrm{d}A_i-\int \delta N_{\beta Ci}^{\mathrm{T}}(U_{Ci}-U_{\alpha Ci})\,\mathrm{d}C_i=0 \tag{2.67}$$

for individual finite elements; it provides an Euler equation for the integrability of the strains and curvature changes $\bar{\boldsymbol{\varepsilon}}_{\beta i}$. Note that because of the subsidiary condition on $\overline{N}_{\beta i}$, as expressed by equations (2.66), this variational principle enforces

$$\iint \overline{N}_{\beta i}^{\mathrm{T}} \bar{\boldsymbol{\varepsilon}}_{\beta i}\,\mathrm{d}A_i-\int N_{\beta Ci}^{\mathrm{T}}(U_{Ci}-U_{\alpha Ci})\,\mathrm{d}C_i=0. \tag{2.68}$$

The functional of equation (2.64) can now be reduced to

$$\begin{aligned}\Pi_R'=\sum_i\Big\{&\frac{1}{2}\iint(\overline{N}_{\alpha i}^{\mathrm{T}}+\overline{N}_{\beta i}^{\mathrm{T}})(\bar{\boldsymbol{\varepsilon}}_{\alpha i}+\bar{\boldsymbol{\varepsilon}}_{\beta i})\,\mathrm{d}A_i-\iint p^{*\mathrm{T}}U_i\,\mathrm{d}A_i\\&-\int_{N_C^*} N_C^{*\mathrm{T}}U_{Ci}\,\mathrm{d}C_i\underline{-\iint \overline{N}_{\alpha i}^{\mathrm{T}}\bar{\boldsymbol{\varepsilon}}_{\beta i}\,\mathrm{d}A_i+\int N_{\alpha Ci}^{\mathrm{T}}(U_{Ci}-U_{\alpha Ci})\,\mathrm{d}C_i+\iint p^{*\mathrm{T}}(U_i-U_{\alpha i})\,\mathrm{d}A_i}\Big\},\end{aligned} \tag{2.69}$$

where both $U_{\alpha i}$ and $\overline{N}_{\beta i}$ are regarded as known functions of the remaining independent quantity U_{Ci}. In examining the underlined terms in Π_R', we note that an Euler equation of the part functional

$$\Pi_R''=\sum_i\left\{\frac{1}{2}\iint(\overline{N}_{\alpha i}^{\mathrm{T}}+\overline{N}_{\beta i}^{\mathrm{T}})(\bar{\boldsymbol{\varepsilon}}_{\alpha i}+\bar{\boldsymbol{\varepsilon}}_{\beta i})\,\mathrm{d}A_i-\iint p^{*\mathrm{T}}U_i\,\mathrm{d}A_i-\int_{N_C^*} N_C^{*\mathrm{T}}U_{Ci}\,\mathrm{d}C_i\right\} \tag{2.70}$$

ensures that

$$\underline{-\iint \overline{N}_{\alpha i}^{\mathrm{T}}\boldsymbol{\varepsilon}_{\beta i}\,\mathrm{d}A_1+\int N_{\alpha Ci}^{\mathrm{T}}(U_{Ci}-U_{\alpha Ci})\,\mathrm{d}C_i+\int p^*(U_i-U_{\alpha i})\,\mathrm{d}A_i=0} \tag{2.71}$$

when the restored integrability of $\bar{\varepsilon}_{\beta i}$ (see equation (2.67)) is acknowledged. The premise is that the stationary value of Π''_R may be identified with that of Π'_R so that the second principle may be written

$$\sum_i \left\{ \iint (\bar{N}^{\mathrm{T}}_{\alpha i} + \bar{N}^{\mathrm{T}}_{\beta i})\,(\delta\bar{\varepsilon}_{\alpha i} + \delta\bar{\varepsilon}_{\beta i})\,\mathrm{d}A_i - \iint p^{*\mathrm{T}}\,\delta U_i\,\mathrm{d}A_i - \int_{N^*_C} N^{*\mathrm{T}}_C\,\delta U_{Ci}\,\mathrm{d}C_i \right\} = 0. \qquad (2.72)$$

Note, however, that U_i is not described over A_i and so the virtual work of the surface forces p^* has to be approximated. This can be achieved by introducing a column matrix $\bar{N}_p$ of stress resultants and stress couples, see equations (2.51), which satisfies the equations (2.43) of equilibrium in the presence of surface forces $p^* = (p^*_1\,p^*_2\,p^*)^{\mathrm{T}}$. Then, by making use of Green's theorem, the equations (2.72) may be rewritten

$$\sum_i \left\{ \iint (\bar{N}^{\mathrm{T}}_{\alpha i} + \bar{N}^{\mathrm{T}}_{\beta i} - \bar{N}^{\mathrm{T}}_{pi})\,(\delta\bar{\varepsilon}_{\alpha i} + \delta\bar{\varepsilon}_{\beta i})\,\mathrm{d}A_i + \int N^{\mathrm{T}}_{pCi}\,\delta U_{Ci}\,\mathrm{d}C_i - \int_{N^*_C} N^{*\mathrm{T}}_C\,\delta U_{Ci}\,\mathrm{d}C_i \right\} = 0, \qquad (2.73)$$

where N_{pC} is defined in equations (2.51).

3. The general developable surface

Mention is made in the Introduction that some special analytical techniques remain to be evolved before the practical and efficient finite element analysis of shells becomes a reality. In first developing these techniques it is sensible to simplify matters as much as possible and this is the reason why attention is to be specialized to developable surfaces, sometimes called surfaces of zero (Gaussian) curvature.

The finite element method is basically a piecewise application of the Rayleigh–Ritz process. The conditions of the process are formally satisfied by the selection of (admissible) trial functions which are complete in the sense that the strain energy norm converges in the mean as the finite element mesh is made progressively finer. Now, the four basic states of static response, which are described in the Introduction, correspond to intrinsic levels of comparative magnitude in the bending and stretching contributions to the strain energy $\frac{1}{2}\iint \bar{N}^{\mathrm{T}}\bar{\varepsilon}\,\mathrm{d}A$, equation (2.54). Thus, an arbitrary choice of trial functions in displacements $U = (U_1\,U_2\,W)^{\mathrm{T}}$ which, nevertheless, meet the requirements of the membrane actions of state (I) leads to

$$\iint_A (M_{11}\kappa_{11} + M_{22}\kappa_{22} + 2M_{12}\bar{\kappa}_{12})\,\alpha_1\alpha_2\,\mathrm{d}\xi_1\,\mathrm{d}\xi_2 = O\left\{k \iint \bar{N}^{\mathrm{T}}\bar{\varepsilon}\,\mathrm{d}A\right\}, \qquad (3.1)$$

where the non-dimensional parameter k, defined in equations (2.50), is very small with a value somewhat less than 10^{-5} for the thin walled shells of first approximation theory. On the other hand, the inextensional solutions of state (II) require special displacement trial functions which are complementary function solutions to the partial differential equations which govern $\epsilon_{11} = \epsilon_{22} = \epsilon_{12} = 0$. For these trial functions, signified by inext.,

$$\iint_A (M_{11}\kappa_{11} + M_{22}\kappa_{22} + 2M_{12}\bar{\kappa}_{12})^{(\mathrm{inext.})}\,\alpha_1\alpha_2\,\mathrm{d}\xi_1\,\mathrm{d}\xi_2 \equiv \iint (\bar{N}^{\mathrm{T}}\bar{\varepsilon})^{(\mathrm{inext.})}\,\mathrm{d}A. \qquad (3.2)$$

The six trial functions of state (III) which describe an arbitrary rigid body movement of the shell, contribute nothing to the stresses or strains so that

$$\iint (\bar{N}^{\mathrm{T}}\bar{\varepsilon})^{(\mathrm{r.b.})}\,\mathrm{d}A \equiv 0. \qquad (3.3)$$

Lastly, the nature of the transcendental trial functions which describe the simple edge effects of state (IV) is such that they are not susceptible to decomposition into separate inextensional and membrane components.† They contribute to another intrinsic level of comparative magnitude in the strain energy where

$$\iint_A (N_{11}\epsilon_{11}+N_{22}\epsilon_{22}+2\bar{N}_{12}\epsilon_{12})^{(\mathrm{edge})}\alpha_1\alpha_2\,\mathrm{d}\xi_1\,\mathrm{d}\xi_2 \doteqdot \iint_A (M_{11}\kappa_{11}+M_{22}\kappa_{22}+2M_{12}\bar{\kappa}_{12})^{(\mathrm{edge})}\alpha_1\alpha_2\,\mathrm{d}\xi_1\,\mathrm{d}\xi_2.$$

It is evident that (so called) general solution processes for shell problems are inadequate for purposes of practical computation when they cannot exhibit strong recovery qualities at each of the above mentioned intrinsic levels of comparative magnitude. It is appropriate, therefore, to make clear that the present objective is limited to the recovery of those smoothly varying distributions of stress and strain which can be piecewise described through the basic states (I), (II) and (III) of static response. In other words, questions of edge effect are specifically excluded from present consideration.

Complementary function solutions to the partial differential equations which govern inextensional deformation are readily available only for certain shell shapes, such as the developable surface. It is the relative simplicity of this analysis which presents the prime motive in so specializing the investigation from the arbitrary shell. Note that if shell problems are solved by selecting trial functions for stress resultants and stress couples, e.g. through the stress functions of equations (2.44), it is then necessary to consider complementary functions which recover purely membrane actions where the stress couples $M_{11} = M_{22} = M_{12} = 0$. The theory of these purely membrane actions is intimately related to inextensional theory by the static-geometric analogy. For these trial functions, denoted by memb.,

$$\iint_A (N_{11}\epsilon_{11}+N_{22}\epsilon_{22}+2\bar{N}_{12}\epsilon_{12})^{(\mathrm{memb.})}\alpha_1\alpha_2\,\mathrm{d}\xi_1\,\mathrm{d}\xi_2 \equiv \iint (\mathsf{N}^{\mathrm{T}}\bar{\varepsilon})^{(\mathrm{memb.})}\,\mathrm{d}A. \tag{3.4}$$

The purpose of the present section is to supply the working formulae for developable surfaces which describe in general terms the inextensional deformations, membrane actions and particularized strains, rigid body movements and sensitive solutions.

3.1. *Specialization of results*

The developable surface in a lines of curvature coordinate system is identified by

$$1/R_1 = 0, \tag{3.5}$$

where the lines ξ_2 = constant are the generators; the Codazzi relations of equation (2.11) then show that

$$\alpha_1 = \alpha_1(\xi_1) \quad \text{and} \quad R_2(\xi_1,\xi_2) = \alpha_2 R_{20}(\xi_2) \tag{3.6}$$

which introduces R_{20} as a function only of ξ_2. Since the line element along a generator (see equation (2.8)) is

$$|\mathrm{d}\boldsymbol{r}| = \alpha_1(\xi_1)\,\mathrm{d}\xi_1,$$

it is clear that ξ_1 may always be identified with arc length so that if we put

$$\alpha_1 = 1 \tag{3.7}$$

† It is observed, for example, that in a shell with developable reference surface where the lines ξ_2 = constant are the generators, the curvature change $\kappa_{11}^{(\mathrm{inext.})} \equiv 0$ and therefore cannot contribute to $\kappa_{11}^{(\mathrm{edge})}$.

there is no ensuing loss of generality. The first of each of equations (2.5), (2.6) and (2.10) reveals that the form of equation (2.3) for the position vector of the general developable surface is

$$\boldsymbol{r} = \boldsymbol{r}_0(\xi_2) + \xi_1 \boldsymbol{t}_1(\xi_2), \tag{3.8}$$

where $\boldsymbol{t}_1$ is, as already described, the unit tangent vector in the ξ_1 direction. The Gauss relation of equation (2.12) shows that

$$\alpha_2(\xi_1, \xi_2) = \alpha_{20}(\xi_2) + \xi_1 \alpha_{21}(\xi_2), \tag{3.9}$$

where, in view of the requirement from equations (2.10) that

$$\frac{\partial \boldsymbol{t}_1}{\partial \xi_2} = \frac{1}{\alpha_1}\frac{\partial \alpha_2}{\partial \xi_1}\boldsymbol{t}_2,$$

it is necessary for

$$\alpha_{20}\frac{\mathrm{d}\boldsymbol{t}_1}{\mathrm{d}\xi_2} = \alpha_{21}\frac{\mathrm{d}\boldsymbol{r}_0}{\mathrm{d}\xi_2}. \tag{3.10}$$

It follows from equations (2.6) and (3.8)–(3.10) that

$$\alpha_{20}(\xi_2) = \left|\frac{\mathrm{d}\boldsymbol{r}_0}{\mathrm{d}\xi_2}\right| \quad \text{and} \quad \alpha_{21}(\xi_2) = \left|\frac{\mathrm{d}\boldsymbol{t}_1}{\mathrm{d}\xi_2}\right|, \tag{3.11}$$

where one of α_{20}, α_{21} may turn out to be zero, but never both simultaneously.† The unit tanget vector $\boldsymbol{t}_2$ in the ξ_2 direction is given by

$$\boldsymbol{t}_2(\xi_2) = \frac{1}{\alpha_2}\frac{\mathrm{d}\boldsymbol{r}}{\mathrm{d}\xi_2} = \frac{1}{\alpha_{20}}\frac{\mathrm{d}\boldsymbol{r}_0}{\mathrm{d}\xi_2} \quad \text{and/or} \quad = \frac{1}{\alpha_{21}}\frac{\mathrm{d}\boldsymbol{t}_1}{\mathrm{d}\xi_2}. \tag{3.12}$$

Consequently, the unit normal vector $\boldsymbol{n}$ of equation (2.9) is

$$\boldsymbol{n}(\xi_2) = \boldsymbol{t}_1(\xi_2) \times \boldsymbol{t}_2(\xi_2), \tag{3.13}$$

while the function R_{20} of equation (3.6) is given by

$$\frac{1}{R_{20}(\xi_2)} = \frac{\mathrm{d}\boldsymbol{n}}{\mathrm{d}\xi_2}\cdot\boldsymbol{t}_2 = -\boldsymbol{n}\cdot\frac{\mathrm{d}\boldsymbol{t}_2}{\mathrm{d}\xi_2}. \tag{3.14}$$

In the alternative form for the position vector $\boldsymbol{r}$, see equations (2.13) and (2.14), the components ρ_1, ρ_2 and ρ_n become

$$\left.\begin{aligned} \rho_1 &= (\boldsymbol{r}_0 + \xi_1\boldsymbol{t}_1)\cdot\boldsymbol{t}_1 = \rho_{10}(\xi_2) + \xi_1 \quad \text{with} \quad \rho_{10}(\xi_2) = \boldsymbol{r}_0\cdot\boldsymbol{t}_1, \\ \rho_2(\xi_2) &= (\boldsymbol{r}_0 + \xi_1\boldsymbol{t}_1)\cdot\boldsymbol{t}_2 = \boldsymbol{r}_0\cdot\boldsymbol{t}_2, \\ \rho_n(\xi_2) &= (\boldsymbol{r}_0 + \xi_1\boldsymbol{t}_1)\cdot\boldsymbol{n} = \boldsymbol{r}_0\cdot\boldsymbol{n}, \end{aligned}\right\} \tag{3.15}$$

where attention is drawn to the fact that ρ_{10}, ρ_2 and ρ_n are here functions only of ξ_2. The first derivatives of these components with respect to the coordinate ξ_2 are required in the sequel. When equations (2.10) are specialized for developable surfaces so that

$$\left.\begin{aligned} \frac{\mathrm{d}\boldsymbol{t}_1}{\mathrm{d}\xi_2} &= \alpha_{21}\boldsymbol{t}_2, \\ \frac{\mathrm{d}\boldsymbol{t}_2}{\mathrm{d}\xi_2} &= -\alpha_{21}\boldsymbol{t}_1 - \frac{\boldsymbol{n}}{R_{20}}, \\ \frac{\mathrm{d}\boldsymbol{n}}{\mathrm{d}\xi_2} &= \frac{\boldsymbol{t}_2}{R_{20}}, \end{aligned}\right\} \tag{3.16}$$

† In fact, $\alpha_{20} = 0$ for conical surfaces with vertex at $\xi_1 = 0$, while $\alpha_{21} = 0$ for cylindrical and plane surfaces. Both α_{20} and α_{21} are non zero for the general developable derived from the tangent surface to a curve.

the required derivatives are readily found to be

$$\left.\begin{aligned}\frac{\mathrm{d}\rho_{10}}{\mathrm{d}\xi_2} &= \alpha_{21}\rho_2,\\ \frac{\mathrm{d}\rho_2}{\mathrm{d}\xi_2} &= \alpha_{20}-\alpha_{21}\rho_{10}-\frac{\rho_n}{R_{20}},\\ \frac{\mathrm{d}\rho_n}{\mathrm{d}\xi_2} &= \frac{\rho_2}{R_{20}}.\end{aligned}\right\} \tag{3.17}$$

The rotation components in the ξ_1, ξ_2 lines of curvature coordinate system for the developable surface are, see equations (2.17),

$$\left.\begin{aligned}\phi_1 &= -\frac{\partial W}{\partial \xi_1},\\ \phi_2 &= \frac{1}{\alpha_2}\left(\frac{U_2}{R_{20}}-\frac{\partial W}{\partial \xi_2}\right),\\ \phi_n &= \frac{1}{2\alpha_2}\left(-\frac{\partial U_1}{\partial \xi_2}+\alpha_2\frac{\partial U_2}{\partial \xi_1}+\alpha_{21}U_2\right),\end{aligned}\right\} \tag{3.18}$$

while the strains are given by, see equations (2.18),

$$\left.\begin{aligned}\epsilon_{11} &= \frac{\partial U_1}{\partial \xi_1},\\ \epsilon_{22} &= \frac{1}{\alpha_2}\left(\frac{\partial U_2}{\partial \xi_2}+\alpha_{21}U_1+\frac{W}{R_{20}}\right),\\ \epsilon_{12} = \epsilon_{21} &= \frac{1}{2\alpha_2}\left(\frac{\partial U_1}{\partial \xi_2}+\alpha_2\frac{\partial U_2}{\partial \xi_1}-\alpha_{21}U_2\right).\end{aligned}\right\} \tag{3.19}$$

The curvature changes are obtained from equations (2.19) and (2.21), they are

$$\left.\begin{aligned}\kappa_{11} &= \frac{\partial \phi_1}{\partial \xi_1},\\ \kappa_{22} &= \frac{1}{\alpha_2}\left(\frac{\partial \phi_2}{\partial \xi_2}+\alpha_{21}\phi_1\right),\\ \bar{\kappa}_{12} &= \frac{1}{2\alpha_2}\left(\frac{\partial \phi_1}{\partial \xi_2}+\frac{\phi_n}{R_{20}}-\alpha_{21}\phi_2+\alpha_2\frac{\partial \phi_2}{\partial \xi_1}\right).\end{aligned}\right\} \tag{3.20}$$

The equations (2.23) *et seq.* were developed in a general way so that the behaviour of the reference surface can be studied along arbitrary orthogonal curvilinear coordinates ν = constant, σ = constant which are not necessarily coincident with the lines of curvature coordinate system. These equations may be simplified for the developable surface. They are particularly appropriate to situations where the geodesic curvatures $-k_\nu$ and k_σ of equations (2.29) are both zero, i.e. where the angle γ between tangent vectors $\boldsymbol{t}_\nu$ and $\boldsymbol{t}_1$ is determined in such a way that

$$\frac{\partial}{\partial \xi_2}(\alpha_1\cos\gamma)-\frac{\partial}{\partial \xi_1}(\alpha_2\sin\gamma) = \frac{\partial}{\partial \xi_2}(\alpha_1\sin\gamma)+\frac{\partial}{\partial \xi_1}(\alpha_2\cos\gamma) = 0, \tag{3.21}$$

which becomes, after substitution from equations (3.7) and (3.9),

$$-\sin\gamma\frac{\partial \gamma}{\partial \xi_2}-\alpha_{21}\sin\gamma-\alpha_2\cos\gamma\frac{\partial \gamma}{\partial \xi_1} = \cos\gamma\frac{\partial \gamma}{\partial \xi_2}+\alpha_{21}\cos\gamma-\alpha_2\sin\gamma\frac{\partial \gamma}{\partial \xi_1} = 0. \tag{3.22}$$

Thus, for both k_ν and k_σ to be zero the angle γ has to be determined so that

$$\gamma(\xi_2) = -\int \alpha_{21}(\xi_2)\,\mathrm{d}\xi_2 + \text{constant}. \tag{3.23}$$

The coordinates ν, σ then form an orthogonal geodesic coordinate system which appear as rectangular Cartesian coordinates when the reference surface is developed onto the plane. It is only on developable surfaces that both geodesic curvatures $-k_\nu$ and k_σ can be made zero such that equations (2.29) imply

$$\partial\alpha_\nu/\partial\sigma = \partial\alpha_\sigma/\partial\nu = 0. \tag{3.24}$$

The line elements along the orthogonal network of geodesics are therefore $\alpha_\nu(\nu)\,\mathrm{d}\nu$ and $\alpha_\sigma(\sigma)\,\mathrm{d}\sigma$ so that both ν and σ may always be identified with arc length and we may put

$$\alpha_\nu = \alpha_\sigma = 1 \tag{3.25}$$

without loss of generality.

Two cases are worthy of special note because of their importance in engineering applications. Consider first the situation where the reference surface lies on an arbitrary cylinder so that, in equation (3.9),

$$\alpha_2(\xi_2) = \alpha_{20}(\xi_2), \quad \text{i.e.} \quad \alpha_{21}(\xi_2) = 0. \tag{3.26}$$

Equation (3.23) then reveals that the angle γ is given by

$$\gamma = \text{constant}, \tag{3.27}$$

while the first of equations (2.25) shows, for $\mathrm{d}\nu = 0$, that the relation

$$\xi_1 = -\alpha_{20}\xi_2 \tan\gamma \tag{3.28}$$

defines geodesics which pass through the origin of coordinates $\xi_1, \xi_2 = 0$. Moreover, the integral of the second of equations (2.25) shows that the arc length σ of these geodesics, as measured in the positive direction from the coordinate origin, is related to ξ_1 and ξ_2 by

$$\xi_1 = -\sigma\sin\gamma, \quad \alpha_{20}\xi_2 = \sigma\cos\gamma. \tag{3.29}$$

The other important situation occurs when the middle surface of the shell lies on an arbitrary cone with vertex at $\xi_1 = -\xi_1'$, $\xi_1' > 0$, so that in equation (3.9)

$$\alpha_2(\xi_1, \xi_2) = (\xi_1 + \xi_1')\,\alpha_{21}(\xi_2), \quad \text{i.e.} \quad \alpha_{20}(\xi_2) = \xi_1'\alpha_{21}(\xi_2). \tag{3.30}$$

Let us again consider the geodesics which pass through the coordinate origin ξ_1, $\xi_2 = 0$. The angle γ now depends upon the coordinate ξ_2,

$$\gamma(\xi_2) = \gamma' - \int_0^{\xi_2} \alpha_{21}\,\mathrm{d}\xi_2, \tag{3.31}$$

where γ' is the angle between the unit tangent vectors $\boldsymbol{t}_\nu$ and $\boldsymbol{t}_1$ at the coordinate origin. From the first of equations (2.25) we obtain, for $\mathrm{d}\nu = 0$, the condition that

$$(\xi_1 + \xi_1')\cos\gamma = \xi_1'\cos\gamma', \quad (\xi_1 + \xi_1') > 0, \tag{3.32}$$

which defines the geodesics. Similarly as above, the integral of the second of equations (2.25) shows that the arc length σ of these geodesics, as measured in the positive direction from the coordinate origin, is

$$\sigma = -(\xi_1 + \xi_1')\sin\gamma - \xi_1'\sin\gamma'. \tag{3.33}$$

Returning now to the general developable surface, the quantities R_ν, R_σ, $R_{\nu\sigma}$ of equations (2.30) for orthogonal geodesic coordinates ν and σ become

$$\frac{1}{R_\nu} = \frac{\sin^2\gamma}{\alpha_2 R_{20}}, \quad \frac{1}{R_\sigma} = \frac{\cos^2\gamma}{\alpha_2 R_{20}}, \quad \frac{1}{R_{\nu\sigma}} = -\frac{\sin\gamma\cos\gamma}{\alpha_2 R_{20}} \tag{3.34}$$

while the list of slopes, strains and curvature changes of equations (2.34)–(2.36) simplify to

$$\left.\begin{aligned} \phi_\nu &= \frac{\sin\gamma}{\alpha_2 R_{20}}(U_\nu \sin\gamma + U_\sigma \cos\gamma) - \frac{\partial W}{\partial \nu} = \frac{U_2 \sin\gamma}{\alpha_2 R_{20}} - \frac{\partial W}{\partial \nu}, \\ \phi_\sigma &= \frac{\cos\gamma}{\alpha_2 R_{20}}(U_\nu \sin\gamma + U_\sigma \cos\gamma) - \frac{\partial W}{\partial \sigma} = \frac{U_2 \cos\gamma}{\alpha_2 R_{20}} - \frac{\partial W}{\partial \sigma}, \\ \phi_n &= \frac{1}{2}\left(\frac{\partial U_\sigma}{\partial \nu} - \frac{\partial U_\nu}{\partial \sigma}\right), \end{aligned}\right\} \tag{3.35}$$

$$\left.\begin{aligned} \epsilon_{\nu\nu} &= \frac{\partial U_\nu}{\partial \nu} + \frac{W\sin^2\gamma}{\alpha_2 R_{20}}, \\ \epsilon_{\sigma\sigma} &= \frac{\partial U_\sigma}{\partial \sigma} + \frac{W\cos^2\gamma}{\alpha_2 R_{20}}, \\ \epsilon_{\nu\sigma} &= \frac{1}{2}\left(\frac{\partial U_\sigma}{\partial \nu} + \frac{\partial U_\nu}{\partial \sigma} + \frac{2W\sin\gamma\cos\gamma}{\alpha_2 R_{20}}\right), \end{aligned}\right\} \tag{3.36}$$

and finally

$$\left.\begin{aligned} \kappa_{\nu\nu} &= \frac{\partial \phi_\nu}{\partial \nu} + \frac{\phi_n \sin\gamma\cos\gamma}{\alpha_2 R_{20}}, \\ \kappa_{\sigma\sigma} &= \frac{\partial \phi_\sigma}{\partial \sigma} - \frac{\phi_n \sin\gamma\cos\gamma}{\alpha_2 R_{20}}, \\ \bar{\kappa}_{\nu\sigma} &= \frac{1}{2}\left\{\frac{\partial \phi_\nu}{\partial \sigma} + \frac{\partial \phi_\sigma}{\partial \nu} + \frac{\phi_n}{\alpha_2 R_{20}}(\cos^2\gamma - \sin^2\gamma)\right\}. \end{aligned}\right\} \tag{3.37}$$

3.2. *Inextensional deformations*

The ξ_1, ξ_2 lines of curvature coordinate system provides a suitable basis to examine the inextensional deformations of a developable surface.

The strains ϵ_{11}, ϵ_{22} and $\epsilon_{12} = \epsilon_{21}$ of equations (3.19) must separately vanish for inextensional deformation to occur, satisfaction of the resulting differential equations then requires that displacements $U^{(\text{inext.})} = (U_1^{(\text{inext.})}\, U_2^{(\text{inext.})}\, W^{(\text{inext})})^{\mathrm{T}}$ be expressed in the form

$$\left.\begin{aligned} U_1^{(\text{inext.})} &= U_{10}(\xi_2), \\ U_2^{(\text{inext.})} &= U_{20}(\xi_2) + \xi_1 U_{21}(\xi_2), \\ W^{(\text{inext}).} &= W_0(\xi_2) + \xi_1 W_1(\xi_2), \end{aligned}\right\} \tag{3.38}$$

where

$$\left.\begin{aligned} U_{10}(\xi_2) &= \int (\alpha_{21} U_{20} - \alpha_{20} U_{21})\, \mathrm{d}\xi_2, \\ W_0(\xi_2) &= -R_{20}\left(\frac{\mathrm{d}U_{20}}{\mathrm{d}\xi_2} + \alpha_{21} U_{10}\right), \\ W_1(\xi_2) &= -R_{20}\frac{\mathrm{d}U_{21}}{\mathrm{d}\xi_2}. \end{aligned}\right\} \tag{3.39}$$

Inextensional deformations of a developable surface may therefore be characterized in terms of two arbitrary functions $U_{20}(\xi_2)$ and $U_{21}(\xi_2)$. The $U^{(\text{inext.})}$ of equations (3.38) are seen to be linear in the coordinate ξ_1 and, in selecting the trial functions for the Rayleigh–Ritz process, consideration may be given towards a choice of $U_{20}(\xi_2)$ and $U_{21}(\xi_2)$ such that the component $U_2^{(\text{inext.})}$ is described entirely as a polynomial. It is evident, however, that the remaining components $U_1^{(\text{inext.})}$ and $W^{(\text{inext.})}$ may not be then described in polynomial terms except in special cases such as where R_{20}, α_{20} and α_{21} are constant.

When equations (3.38) and (3.39) are substituted into equations (3.18) it is found that the rotations which accompany this inextensional deformation are interrelated by

$$\left.\begin{aligned}\phi_n^{(\text{inext.})}(\xi_2) &= U_{21},\\ \phi_1^{(\text{inext.})}(\xi_2) &= R_{20}\frac{\mathrm{d}\phi_n^{(\text{inext.})}}{\mathrm{d}\xi_2},\\ \frac{\partial}{\partial\xi_1}(\alpha_2\phi_2^{(\text{inext.})}) &= \frac{\mathrm{d}\phi_1^{(\text{inext.})}}{\mathrm{d}\xi_2}+\frac{\phi_n^{(\text{inext.})}}{R_{20}}.\end{aligned}\right\} \tag{3.40}$$

These show that the rotation component $\phi_2^{(\text{inext.})}$ must have the form

$$\phi_2^{(\text{inext.})}(\xi_1,\xi_2) = \frac{\phi_{20}(\xi_2)+\xi_1\phi_{21}(\xi_2)}{\alpha_{20}(\xi_2)+\xi_1\alpha_{21}(\xi_2)}, \quad \text{with} \quad \phi_{21}(\xi_2) = \frac{\mathrm{d}\phi_1^{(\text{inext.})}}{\mathrm{d}\xi_2}+\frac{\phi_n^{(\text{inext.})}}{R_{20}}. \tag{3.41}$$

The curvature changes of this inextensional deformation are, see equations (3.20),

$$\left.\begin{aligned}\kappa_{11}^{(\text{inext.})} &= 0,\\ \kappa_{22}^{(\text{inext.})} &= \frac{1}{\alpha_2}\left(\frac{\partial\phi_2^{(\text{inext.})}}{\partial\xi_2}+\alpha_{21}\phi_1^{(\text{inext.})}\right),\\ \bar{\kappa}_{12}^{(\text{inext.})} &= \frac{\partial\phi_2^{(\text{inext.})}}{\partial\xi_1},\end{aligned}\right\} \tag{3.42}$$

In the conditions for convergence of finite element displacement analysis, reference is made, see Introduction, to particularized responses for use as trial functions in the piecewise description of general curvature change. The above equations confirm, however, the statement that arbitrary states of constant curvature change cannot be sustained in shells. Moreover, it is seen to be generally a matter of considerable difficulty to find functions $U_{20}(\xi_2)$ and $U_{21}(\xi_2)$ which provide constant values for just $\kappa_{22}^{(\text{inext.})}$ and $\bar{\kappa}_{12}^{(\text{inext.})}$ in the developable shell; a simpler criterion is given in the sequel for particularized responses referred to as sensitive inextensional solutions by Morley (1972) and Morris (1974).

The stress resultants $N_{11}^{(\text{inext.})}$, $N_{22}^{(\text{inext.})}$ and $\bar{N}_{12}^{(\text{inext.})}$ of inextensional theory do not necessarily vanish. They cannot be determined from the constitutive relations (2.48), instead they follow from considerations of equilibrium, either from equations (2.43) or by way of stress functions $\chi_1^{(\text{inext.})}$, $\chi_2^{(\text{inext.})}$ and $\psi^{(\text{inext.})}$. Consequently, inextensional solutions may not satisfy exactly all the equations of the agreed first approximation shell theory. They are, nonetheless, perfectly adequate when taken in comparison with exact solutions to the agreed first approximation shell theory as may be confirmed by appeal to equations (2.50) or their static-geometric counterpart.

PHILOSOPHICAL TRANSACTIONS OF THE ROYAL SOCIETY A MATHEMATICAL, PHYSICAL & ENGINEERING SCIENCES

3.3. *Membrane action*

In finite element analysis by the displacement method, there is generally no need to dwell upon the role of stress resultants as derived from membrane theory although instances do occur where it is practicable to select trial functions $\mathbf{U} = (U_1 U_2 W)^{\mathrm{T}}$ which allow direct recovery of these actions for what may be regarded as the more basic distributions appropriate to zero and to specific surface forces, e.g. appropriate to such as the surface force which occurs in a pressurized vessel. One such instance occurs in the technologically important circular cylindrical shell with uniform wall thickness and uniform material properties; other shapes of shell may require variation in wall thickness or material properties to achieve this recovery in a practical way.

Study of purely membrane actions assumes greater significance, however, in applying the variational principles of the assumed stress hybrid finite element and similar models (see Pian & Tong 1969), and in applying the principle of minimum complementary energy. For this reason, the working formulae which describe these actions are listed for the developable shell. The static-geometric analogy with inextensional theory facilitates the preparation of this list. In a purely membrane action the stress couples M_{11}, M_{22}, M_{12}, M_{21} as well as the out of surface shears Q_1 and Q_2 are assumed to vanish.

The correspondence of variables in the static-geometric analogy is expressed by equations (2.42), (2.44) and (2.46). Equations (3.38) and (3.39) then show, in the absence of surface forces $p^* = (p_1^* p_2^* p^*)^{\mathrm{T}}$, that the purely membrane actions in a shell with a developable reference surface can be expressed by stress functions $\chi_1^{(\mathrm{memb.})}$, $\chi_2^{(\mathrm{memb.})}$ and $\psi^{(\mathrm{memb.})}$ which have the form

$$\left.\begin{aligned} \chi_1^{(\mathrm{memb.})} &= \chi_{10}(\xi_2), \\ \chi_2^{(\mathrm{memb.})} &= \chi_{20}(\xi_2) + \xi_1 \chi_{21}(\xi_2), \\ \psi^{(\mathrm{memb.})} &= \psi_0(\xi_2) + \xi_1 \psi_1(\xi_2), \end{aligned}\right\} \tag{3.43}$$

where

$$\left.\begin{aligned} \chi_{10}(\xi_2) &= \int (\alpha_{21}\chi_{20} - \alpha_{20}\chi_{21})\, \mathrm{d}\xi_2, \\ \psi_0(\xi_2) &= -R_{20}\left(\frac{\mathrm{d}\chi_{20}}{\mathrm{d}\xi_2} + \alpha_{21}\chi_{10}\right), \\ \psi_1(\xi_2) &= -R_{20}\frac{\mathrm{d}\chi_{21}}{\mathrm{d}\xi_2}. \end{aligned}\right\} \tag{3.44}$$

These membrane actions are seen to be characterized by the two arbitrary functions $\chi_{20}(\xi_2)$ and $\chi_{21}(\xi_2)$. Formulae which express the stress resultants $N_{11}^{(\mathrm{memb.})}$, $N_{22}^{(\mathrm{memb.})}$ and $\bar{N}_{12}^{(\mathrm{memb.})}$ in terms of the stress functions may be written down from the static-geometric analogy to equations (3.18) and (3.20); subsequent appeal to the equations (2.43) of equilibrium allows the determination of extra contributions which are caused by the surface forces, thus

$$\left.\begin{aligned} N_{11}^{(\mathrm{memb.})} &= -\frac{1}{\alpha_2}\left\{\frac{\partial}{\partial \xi_2}\frac{1}{\alpha_2}\left(\frac{\chi_2^{(\mathrm{memb.})}}{R_{20}} - \frac{\partial \psi^{(\mathrm{memb.})}}{\partial \xi_2}\right) + \alpha_{21}R_{20}\frac{\mathrm{d}\chi_{21}^{(\mathrm{memb.})}}{\mathrm{d}\xi_2} + \int\left(\frac{\partial I_p}{\partial \xi_2} - \alpha_{21}R_2 p^* + \alpha_2 p_1^*\right)\mathrm{d}\xi_1\right\}, \\ N_{22}^{(\mathrm{memb.})} &= R_2 p^*, \\ \bar{N}_{12}^{(\mathrm{memb.})} &= \frac{\partial}{\partial \xi_1}\frac{1}{\alpha_2}\left(\frac{\chi_2^{(\mathrm{memb.})}}{R_{20}} - \frac{\partial \psi^{(\mathrm{memb.})}}{\partial \xi_2}\right) + I_p, \end{aligned}\right\} \tag{3.45}$$

where $R_2 = \alpha_2 R_{20}$ (see equations (3.6)) and

$$I_p = -\frac{1}{\alpha_2^2}\int \alpha_2\left(\frac{\partial R_2 p^*}{\partial \xi_2} + \alpha_2 p_2^*\right)\mathrm{d}\xi_1. \tag{3.46}$$

11-2

The constitutive relations of equations (2.48), taken in conjunction with equations (3.19), provide

$$\left.\begin{aligned} \epsilon_{11}^{(\text{memb.})} &= \frac{1}{Eh}(N_{11}^{(\text{memb.})} - \nu N_{22}^{(\text{memb.})}) = \frac{\partial U_1^{(\text{memb.})}}{\partial \xi_1}, \\ \epsilon_{22}^{(\text{memb.})} &= \frac{1}{Eh}(N_{22}^{(\text{memb.})} - \nu N_{11}^{(\text{memb.})}) = \frac{1}{\alpha_2}\left(\frac{\partial U_2^{(\text{memb.})}}{\partial \xi_2} + \alpha_{21} U_1^{(\text{memb.})} + \frac{W^{(\text{memb.})}}{R_{20}}\right), \\ \epsilon_{12}^{(\text{memb.})} &= \frac{(1+\nu)}{Eh}\bar{N}_{12}^{(\text{memb.})} = \frac{1}{2}\left\{\frac{1}{\alpha_2}\frac{\partial U_1^{(\text{memb.})}}{\partial \xi_2} + \alpha_2 \frac{\partial}{\partial \xi_1}\left(\frac{U_2^{(\text{memb.})}}{\alpha_2}\right)\right\}, \end{aligned}\right\} \tag{3.47}$$

and these may be integrated to provide $U^{(\text{memb.})} = (U_1^{(\text{memb.})}\, U_2^{(\text{memb.})}\, W^{(\text{memb.})})^{\text{T}}$ where

$$\left.\begin{aligned} U_1^{(\text{memb.})} &= \int \epsilon_{11}^{(\text{memb.})}\, \mathrm{d}\xi_1, \\ U_2^{(\text{memb.})} &= \alpha_2 \int \frac{1}{\alpha_2}\left(2\epsilon_{12}^{(\text{memb.})} - \frac{1}{\alpha_2}\frac{\partial U_1^{(\text{memb.})}}{\partial \xi_2}\right) \mathrm{d}\xi_1, \\ W^{(\text{memb.})} &= R_{20}\left(\alpha_2 \epsilon_{22}^{(\text{memb.})} - \frac{\partial U_2^{(\text{memb.})}}{\partial \xi_2} - \alpha_{21} U_1^{(\text{memb.})}\right). \end{aligned}\right\} \tag{3.48}$$

The displacements $U^{(\text{memb.})}$ are particular integrals of equations (3.47), they require to be augmented with complementary functions $U^{(\text{inext.})}$ from the inextensional deformations of equations (3.38) where $\epsilon_{11} = \epsilon_{22} = \epsilon_{12} = 0$.

Purely membrane action solutions may not satisfy exactly all the equations of the agreed first approximation shell theory. Like the inextensional solutions discussed earlier they are, nonetheless, perfectly adequate solutions when taken in comparison with the exact solutions to the agreed first approximation shell theory.

3.4. *Rigid body movement and sensitive solutions*

The vector $\boldsymbol{U}^{(\text{r.b.})}$ which describes the rigid body movement of a particle on the shell reference surface can be described in terms of a constant translation vector $\boldsymbol{\Delta}$ and a constant (small) rotation vector $\boldsymbol{\Omega}$ by

$$\boldsymbol{U}^{(\text{r.b.})} = \boldsymbol{\Delta} + \boldsymbol{\Omega} \times \boldsymbol{r}, \tag{3.49}$$

where

$$\left.\begin{aligned} \boldsymbol{\Delta} &= c_1 \boldsymbol{e}_1 + c_2 \boldsymbol{e}_2 + c_3 \boldsymbol{e}_3, \\ \boldsymbol{\Omega} &= c_4 \boldsymbol{e}_1 + c_5 \boldsymbol{e}_2 + c_6 \boldsymbol{e}_3, \end{aligned}\right\} \tag{3.50}$$

with constant coefficients $c_1, c_2, \ldots, c_6$. All these vectors may be defined alternatively in the ξ_1, ξ_2 lines of curvature coordinate system by

$$\left.\begin{aligned} \boldsymbol{\Delta} &= \delta_1 \boldsymbol{t}_1 + \delta_2 \boldsymbol{t}_2 + \delta_n \boldsymbol{n}, \\ \boldsymbol{\Omega} &= -\omega_2 \boldsymbol{t}_1 + \omega_1 \boldsymbol{t}_2 + \omega_n \boldsymbol{n}, \\ \boldsymbol{U}^{(\text{r.b.})} &= U_1^{(\text{r.b.})} \boldsymbol{t}_1 + U_2^{(\text{r.b.})} \boldsymbol{t}_2 + W^{(\text{r.b.})} \boldsymbol{n}, \end{aligned}\right\} \tag{3.51}$$

see also equations (2.15) and (2.16). The translation and rotation components δ_i and ω_i are functions only of ξ_2 and may be derived in terms of the $c_1, c_2, \ldots, c_6$ from

$$\left.\begin{aligned} \delta_1(\xi_2) &= \boldsymbol{\Delta}\cdot\boldsymbol{t}_1, & \omega_1(\xi_2) &= \boldsymbol{\Omega}\cdot\boldsymbol{t}_2, \\ \delta_2(\xi_2) &= \boldsymbol{\Delta}\cdot\boldsymbol{t}_2, & \omega_2(\xi_2) &= -\boldsymbol{\Omega}\cdot\boldsymbol{t}_1, \\ \delta_n(\xi_2) &= \boldsymbol{\Delta}\cdot\boldsymbol{n}, & \omega_n(\xi_2) &= \boldsymbol{\Omega}\cdot\boldsymbol{n}. \end{aligned}\right\} \tag{3.52}$$

After substituting from equations (2.13) and (3.15) into (3.49), the rigid body displacements $U^{(\mathrm{r.b.})} = (U_1^{(\mathrm{r.b.})}\, U_2^{(\mathrm{r.b.})}\, W^{(\mathrm{r.b.})})^{\mathrm{T}}$ may subsequently be expressed in terms of these δ_i and ω_i by

$$\left.\begin{aligned} U_1^{(\mathrm{r.b.})} &= U_{10}^{(\mathrm{r.b.})}(\xi_2), \\ U_2^{(\mathrm{r.b.})} &= U_{20}^{(\mathrm{r.b.})}(\xi_2) + \xi_1 U_{21}^{(\mathrm{r.b.})}(\xi_2), \\ W^{(\mathrm{r.b.})} &= W_0^{(\mathrm{r.b.})}(\xi_2) + \xi_1 W_1^{(\mathrm{r.b.})}(\xi_2), \end{aligned}\right\} \tag{3.53}$$

where

$$\left.\begin{aligned} U_{10}^{(\mathrm{r.b.})}(\xi_2) &= \delta_1 + \rho_n \omega_1 - \rho_2 \omega_n, \\ U_{20}^{(\mathrm{r.b.})}(\xi_2) &= \delta_2 + \rho_n \omega_2 + \rho_{10} \omega_n, \\ U_{21}^{(\mathrm{r.b.})}(\xi_2) &= \omega_n, \\ W_0^{(\mathrm{r.b.})}(\xi_2) &= \delta_n - \rho_{10}\omega_1 - \rho_2 \omega_2, \\ W_1^{(\mathrm{r.b.})}(\xi_2) &= -\omega_1. \end{aligned}\right\} \tag{3.54}$$

Equations (3.38) and (3.39) show that the general inextensional deformation may be characterized by two functions $U_{20}^{(\mathrm{inext.})}(\xi_2)$ and $U_{21}^{(\mathrm{inext.})}(\xi_2)$ and, since the movement of the whole shell as a rigid body is just a special case of inextensional deformation, the rigid body movement may also be characterized by two functions $U_{20}^{(\mathrm{r.b.})}(\xi_2)$ and $U_{21}^{(\mathrm{r.b.})}(\xi_2)$.

Now, piecewise representation of the curvature changes throughout the shell requires the selection of smoothly varying particularized responses from inextensional theory, section (3.2). The 'smoothest' of such responses are described in the literature as sensitive inextensional solutions. They are best derived by approximating the rigid body movement over a small region by an inextensional deformation $U_{20}^{(\mathrm{inext.})}(\xi_2)$ and $U_{21}^{(\mathrm{inext.})}(\xi_2)$ where, say, $U_{20}^{(\mathrm{r.b.})}(\xi_2)$ and $U_{21}^{(\mathrm{r.b.})}(\xi_2)$ are expanded about the line $\xi_2 = 0$ in terms of a truncated Taylor series,

$$\left.\begin{aligned} U_{20}^{(\mathrm{inext.})}(\xi_2) &= \sum_{j=0,1,2,\ldots} \left[\frac{\mathrm{d}^j U_{20}^{(\mathrm{r.b.})}}{\mathrm{d}\xi_2^j}\right]^{\xi_2=0} \left(\frac{\xi_2^j}{j!}\right), \\ U_{21}^{(\mathrm{inext.})}(\xi_2) &= \sum_{j=0,1,2,\ldots} \left[\frac{\mathrm{d}^j U_{21}^{(\mathrm{r.b.})}}{\mathrm{d}\xi_2^j}\right]^{\xi_2=0} \left(\frac{\xi_2^j}{j!}\right). \end{aligned}\right\} \tag{3.55}$$

The two particularized responses best suitable for piecewise representation of curvature changes throughout the shell, and hence for convergence in the finite element method, are given by the first term, from each series, which provides non-zero curvature change.

3.5. *Particularized strains*

The discussion on practical conditions for convergence in the finite element analysis of shells (see Introduction) draws attention to the fact that arbitrary choice of (low degree polynomial) displacement trial functions in $U = (U_1 U_2 W)^{\mathrm{T}}$ leads to significant membrane actions where the curvature changes $\kappa_{11}, \kappa_{22}, \bar{\kappa}_{12}$ are negligible. Smoothly varying particularized strains are required for each of ϵ_{11}, ϵ_{22} and ϵ_{12}, in the chosen coordinate system, if convergence of the piecewise representation is to be assured for general states of membrane response calculated by the finite element displacement method. The effects of (the negligible) curvature changes can be ignored in these considerations.

Strains $\epsilon_{11}, \epsilon_{22}, \epsilon_{12}$ in the ξ_1, ξ_2 lines of curvature coordinate system for the developable surface are given in terms of the displacements by equations (3.19). Smoothly varying particularized responses in this coordinate system are given by

$$\left.\begin{aligned} U_1 &= c_1\xi_1 + c_2 \int \alpha_{21}\xi_2 \,\mathrm{d}\xi_2 + 2c_3\xi_2, \\ U_2 &= c_2\xi_2 + 2c_4\xi_1, \\ W &= -R_{20}\alpha_{21} U_1, \end{aligned}\right\} \tag{3.56}$$

where c_1, c_2, c_3 and c_4 are constants. This gives rise to strains

$$\epsilon_{11} = c_1, \quad \epsilon_{22} = c_2/\alpha_2, \quad \epsilon_{12} = (c_3 + \alpha_{20} c_4)/\alpha_2, \tag{3.57}$$

where it is recalled that

$$\alpha_2 = \alpha_{20}(\xi_2) + \xi_1 \alpha_{21}(\xi_2) \tag{3.9 bis}$$

for developable surfaces.

Rather more satisfactory particularized responses are derived from strains $\epsilon_{\nu\nu}$, $\epsilon_{\sigma\sigma}$, $\epsilon_{\nu\sigma}$ in the ν, σ geodesic coordinate system, equations (3.36). Here we write

$$\left.\begin{aligned} U_\nu &= c_1' \nu + 2c_3' \sigma, \\ U_\sigma &= c_2' \sigma + 2c_4' \nu, \\ W &= 0, \end{aligned}\right\} \tag{3.58}$$

where c_1', c_2', c_3' and c_4' are further constants. This gives rise to *constant* strains

$$\epsilon_{\nu\nu} = c_1', \quad \epsilon_{\sigma\sigma} = c_2', \quad \epsilon_{\nu\sigma} = c_3' + c_4', \tag{3.59}$$

just as occurs in problems of plane stress. Equations (2.35) can be used to transform these into strains of the lines of curvature coordinate system but, in this connexion, it should be noted that equation (3.23) shows the angle γ to be constant only when $\alpha_{21} \equiv 0$, i.e. as for arbitrary cylinders.

4. The circular cylindrical shell

Application of the formulae just derived for the general developable surface is now demonstrated in the development of finite element methods specifically for circular cylindrical shells. It is emphasized that attention is restricted to the smoothly varying distributions of stress and strain which can be piecewise described through the basic states (I), (II) and (III) of static response which are described in the Introduction.

Central to the finite element development are the trial functions in U_{ci}, see equations (2.51), which interpolate the kinematic conditions along a geodesic boundary of the (ith) element. It is an unfortunate fact, however, that casual embodiment of the formulae of § 3 leads to numerical difficulties when evaluating the component trial functions in U_{ci}. In consequence, it is necessary to express these trial functions in terms of special transcendental functions defined along the geodesic.

This interpolation is then used in the guise of Hermitian interpolation to develop a lines of curvature rectangular finite element, which is distinguished from all other known shell finite elements because it directly recovers (I) membrane actions, including the particularized strains; (II) four sensitive inextensional solutions; (III) arbitrary rigid body movements, and satisfies all inter-element continuities as are demanded by the underlying principle of minimum total potential energy.

It is recognized that useful application of this rectangular finite element is limited to special problems where the boundary contours of the shell coincide with the lines of curvature. Consequently, attention is next given to the development of a more practically useful finite element which is triangularly shaped with each side coinciding with a geodesic line. The possibility of development by using Pian's (1964) assumed stress hybrid finite element model is first discussed before making recourse to the more versatile variational principle introduced in § 2.4.

Problems in circular cylindrical shells are so frequently occurring that they have attracted an almost standard notation. Thus, it is more usual to work in terms of x, θ and s rather than ξ_1, ξ_2 and σ. Accordingly, let

$$\left.\begin{array}{lllll} \xi_1 = Rx, & \sigma = Rs, & U_1 = U_x, & U_\sigma = U_s, & \epsilon_{11} = \epsilon_{xx}, \\ \xi_2 = \theta, & & U_2 = U_\theta, & & \epsilon_{22} = \epsilon_{\theta\theta}, \quad \text{etc.} \end{array}\right\} \tag{4.1}$$

where R is the radius of the reference surface and x, θ, s are non-dimensional coordinates. The position vector $\boldsymbol{r}$ to the reference surface is given by (see figure 2)

$$\boldsymbol{r} = R(\sin\theta\,\boldsymbol{e}_1 + \cos\theta\,\boldsymbol{e}_2 + x\boldsymbol{e}_3) \tag{4.2}$$

so that the vectors $\boldsymbol{r}_0$ and $\boldsymbol{t}_x$ of equation (3.8) are

$$\boldsymbol{r}_0 = R(\sin\theta\,\boldsymbol{e}_1 + \cos\theta\,\boldsymbol{e}_2), \quad \boldsymbol{t}_x = \boldsymbol{e}_3. \tag{4.3}$$

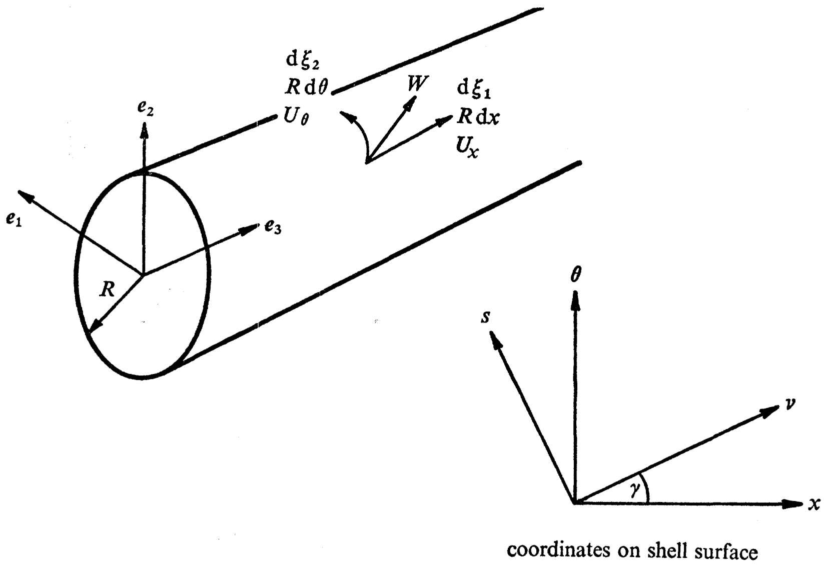

FIGURE 2. Notation for circular cylindrical shell.

The modulus $|\boldsymbol{t}_x| = 1$ as is required and, from equations (3.9) and (3.11),

$$\alpha_\theta = \alpha_{\theta 0} = R, \quad \alpha_{\theta 1} = 0. \tag{4.4}$$

The unit tangent vector $\boldsymbol{t}_\theta$ in the θ direction, equation (3.12), is

$$\boldsymbol{t}_\theta = \cos\theta\,\boldsymbol{e}_1 - \sin\theta\,\boldsymbol{e}_2 \tag{4.5}$$

while the unit normal vector to the reference surface, equation (3.13), is

$$\boldsymbol{n} = \sin\theta\,\boldsymbol{e}_1 + \cos\theta\,\boldsymbol{e}_2. \tag{4.6}$$

Thus, the function $R_{\theta 0}$ of equation (3.14) is the unit constant,

$$R_{\theta 0} = 1 \quad (\text{so that } R_\theta = R), \tag{4.7}$$

and the components ρ_x, ρ_θ and ρ_n of equations (3.15) are

$$\rho_x = Rx, \quad \rho_{x0} = \rho_\theta = 0, \quad \rho_n = R, \tag{4.8}$$

so that when the position vector $\boldsymbol{r}$ of equation (4.2) is expressed in terms of the moving triad $\boldsymbol{t}_x$, $\boldsymbol{t}_\theta$ and $\boldsymbol{n}$ it is simply

$$\boldsymbol{r} = R(x\boldsymbol{t}_x + \boldsymbol{n}). \tag{4.9}$$

The rotations, strains and curvature changes in the x, θ coordinate system are, see equations (3.18)–(3.20),

$$\left.\begin{aligned} R\phi_x &= -\frac{\partial W}{\partial x}, \\ R\phi_\theta &= U_\theta - \frac{\partial W}{\partial \theta}, \\ R\phi_n &= \frac{1}{2}\left(-\frac{\partial U_x}{\partial \theta} + \frac{\partial U_y}{\partial x}\right), \end{aligned}\right\} \tag{4.10}$$

$$\left.\begin{aligned} R\epsilon_{xx} &= \frac{\partial U_x}{\partial x}, & R^2\kappa_{xx} &= -\frac{\partial^2 W}{\partial x^2}, \\ R\epsilon_{\theta\theta} &= \frac{\partial U_\theta}{\partial \theta} + W, & R^2\kappa_{\theta\theta} &= -\frac{\partial^2 W}{\partial \theta^2} + \frac{\partial U_\theta}{\partial \theta}, \\ R\epsilon_{x\theta} &= \frac{1}{2}\left(\frac{\partial U_x}{\partial \theta} + \frac{\partial U_\theta}{\partial x}\right), & R^2\bar{\kappa}_{x\theta} &= -\frac{\partial^2 W}{\partial x \partial \theta} + \frac{3}{4}\frac{\partial U_\theta}{\partial x} - \frac{1}{4}\frac{\partial U_x}{\partial \theta}. \end{aligned}\right\} \tag{4.11}$$

The equations (2.43) and (2.47) of equilibrium reduce to

$$\left.\begin{aligned} \frac{\partial N_{xx}}{\partial x} + \frac{\partial \bar{N}_{x\theta}}{\partial \theta} - \frac{1}{2R}\frac{\partial M_{x\theta}}{\partial \theta} &= -Rp_x^*, \\ \frac{\partial \bar{N}_{x\theta}}{\partial x} + \frac{\partial N_{\theta\theta}}{\partial \theta} + \frac{3}{2R}\frac{\partial M_{x\theta}}{\partial x} + \frac{1}{R}\frac{\partial M_{\theta\theta}}{\partial \theta} &= -Rp_\theta^*, \\ \frac{1}{R}\frac{\partial^2 M_{xx}}{\partial x^2} + \frac{2}{R}\frac{\partial^2 M_{x\theta}}{\partial x \partial \theta} + \frac{1}{R}\frac{\partial^2 M_{\theta\theta}}{\partial \theta^2} - N_{\theta\theta} &= -Rp^*. \end{aligned}\right\} \tag{4.12}$$

The expressions for the stress resultants and stress couples in terms of arbitrary stress functions χ_x, χ_θ and ψ are, see equations (2.42), (2.44), (2.46) and (4.11),

$$\left.\begin{aligned} R^2N_{xx} &= \frac{\partial^2 \psi}{\partial \theta^2} - \frac{\partial \chi_\theta}{\partial \theta}, & RM_{xx} &= \frac{\partial \chi_\theta}{\partial \theta} + \psi, \\ R^2N_{\theta\theta} &= \frac{\partial^2 \psi}{\partial x^2}, & RM_{\theta\theta} &= \frac{\partial \chi_x}{\partial x}, \\ R^2\bar{N}_{x\theta} &= -\frac{\partial^2 \psi}{\partial x \partial \theta} + \frac{3}{4}\frac{\partial \chi_\theta}{\partial x} - \frac{1}{4}\frac{\partial \chi_x}{\partial \theta}, & RM_{x\theta} &= -\frac{1}{2}\left(\frac{\partial \chi_x}{\partial \theta} + \frac{\partial \chi_\theta}{\partial x}\right), \end{aligned}\right\} \tag{4.13}$$

and these provide solutions to the equations of equilibrium (4.12) when the surface forces $p_x^* = p_\theta^* = p^* = \theta$.

The inextensional displacements $U^{(\text{inext.})}$ are given by equations (3.38) and (3.39) and when hese are specialized for the circular cylindrical shell they are

$$\left.\begin{aligned} U_x^{(\text{inext.})} &= U_{x0}(\theta), \\ U_\theta^{(\text{inext.})} &= U_{\theta 0}(\theta) + RxU_{\theta 1}(\theta), \\ W^{(\text{inext.})} &= W_0(\theta) + RxW_1(\theta), \end{aligned}\right\} \tag{4.14}$$

where
$$\left.\begin{aligned} U_{x0}(\theta) &= -R\int U_{\theta 1}\,\mathrm{d}\theta,\\ W_0(\theta) &= -\frac{\mathrm{d}U_{\theta 0}}{\mathrm{d}\theta},\\ W_1(\theta) &= -\frac{\mathrm{d}U_{\theta 1}}{\mathrm{d}\theta},\end{aligned}\right\} \tag{4.15}$$

with $U_{\theta 0}(\theta)$ and $U_{\theta 1}(\theta)$ as arbitrary functions.

In a purely membrane action the stress functions in the circular cylindrical shell are, see equations (3.43) *et seq.*,
$$\left.\begin{aligned} \chi_x^{(\text{memb.})} &= \chi_{x0}(\theta),\\ \chi_\theta^{(\text{memb.})} &= \chi_{\theta 0}(\theta)+Rx\chi_{\theta 1}(\theta),\\ \psi^{(\text{memb.})} &= \psi_0(\theta)+Rx\psi_1(\theta),\end{aligned}\right\} \tag{4.16}$$

where
$$\left.\begin{aligned} \chi_{x0}(\theta) &= -R\int \chi_{\theta 1}\,\mathrm{d}\theta,\\ \psi_0(\theta) &= -\frac{\mathrm{d}\chi_{\theta 0}}{\mathrm{d}\theta},\\ \psi_1(\theta) &= -\frac{\mathrm{d}\chi_{\theta 1}}{\mathrm{d}\theta},\end{aligned}\right\} \tag{4.17}$$

with $\chi_{\theta 0}(\theta)$ and $\chi_{\theta 1}(\theta)$ as arbitrary functions. These stress functions, together with surface forces p_x^*, p_θ^* and p^*, produce stress resultants
$$\left.\begin{aligned} R^2N_{xx}^{(\text{memb.})} &= -\frac{\partial}{\partial\theta}\left(\frac{\partial^2}{\partial\theta^2}+1\right)(\chi_{\theta 0}+Rx\chi_{\theta 1})-R^2\int\left(\frac{\partial I_p}{\partial\theta}+Rp_x^*\right)\mathrm{d}x,\\ R^2N_{\theta\theta}^{(\text{memb.})} &= R^3p^*,\\ R^2\bar{N}_{x\theta}^{(\text{memb.})} &= \left(\frac{\mathrm{d}^2}{\mathrm{d}\theta^2}+1\right)R\chi_{\theta 1}+R^2I_p,\end{aligned}\right\} \tag{4.18}$$

where
$$I_p = -R\int\left(\frac{\partial p^*}{\partial\theta}+p_\theta^*\right)\mathrm{d}x. \tag{4.19}$$

The strains in this purely membrane action
$$\left.\begin{aligned} \epsilon_{xx}^{(\text{memb.})} &= \frac{1}{Eh}\left(N_{xx}^{(\text{memb.})}-\nu N_{\theta\theta}^{(\text{memb.})}\right),\\ \epsilon_{\theta\theta}^{(\text{memb.})} &= \frac{1}{Eh}\left(N_{\theta\theta}^{(\text{memb.})}-\nu N_{xx}^{(\text{memb.})}\right),\\ \epsilon_{x\theta}^{(\text{memb.})} &= \frac{(1+\nu)}{Eh}\bar{N}_{x\theta}^{(\text{memb.})},\end{aligned}\right\} \tag{4.20}$$

give rise to displacements $U^{(\text{memb.})}$
$$\left.\begin{aligned} U_x^{(\text{memb.})} &= R\int \epsilon_{xx}^{(\text{memb.})}\,\mathrm{d}x,\\ U_\theta^{(\text{memb.})} &= R\int\left(2\epsilon_{x\theta}^{(\text{memb.})}-\frac{1}{R}\frac{\partial U_x^{(\text{memb.})}}{\partial\theta}\right)\mathrm{d}x,\\ W^{(\text{memb.})} &= R\epsilon_{\theta\theta}^{(\text{memb.})}-\frac{\partial U_\theta^{(\text{memb.})}}{\partial\theta},\end{aligned}\right\} \tag{4.21}$$

see equations (3.48) and subsequent sentence.

The rigid body movements are obtained by substituting equations (4.3), (4.5), (4.6) and (4.8) into equations (3.49)–(3.54). Rigid body movements are special instances of inextensional deformation (see equations (4.14) and (4.15)) and so may be characterized by two functions as follows

$$\left.\begin{aligned} U^{(\mathrm{r.b.})}_{\theta 0}(\theta) &= c_1\cos\theta - c_2\sin\theta - Rc_6,\\ U^{(\mathrm{r.b.})}_{\theta 1}(\theta) &= c_4\sin\theta + c_5\cos\theta.\end{aligned}\right\} \tag{4.22}$$

4.1. *Interpolation of kinematic conditions along a geodesic line*

Equations (2.51) define column matrices $\boldsymbol{U}$ and $\boldsymbol{U}_C$ respectively for the distribution of displacements in the interior and for kinematic conditions on the boundary C,

$$\left.\begin{aligned} \boldsymbol{U} &= (U_x\, U_\theta\, W)^{\mathrm{T}},\\ \boldsymbol{U}_C &= (U_\nu\, U_s \phi_\nu\, W)^{\mathrm{T}}.\end{aligned}\right\} \tag{4.23}$$

The matrix $\boldsymbol{U}_C$ is related to $\boldsymbol{U}$ through equations (2.32), (2.34), (4.1) and (4.10). For the circular cylindrical shell, on C,

$$\left.\begin{aligned} U_\nu &= U_x\cos\gamma + U_\theta\sin\gamma,\\ U_s &= -U_x\sin\gamma + U_\theta\cos\gamma,\\ R\phi_\nu &= \left(U_\theta - \frac{\partial W}{\partial\theta}\right)\sin\gamma - \frac{\partial W}{\partial x}\cos\gamma.\end{aligned}\right\} \tag{4.24}$$

In the variational principles described by equations (2.67) and (2.73), $\boldsymbol{U}_{Ci}$ denotes trial functions which interpolate kinematic conditions along the boundary C_i of the ith finite element. The interpolation must be capable of recovering directly the particularized strains, sensitive inextensional solutions as well as arbitrary rigid body movements. Let us begin by writing these expressions out in detail.

Complete expressions for the rigid body movements are obtained by substituting equations (4.22) into (4.14) and (4.15), they are

$$\left.\begin{aligned} U^{(\mathrm{r.b.})}_x &= c_3 + R(c_4\cos\theta - c_5\sin\theta),\\ U^{(\mathrm{r.b.})}_\theta &= c_1\cos\theta - c_2\sin\theta + Rx(c_4\sin\theta + c_5\cos\theta) - Rc_6,\\ W^{(\mathrm{r.b.})} &= c_1\sin\theta + c_2\cos\theta - Rx(c_4\cos\theta - c_5\sin\theta),\\ R\phi^{(\mathrm{r.b.})}_\nu &= R(c_4\cos\theta - c_5\sin\theta)\cos\gamma - Rc_6\sin\gamma.\end{aligned}\right\} \tag{4.25}$$

The first few terms of the Taylor series expansions given in equations (3.55) provide the sensitive inextensional solutions. Substituting from equations (4.22), we obtain

$$\left.\begin{aligned} U^{(\mathrm{inext.})}_{\theta 0}(\theta) &= c_1'(1-\tfrac{1}{2}\theta^2) - c_2'\theta - Rc_6,\\ U^{(\mathrm{inext.})}_{\theta 1}(\theta) &= c_4'\theta + c_5',\end{aligned}\right\} \tag{4.26}$$

and these characterize inextensional approximations to the rigid body movements. The terms which belong to the constants c_2' and c_5' are the most important for they provide constant particularized values of the curvature changes $\kappa^{(\mathrm{inext.})}_{\theta\theta}$ and $\kappa^{(\mathrm{inext.})}_{x\theta}$; the terms which belong to the constants c_1' and c_4' provide interrelated linearly varying expressions in the curvature changes.† Note

† The actual expressions for these curvature changes are

$$R^2\kappa^{(\mathrm{inext.})}_{\theta\theta} = -c_1'\theta - c_2' + Rxc_4',$$

$$R^2\overline{\kappa}^{(\mathrm{inext.})}_{x\theta} = Rc_4'\theta + c_5'.$$

that $\kappa_{xx}^{(\text{inext.})} \equiv 0$. Substitution into equations (4.14) and (4.15) now provides

$$\left.\begin{aligned} U_x^{(\text{inext.})} &= c_3 + R\,\{c_4'(1-\tfrac{1}{2}\theta^2) - c_5'\theta\},\\ U_\theta^{(\text{inext.})} &= c_1'(1-\tfrac{1}{2}\theta^2) - c_2'\theta + Rx(c_4'\theta + c_5') - Rc_6,\\ W^{(\text{inext.})} &= c_1'\theta + c_2' - c_4' Rx,\\ R\phi_\nu^{(\text{inext.})} &= U_\theta^{(\text{inext.})}\sin\gamma - c_1'\sin\gamma + Rc_4'\cos\gamma, \end{aligned}\right\} \tag{4.27}$$

where c_3 arises as a constant of integration.

Now, the circular cylindrical shell with uniform wall thickness and uniform material properties provides an instance where it is practicable to directly recover, in analysis by the displacement method, the more basic distributions of purely membrane actions appropriate to both zero and specific surface forces, e.g. such as is caused by internal pressure. Accordingly, consider stress function components analogous to equations (4.25)

$$\left.\begin{aligned} \chi_{\theta 0}^{(\text{memb.})}(\theta) &= c_1''(1-\tfrac{1}{2}\theta^2) - c_2''\theta - Rc_6'',\\ \chi_{\theta 1}^{(\text{memb.})}(\theta) &= c_4''\theta + c_5'', \end{aligned}\right\} \tag{4.28}$$

and substitute into equations (4.16) and (4.17); consider also the membrane actions which correspond to uniformly distributed surface forces p_x^*, p_θ^* and to linearly varying surface forces p^* where

$$p_x^* = p_{x0}^*, \quad p_\theta^* = p_{\theta 0}^*, \quad p^* = p_0^* + xp_1^* + \theta p_2^* \tag{4.29}$$

with p_{x0}^*, $p_{\theta 0}^*$, p_0^*, p_1^* and p_2^* constants. The stress resultants are obtained from equations (4.16) to (4.19),

$$\left.\begin{aligned} R^2N_{xx}^{(\text{memb.})} &= c_1''\theta + c_2'' - c_4''Rx - R^3xp_{x0}^*,\\ R^2N_{\theta\theta}^{(\text{memb.})} &= R^3(p_0^* + xp_1^* + \theta p_2^*),\\ R^2\bar{N}_{x\theta}^{(\text{memb.})} &= R(c_4''\theta + c_5'') - R^3x(p_{\theta 0}^* + p_2^*). \end{aligned}\right\} \tag{4.30}$$

Note that neither the inextensional displacements of equations (4.27) nor the stress resultants of equations (4.30) are exact solutions of the agreed first approximation shell theory. Exact solutions require the addition of small order terms as follows

$$\left.\begin{aligned} &U_x^{(\text{inext.})} + \frac{k}{8(1-\nu)}\{12c_1'x\theta + 3(1-\nu)\,c_4'R\theta^2\},\\ &U_\theta^{(\text{inext.})} + \frac{k}{8(1-\nu)}\{2c_1'x^2 + 2(1-\nu)\,c_4'Rx\theta\},\\ &W^{(\text{inext.})} - \frac{k}{8(1-\nu)}\{12\nu c_1'\theta + 2(1-\nu)\,c_4'Rx\}, \end{aligned}\right\} \tag{4.31}$$

and

$$\left.\begin{aligned} &R^2N_{xx}^{(\text{memb.})} - \frac{k}{4}c_4''Rx,\\ &R^2N_{\theta\theta}^{(\text{memb.})} + 0,\\ &R^2\bar{N}_{x\theta}^{(\text{memb.})} + \frac{3kR^3x}{(4+9k)}\left(3p_{\theta 0}^* + \frac{3+\nu}{1+\nu}p_2^*\right),\\ &RM_{xx}^{(\text{memb.})} = \frac{k}{2(1+\nu)}\,3\nu c_1''\theta,\\ &RM_{\theta\theta}^{(\text{memb.})} = \frac{k}{2(1+\nu)}\,3c_1''\theta,\\ &RM_{x\theta}^{(\text{memb.})} = -\frac{k}{2(1+\nu)}\{2c_1''x + (1+\nu)c_4''R\theta\} - \frac{2kR^3x}{(4+9k)}\left(3p_{\theta 0}^* + \frac{3+\nu}{1+\nu}p_2^*\right), \end{aligned}\right\} \tag{4.32}$$

where the small parameter k, see equations (2.50), is defined by

$$k = h^2/12R^2. \tag{4.33}$$

The small order items listed in equations (4.31) and (4.32) play a relatively inconsequential rôle in first approximation shell theory. The stress resultants and stress couples of equations (4.30), (4.32) give rise to the following displacements, exact according to the agreed first approximation shell theory,

$$\left.\begin{aligned}
U_x^{(\mathrm{memb.})} &= \frac{1}{REh}\Big[c_1'' x\theta + c_2'' x + \frac{c_4'' R}{8}\{8(1+\nu)\theta^2 - (4+k)x^2\} \\
&\qquad + \frac{3c_5'' R}{2}(1+\nu)\theta - \frac{R^3}{2}(x^2 p_{x0}^* + 2\nu x p_0^* + \nu x^2 p_1^* + 2\nu x\theta p_2^*)\Big], \\
U_\theta^{(\mathrm{memb.})} &= \frac{1}{REh}\Big[-\frac{c_1''}{4}\{2x^2 - 3(1-\nu)\theta^2\} + \frac{c_5'' R}{2}(1+\nu)x \\
&\qquad - \frac{R^3}{2(4+9k)}\{8(1+\nu)x^2 p_{\theta 0}^* + (8+4\nu+3k)x^2 p_2^*\}\Big], \\
W^{(\mathrm{memb.})} &= \frac{1}{REh}\Big[-\frac{c_1''}{2}(3-\nu)\theta - \nu c_2'' + \frac{c_4'' R\nu}{4}(4+k)x + R^3(\nu x p_{x0}^* + p_0^* + x p_1^* + \theta p_2^*)\Big].
\end{aligned}\right\} \tag{4.34}$$

Equations (4.31), (4.32) and (4.34) are also exact in the Sanders–Koiter theory of circular cylindrical shells for which more comprehensive details are given by Morley & Merrifield (1974).

The geodesic line which defines part of the boundary C_i of the ith finite element and which passes through the origin of the surface coordinates x and θ is given by equations (3.29) as

$$x = -s\sin\gamma, \quad \theta = s\cos\gamma, \tag{4.35}$$

where the angle γ is constant and s is measured along the geodesic line, see equation (4.1). The interpolating trial functions in U_{Ci} are now determined so that direct recovery is secured of equations (4.35), (4.27), (4.31), (4.34) as well as of particularized strains appropriate to equations (3.56)–(3.59). This more than fulfills the requirements which have been laid down to ensure convergence in a piecewise representation. Thus

$$\left.\begin{aligned}
U_x &= \alpha_1 + \alpha_2 s + \alpha_3 s^2 + \alpha_{12}\sin\theta + \alpha_{13}\cos\theta, \\
U_\theta &= \alpha_4 + \alpha_5 s + \alpha_6 s^2 - \alpha_9\sin\theta + \alpha_{10}\cos\theta + x(-\alpha_{12}\cos\theta + \alpha_{13}\sin\theta), \\
W &= \alpha_7 + \alpha_8 s + \alpha_9\cos\theta + \alpha_{10}\sin\theta + x(-\alpha_{12}\sin\theta - \alpha_{13}\cos\theta), \\
R\phi_\nu &= \alpha_{11} + (\alpha_{12}\sin\theta + \alpha_{13}\cos\theta)\cos\gamma + (\alpha_5 s + \alpha_6 s^2)\sin\gamma,
\end{aligned}\right\} \tag{4.36}$$

where $\alpha_1, \alpha_2, \ldots, \alpha_{13}$ are constants. The rigid body movement of equations (4.25) is directly recovered when the substitutions

$$\left.\begin{aligned}
c_1 &= \alpha_{10}, \quad & Rc_4 &= \alpha_{13}, \\
c_2 &= \alpha_9, \quad & Rc_5 &= -\alpha_{12}, \\
c_3 &= \alpha_1, \quad & Rc_6 &= -\alpha_4,
\end{aligned}\right\} \tag{4.37}$$

are made. Moreover, with the aid of equations (2.32), (3.36), (4.1), (4.4) and (4.7), the strain ϵ_{ss} along the geodesic line is found to be

$$R\epsilon_{ss} = -(\alpha_2 + 2\alpha_3 s)\sin\gamma + (\alpha_5 + 2\alpha_6 s)\cos\gamma + (\alpha_7 + \alpha_8 s)\cos^2\gamma. \tag{4.38}$$

Note that $R\epsilon_{ss} = 0$ for four linearly independent and non-trivial combinations of the constants, i.e.

$$-\alpha_2\sin\gamma + \alpha_5\cos\gamma + \alpha_7\cos^2\gamma = 0,$$

$$-2\alpha_3\sin\gamma + 2\alpha_6\cos\gamma + \alpha_8\cos^2\gamma = 0,$$

and this admits direct recovery of four inextensional solutions.

PHILOSOPHICAL TRANSACTIONS OF THE ROYAL SOCIETY A MATHEMATICAL, PHYSICAL & ENGINEERING SCIENCES

It remains to identify the thirteen constants $\alpha_1, \alpha_2, \ldots, \alpha_{13}$ with thirteen connexion quantities as are depicted in figure 3; these connexion quantities are the values of U_x, U_θ, W, $R\phi_x$, $R\phi_\theta$ at each end and U_x, U_θ, $R\phi_v$ at the mid-point of the geodesic line. It is clear, however, that rearrangement of equations (4.36) is necessary because of the difficulty in distinguishing respectively between the values of 1, $s\cos\gamma$ and of $\cos\theta$, $\sin\theta$ (with $\theta = s\cos\gamma$) when the non-dimensional distance s is small in comparison with unity. Furthermore, the interpolation formulae of equations (4.36) break down when trying to deal with the situation which arises when the geodesic line coincides with a generator, i.e. when $\gamma = \frac{1}{2}\pi, \frac{3}{2}\pi$.

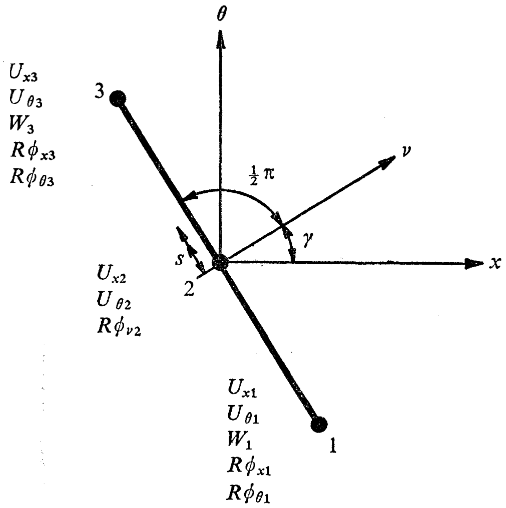

FIGURE 3. Nodal connexion quantities for displacement interpolation along a geodesic on a circular cylinder.

Rearrangement of equations (4.36) is facilitated by introducing special transcendental functions to replace the trigonometric terms. Accordingly, let

$$\left.\begin{aligned} F_j(s,\gamma) &= \frac{j!}{\cos^j\gamma}\left\{\frac{\theta^j}{j!} - \frac{\theta^{j+2}}{(j+2)!} + \frac{\theta^{j+4}}{(j+4)!} - \ldots\right\} \\ &= s^j - \frac{F_{j+2}\cos^2\gamma}{(j+2)(j+1)}, \\ G_j(s,\gamma) &= \tfrac{1}{2}j(sF_{j-1} - F_j) + F_j, \end{aligned}\right\} \tag{4.39}$$

be defined for positive integral suffices. Note that specimen functions F_4 and G_6 may be written

$$\left.\begin{aligned} F_4(s,\gamma) &= \frac{24}{\cos^4\gamma}\left(\tfrac{1}{2}\theta^2 - 1 + \cos\theta\right), \\ G_6(s,\gamma) &= \frac{360}{\cos^6\gamma}\left(\theta^2 - 4 + 4\cos\theta + \theta\sin\theta\right), \end{aligned}\right\} \tag{4.40}$$

and that the following identities are available along the geodesic,

$$\left.\begin{aligned} \cos\theta &= F_0 & \sin\theta &= F_1\cos\gamma \\ &= 1 - \tfrac{1}{2}F_2\cos^2\gamma & &= \theta - \tfrac{1}{6}F_3\cos^3\gamma, \\ &= 1 - \tfrac{1}{2}\theta^2 + \tfrac{1}{24}F_4\cos^4\gamma, \\ x\sin\theta &= -\left(F_2\cos^2\gamma - \tfrac{1}{12}G_4\cos^4\gamma\right)\tan\gamma \\ &= -\left(\theta^2 - \tfrac{1}{6}F_4\cos^4\gamma + \tfrac{1}{360}G_6\cos^6\gamma\right)\tan\gamma, \\ x\cos\theta &= -\left(\theta - \tfrac{1}{2}F_3\cos^3\gamma + \tfrac{1}{60}G_5\cos^5\gamma\right)\tan\gamma. \end{aligned}\right\} \tag{4.41}$$

The functions F and G possess the following qualities,

$$\left.\begin{aligned} F_j(s,\gamma) \to G_j(s,\gamma) \to s^j \quad &\text{as} \quad s\to 0,\\ F_j(s,\tfrac{1}{2}\pi) = G_j(s,\tfrac{1}{2}\pi) = s^j \quad &\text{for all } s,\\ F_j(s,\gamma+\pi) = F_j(s,\gamma), \quad &G_j(s,\gamma+\pi) = G_j(s,\gamma),\\ \partial F_j/\partial s = jF_{j-1}, \quad &\partial G_j/\partial s = jG_{j-1}. \end{aligned}\right\} \tag{4.42}$$

Numerical values may be calculated without difficulty for all angles γ, for example once F_6 and F_5 are evaluated from the series expression in equations (4.39) then the values of $F_0, F_1, \ldots, F_4$ and of $G_1, G_2, \ldots, G_6$ follow directly and accurately from the reduction formulae.

The equations (4.36) may now be rearranged into a more satisfactory form to interpolate the kinematic conditions U_{Ci}. Thus

$$\left.\begin{aligned} U_x &= A_1+A_2s+A_3s^2-\Phi(s,\gamma)\cos^2\gamma,\\ U_\theta &= B_1+B_2s+B_3s^2-\Phi(s,\gamma)\sin\gamma\cos\gamma-\Psi(s,\gamma)\cos\gamma+\Gamma(s,\gamma)\sin\gamma\cos^3\gamma,\\ W &= C_1+C_2s+C_3F_2(s,\gamma)+C_4F_3(s,\gamma)-\Gamma'(s,\gamma)\sin\gamma\cos^2\gamma,\\ R\phi_\nu &= D_1+D_2s+D_3s^2-\Phi(s,\gamma)\cos^3\gamma, \end{aligned}\right\} \tag{4.43}$$

where

$$\left.\begin{aligned} \Phi(s,\gamma) &= \tfrac{1}{6}\Delta_1F_3+\tfrac{1}{12}\Delta_2F_4,\\ \Gamma(s,\gamma) &= \tfrac{1}{60}\Delta_1G_5+\tfrac{1}{180}\Delta_2G_6,\\ \Psi(s,\gamma) &= \tfrac{1}{3}C_3F_3+\tfrac{1}{4}C_4F_4,\\ \Gamma'(s,\gamma) &= \frac{\partial\Gamma}{\partial s},\\ \Delta_1 &= D_2\cos\gamma-B_2\sin\gamma\cos\gamma+2C_3\sin\gamma,\\ \Delta_2 &= D_3\cos\gamma-B_3\sin\gamma\cos\gamma+3C_4\sin\gamma. \end{aligned}\right\} \tag{4.44}$$

The $A_1, A_2, \ldots$ are new constants which are related to $\alpha_1, \alpha_2, \ldots, \alpha_{13}$ by

$$\left.\begin{aligned} A_1 &= \alpha_1+\alpha_{13}, & B_1 &= \alpha_4+\alpha_{10},\\ A_2 &= \alpha_2+\alpha_{12}\cos\gamma, & B_2 &= \alpha_5-\alpha_9\cos\gamma+\alpha_{12}\sin\gamma,\\ A_3 &= \alpha_3-\tfrac{1}{2}\alpha_{13}\cos^2\gamma, & B_3 &= \alpha_6-\tfrac{1}{2}\alpha_{10}\cos^2\gamma-\alpha_{13}\sin\gamma\cos\gamma,\\ C_1 &= \alpha_7+\alpha_9, & D_1 &= \alpha_{11}+\alpha_{13}\cos\gamma,\\ C_2 &= \alpha_8+\alpha_{10}\cos\gamma+\alpha_{13}\sin\gamma, & D_2 &= \alpha_5\sin\gamma+\alpha_{12}\cos^2\gamma,\\ C_3 &= -\tfrac{1}{2}\alpha_9\cos^2\gamma+\alpha_{12}\sin\gamma\cos\gamma, & D_3 &= \alpha_6\sin\gamma-\tfrac{1}{2}\alpha_{13}\cos^3\gamma,\\ C_4 &= -\tfrac{1}{6}\alpha_{10}\cos^3\gamma-\tfrac{1}{2}\alpha_{13}\sin\gamma\cos^2\gamma, & &\\ \Delta_1 &= \alpha_{12}\cos\gamma, & &\\ \Delta_2 &= -\tfrac{1}{2}\alpha_{13}\cos^2\gamma. & & \end{aligned}\right\} \tag{4.45}$$

In contrast with equations (4.36), the rearranged equations (4.43) are free from all numerical hazards; in the special case where $\gamma = \frac{3}{2}\pi$ (say, so that $s = x$) they simplify to

$$\left.\begin{aligned} U_x &= A_1+A_2x+A_3x^2,\\ U_\theta &= B_1+B_2x+B_3x^2,\\ W &= C_1+C_2x+C_3x^2+C_4x^3,\\ R\phi_\nu = -(U_\theta-\partial W/\partial\theta) &= D_1+D_2x+D_3x^2, \end{aligned}\right\} \tag{4.46}$$

which coincide with a form of displacement interpolation which is frequently encountered in the finite element analysis of flat plates. When $\gamma = 0$ (say, so that $s = \theta$) we can produce a similar form of representation by combining equations (4.43) in the following way

$$\left.\begin{aligned} U_x - R\phi_\nu &= U_x + \partial W/\partial x = (A_1 - D_1) + (A_2 - D_2)\,\theta + (A_3 - D_3)\,\theta^2, \\ U_\theta - \partial W/\partial s &= U_\theta - \partial W/\partial\theta = (B_1 - C_2) + (B_2 - 2C_3)\,\theta + (B_3 - 3C_4)\,\theta^2, \\ W &= C_1 + C_2\theta + C_3 F_2(\theta, 0) + C_4 F_3(\theta, 0), \\ R\phi_\nu &= -\partial W/\partial x = D_1 + D_2 F_1(\theta, 0) + D_3 F_2(\theta, 0). \end{aligned}\right\} \tag{4.47}$$

An examination of equations (4.46) and (4.47) reveals that this U_{Ci} can be used in the guise of Hermitian interpolation to develop a lines of curvature compatible rectangular finite element; it is then possible to proceed by straightforward application of the principle of minimum total potential energy Π, see equation (2.62). Details of this finite element are first presented before going on to develop a more generally useful element which is triangular in shape.

4.2. *A lines of curvature compatible rectangular finite element*

In an application of the principle of minimum total potential energy it is necessary for the displacement trial functions in U_i to satisfy inter-element kinematic subsidiary conditions

$$U_{Ci+} - U_{Ci-} = 0, \tag{4.48}$$

see equations (2.63). In the case of the circular cylindrical shell, the column matrices U_i and U_{Ci} are related to each other through equations (4.23) and (4.24); the subscripts + and − refer to the two sides of the boundary C_i of the ith finite element. Inter-element continuity can be achieved

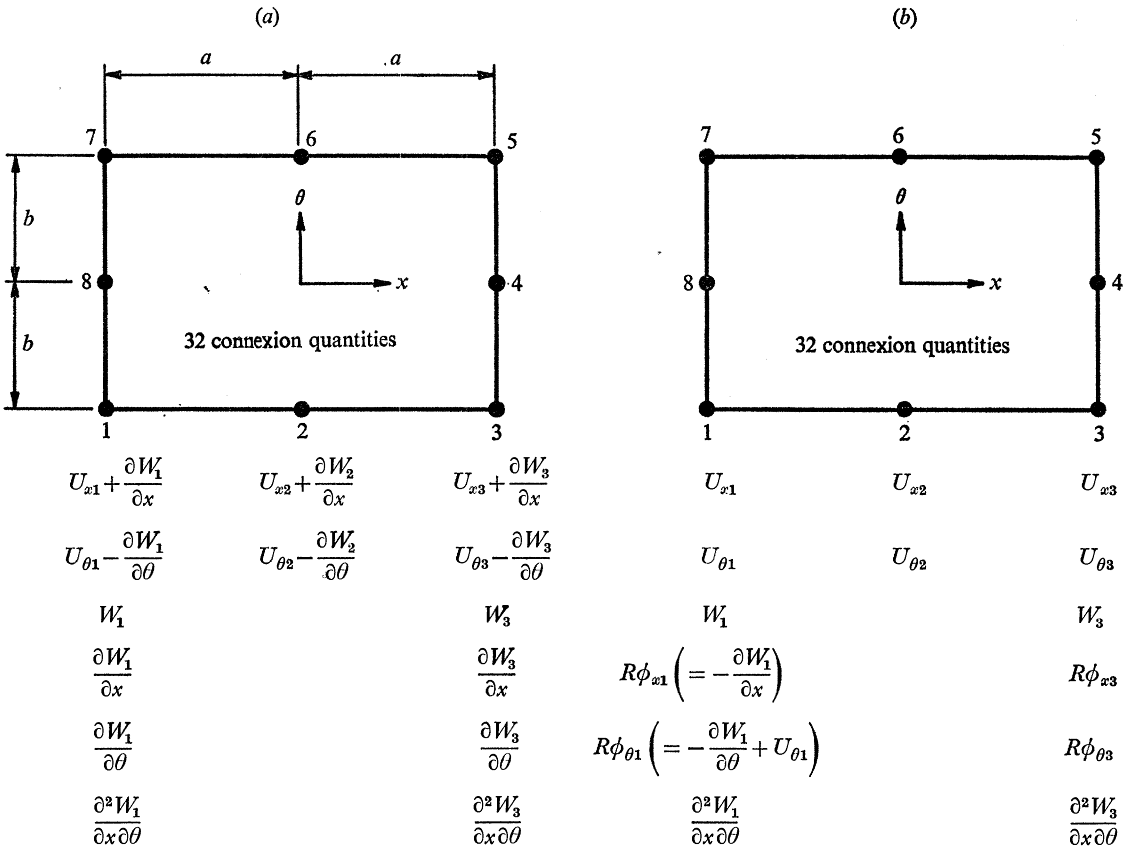

FIGURE 4. Nodal connexion quantities for lines of curvature rectangular finite element on a circular cylinder.

for a lines of curvature rectangular finite element by taking equations (4.46) and (4.47) in association with nodal connexion quantities $U_x + \partial W/\partial x$, $U_\theta - \partial W/\partial \theta$, W, $\partial W/\partial x$, $\partial W/\partial \theta$, $\partial^2 W/\partial x \partial \theta$ at the corner points and $U_x + \partial W/\partial x$, $U_\theta - \partial W/\partial \theta$ at the mid-sides of the rectangle (see figure 4*a*). Thus, compatible trial functions in $\boldsymbol{U}_i = (U_x\, U_\theta\, W)^{\mathrm{T}}$ are calculated from

$$\left.\begin{aligned} U_x + \partial W/\partial x &= A_1 + A_2\theta + A_3\theta^2 + x(A_{1x} + A_{2x}\theta + A_{3x}\theta^2) \\ &\quad + x^2(A_{1xx} + A_{2xx}\theta) + A_{3xx}(a^2 - x^2)\,(b^2 - \theta^2), \\ U_\theta - \partial W/\partial\theta &= B_1 + B_2\theta + B_3\theta^2 + x(B_{1x} + B_{2x}\theta + B_{3x}\theta^2) \\ &\quad + x^2(B_{1xx} + B_{2xx}\theta) + B_{3xx}(a^2 - x^2)\,(b^2 - \theta^2), \\ W &= C_1 + C_2\theta + C_3F_2 + C_4F_3 \\ &\quad + x(C_{1x} + C_{2x}\theta + C_{3x}F_2 + C_{4x}F_3) \\ &\quad + x^2(C_{1xx} + C_{2xx}\theta + C_{3xx}F_2 + C_{4xx}F_3) \\ &\quad + x^3(C_{1xxx} + C_{2xxx}\theta + C_{3xxx}F_2 + C_{4xxx}F_3). \end{aligned}\right\} \tag{4.49}$$

The $A_1, A_2, \dots B_1, \dots C_1, \dots$ are thirty-four (new) constants which have to be expressed in terms of the connexion quantities. Explicit expressions are readily obtainable for all but $C_1, C_2, \dots$ and, if desired, use can be made of Ahlin's (1964) bivariate generalization of the Hermite interpolation formulae in the manner of Bogner *et al.* (1966). The sides of the rectangular finite element are located at $x = \pm a$, $\theta = \pm b$ and so the terms which involve the constants A_{3xx} and B_{3xx} are independent of the requirements for inter-element displacement continuity. It is a little more troublesome to express the constants $C_1, C_2, \dots$ in explicit terms of their connexion quantities; the symbols F_2 and F_3 are written here in abbreviation respectively for $F_2(\theta, 0)$ and $F_3(\theta, 0)$, see equations (4.39) *et seq.*

A 32×32 element stiffness matrix k_i may now be derived by substituting into the strain energy integral $\frac{1}{2}\iint \overline{\boldsymbol{N}}_i^{\mathrm{T}}\bar{\boldsymbol{\varepsilon}}_i\,\mathrm{d}A_i$ of equation (2.54); with the aid of the constitutive relations (2.48) we find that

$$\begin{aligned} \iint \overline{\boldsymbol{N}}_i^{\mathrm{T}}\bar{\boldsymbol{\varepsilon}}_i\,\mathrm{d}A_i = \iint_{A_i} \frac{D}{k} \begin{Bmatrix} \epsilon_{xx} \\ \epsilon_{\theta\theta} \\ \epsilon_{x\theta} \end{Bmatrix}^{\mathrm{T}} \begin{bmatrix} 1 & \nu & 0 \\ \nu & 1 & 0 \\ 0 & 0 & 2(1-\nu) \end{bmatrix} \begin{Bmatrix} \epsilon_{xx} \\ \epsilon_{\theta\theta} \\ \epsilon_{x\theta} \end{Bmatrix} \mathrm{d}x\,\mathrm{d}\theta \\ + \iint_{A_i} R^2 D \begin{Bmatrix} \kappa_{xx} \\ \kappa_{\theta\theta} \\ \bar{\kappa}_{x\theta} \end{Bmatrix}^{\mathrm{T}} \begin{bmatrix} 1 & \nu & 0 \\ \nu & 1 & 0 \\ 0 & 0 & 2(1-\nu) \end{bmatrix} \begin{Bmatrix} \kappa_{xx} \\ \kappa_{\theta\theta} \\ \bar{\kappa}_{x\theta} \end{Bmatrix} \mathrm{d}x\,\mathrm{d}\theta, \end{aligned} \tag{4.50}$$

where the small non-dimensional parameter k is defined by equation (4.33) and the flexural rigidity D is defined by equation (2.49). In carrying out the integrations it is useful to note that

$$\left.\begin{aligned} F_0^2(\theta, 0) &= \tfrac{1}{2}F_0(2\theta, 0) + \tfrac{1}{2}, \\ F_1^2(\theta, 0) &= \tfrac{1}{4}F_2(2\theta, 0), \\ F_2^2(\theta, 0) &= \frac{2}{4!}F_4(2\theta, 0) - \frac{8}{4!}F_4(\theta, 0), \\ F_3^2(\theta, 0) &= \frac{18}{6!}F_6(2\theta, 0) + \frac{72}{6!}F_6(\theta, 0) - \frac{72}{5!}\theta F_5(\theta, 0), \\ F_4^2(\theta, 0) &= \frac{288}{8!}F_8(2\theta, 0) - \frac{2304}{8!}F_8(\theta, 0) \\ &\quad + \frac{1152}{7!}\theta F_7(\theta, 0) - \frac{576}{6!}\theta^2 F_6(\theta, 0), \end{aligned}\right\} \tag{4.51}$$

in addition to the relations already given in equations (4.39)–(4.47).

PHILOSOPHICAL TRANSACTIONS OF THE ROYAL SOCIETY A MATHEMATICAL, PHYSICAL & ENGINEERING SCIENCES

The principle of minimum total potential energy (see equation (2.62)) requires that

$$\sum_i \left\{ \iint \overline{N}_i^{\mathrm{T}}\, \delta\bar{\varepsilon}_i \,\mathrm{d}A_i - \iint p^{*\mathrm{T}}\, \delta U_i \,\mathrm{d}A_i - \int_{N_C^*} N_C^{*\mathrm{T}}\, \delta U_{Ci} \,\mathrm{d}C_i \right\} = 0 \tag{4.52}$$

where the 32×1 matrix of the external work done on the finite element by the prescribed surface loads p^* and boundary tractions N_C^* follows in a straightforward manner on substitutions from equations (4.49) into the integrals of equations (2.55) and (2.56).

Care needs to be exercised at all stages in the numerical work. Large differences occur in the orders of magnitude between the contributions to k_i from the strains/stress resultants and the curvature changes/stress couples, see equations (3.1). The measure of these differences is provided by the small parameter k, typical values of which are listed in table 1. The consequences are that a value $k \approx 10^{-p}$ means at least p significant digits are at risk during the solution of the stiffness equations. *This contribution to the ill-conditioning of the stiffness equations is quite unavoidable in any solution process of a shell problem which considers simultaneously, and in a satisfactory manner, the effects of both bending and stretching actions.*

Table 1. Typical values of the non-dimensional parameter k

R/h	50	100	300	1000
$k = h^2/12R^2$	0.33×10^{-4}	0.83×10^{-5}	0.93×10^{-6}	0.83×10^{-7}

Table 2. Typical values of the M-condition number for a $n \times n$ stiffness matrix of the lines of curvature rectangular finite element for circular cylindrical shells

n	R/h	k	M-condition number	average M-condition number
26	52.7	0.30×10^{-4}	0.3×10^{8}	0.2×10^{2}
72*	52.7	0.30×10^{-4}	0.1×10^{9}	0.4×10^{2}
26	320.0	0.81×10^{-6}	0.4×10^{9}	0.2×10^{2}
72*	320.0	0.81×10^{-6}	0.1×10^{10}	0.4×10^{2}

All these finite elements are of size $2a = 0.52$, $2b = \frac{1}{4}\pi$. The asterisk refers to a 2×2 assembly of these elements. The value of n refers to the reduced size of the stiffness matrix with rigid body freedoms constrained.

Many different criteria are available which indicate the measure of conditioning in a system of simultaneous equations. Fried (1971) and Strang & Fix (1973), for example, favour a condition number which depends upon the ratio of the largest and smallest eigenvalues. In the present paper, we adopt a criterion which, although cruder, is simpler to calculate and is due to Turing (1948). The quantity $nM(k_i)\, M(k_i^{-1})$, called the M-condition number of the $n \times n$ matrix k_i, is taken as the measure with

$$M(A) = \max_{rs} |a_{rs}|.$$

An average value of this M-condition number for a matrix with coefficients chosen at random from a normal population is about $n^{\frac{1}{2}} \ln n$. The values listed in table 2 are those encountered in our numerical work, they are calculated by first condensing the stiffness matrix so as to eliminate the rigid body freedoms. An M-condition number $\approx 10^q$ means that a total of q significant digits may be lost during the solution of the stiffness equations and table 2 shows that a value $q = 10$ can be attained even in a modestly small calculation involving very few finite elements. The indications are that four significant digits are lost additionally to those attributable to smallness of the parameter k, this loss of significant digits is more severe than normally encountered in the solution of ordinary plate bending or plane stress problems and is naturally a matter of serious concern in a major calculation. It is advisable, particularly when solving the stiffness equations, to use double precision arithmetic to avoid further degradation from rounding errors.

An example problem which is often used to test shell finite elements concerns a circular cylinder which is pinched by two concentrated radial loads each of intensity P as shown in figure 5. The radius of the middle surface is $R = 4.953$ units, the uniform wall thickness is $h = 0.094$ units (for

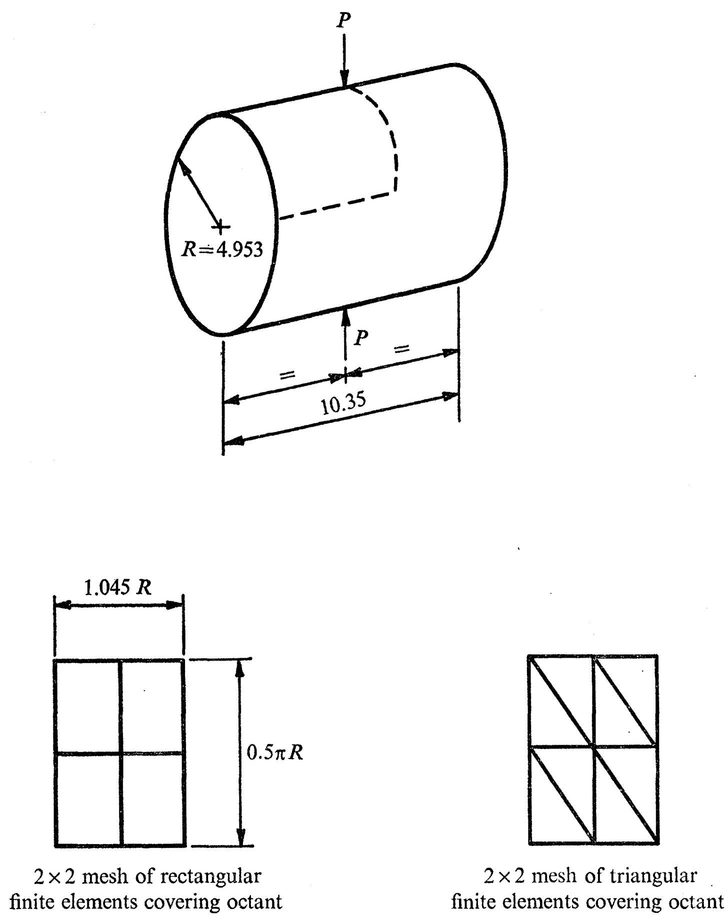

FIGURE 5. Pinched circular cylindrical shell showing the finite element mesh patterns.

the thick cylinder) and 0.01548 units (for the thin cylinder), the material properties are uniform with Young modulus $E = 10.5 \times 10^6$ in units which are the same as for P, R, h and Poisson ratio $\nu = 0.3125$. The approximate values of R/h are 52.7 and 320.0 and the parameter k has approximate values 0.300×10^{-4} and 0.814×10^{-6} respectively for the thick and thin walled cylinders. The overall length of the cylinders is 10.35 units. Attention is drawn to the fact that the above finite element has not been developed to deal either with the simple edge effect which occurs at the free edges or the singular behaviour at the points of application of the concentrated loads. Note also that the bending stresses are predominant over the remainder of the shell; this example problem therefore presents an exceptional situation which is far removed from an ideal practical design.

PHILOSOPHICAL TRANSACTIONS OF THE ROYAL SOCIETY A MATHEMATICAL, PHYSICAL & ENGINEERING SCIENCES

Because of the symmetry, it is possible to confine attention to only one octant of the cylinder. Numerical results are listed in table 3 for the radial deflexion underneath each load, also listed are comparative results from Ashwell & Sabir (1972), Cantin (1970) and Cantin & Clough (1968) all of whom make use of lines of curvature rectangular finite elements. The comparative results are, however, obtained from finite element methods where the requirements of inter-element continuity, see equations (2.63), are only partially satisfied. This is in contrast with the present formulation which, because it provides a correct application of the principle of minimum total potential energy, calculates the deflexion as a lower bound. This deflexion, calculated according to inextensional shell theory, is

$$\frac{W^{(\text{inext.})}}{P} = -\frac{R^2}{2LD}\left(\frac{\pi}{4}-\frac{2}{\pi}\right), \tag{4.53}$$

where L is the overall length of the cylinder; values from this expression are also quoted in table 3 for the purpose of comparison.

Table 3. Radial deflexion W underneath each of the concentrated loads in the pinched circular cylindrical shell for the lines of curvature compatible rectangular finite element

(*a*) Results for thick walled cylinder $R/h \simeq 52.7$

mesh size (see figure 5)	$10^2 W/P$ Ashwell & Sabir (1972)	Cantin (1970)	present
1 by 1	−0.1040	—	−0.1040
2 by 2	−0.1103	−0.0931	−0.1092
4 by 4	−0.1129	−0.1126	−0.1111
6 by 6	−0.1135	−0.1137	−0.1121

Inextensional shell theory gives $10^2 W^{(\text{inext.})}/P = -0.1084$.

(*b*) Results for thin walled cylinder $R/h \simeq 320.0$

mesh size (see figure 5)	W/P Ashwell & Sabir (1972)	Cantin & Clough (1968)†	present
1 by 1	−0.2301	−0.0001	−0.2327
1 by 8	−0.2406	−0.0070	−0.2434
2 by 8	−0.2414	−0.0070	−0.2436
3 by 8	−0.2418	−0.0070	−0.2439

Inextensional shell theory gives $W^{(\text{inext.})}/P = -0.2428$.

† These values were calculated by Ashwell & Sabir (1972) by using the finite element as developed by Cantin & Clough (1968).

The magnitude of the stress couple M_θ at a point underneath either the concentrated loads is infinitely large according to first approximation shell theory. Finite element results are spurious in the vicinity of such points. Another peak value of this stress couple occurs mid-way between the concentrated loads and this is of finite magnitude. Numerical results are listed in table 4 along with the value

$$\frac{M_\theta^{(\text{inext.})}}{P} = \frac{R}{2L}\left(1-\frac{2}{\pi}\right) \tag{4.54}$$

calculated according to inextensional theory. The finite element results confirm that the stress resultants contribute negligibly, in the sense of equations (2.50), to the significant stresses; there is thus no practical interest in recording these values.

Details of a computer program together with further numerical examples are given by Merrifield (1976).

Table 4. Stress couple M_θ mid-way between concentrated loads in the pinched circular cylindrical shell for the lines of curvature compatible rectangular finite element

mesh size (see figure 5)	M_θ/P thick walled cylinder $R/h = 52.7$	M_θ/P thin walled cylinder $R/h = 320.0$
1 by 1	0.1248	0.1249
2 by 2	0.1001	0.0986
4 by 4	0.0919	0.0906
6 by 6	0.0901	0.0889
3 by 8	—	0.0876

Inextensional shell theory gives $M_\theta^{(\text{inext.})}/P = 0.0870$.

4.3. *Discussion on an assumed stress hybrid triangular finite element*

Useful application of rectangular finite elements is limited to special problems where the boundary contours of the shell coincide with the lines of curvature. A more practically useful finite element is triangularly shaped where each side coincides with a geodesic line; the triangular shape can approximate quite closely almost any boundary contour and can be easily varied in size in any region which is of particular interest. The development of such an element for shells is by no means a straightforward task, especially as it is now clear that there are serious difficulties in securing suitable displacement trial functions in U_i, over the element, which satisfy the inter-element kinematic continuities of equations (2.63) and (4.48). In comparison, the difficulties which occur in deriving a triangular finite element for ordinary plate bending problems become almost trivial.

As described in §2, however, many finite element methods have been formulated with underlying variational principles which relax continuity requirements along the element boundaries. A particularly effective application of one of these principles is made by Allman (1970), in an analysis of the ordinary plate bending problem, by using an assumed stress hybrid finite element model first introduced by Pian (1964) in a plane stress context. The functional associated with this model is a limiting case of that given in equation (2.64) where it requires $U_{\alpha i}$, $p^* = 0$. In Allman's application the trial functions in U_{Ci}, which interpolate the kinematic conditions along the boundary C_i, provide a cubically varying interpolation of the displacement W and a linearly varying interpolation of the slope $\partial W/\partial \nu$; the trial functions in $\overline{N}_{\beta i}$ over the element are taken as a complete set of linearly varying distributions of stress couples which automatically satisfy the equations of homogeneous equilibrium.

The success of Allman's finite element provides a compelling incentive to investigate a similar assumed stress hybrid model for the circular cylindrical shell. The interpolation formulae given in equations (4.36) and (4.43) are relevant for use as trial functions in U_{Ci}, but note that it is necessary to interpolate simultaneously the pseudo-quadratic in surface displacements U_x and U_θ which require mid-side connexions as shown in figures 3 and 6. Moreover, the pseudo-quadratic slope $R\phi_\nu$ also requires a mid-side connexion and this is in contrast with Allman's linearly varying $\partial W/\partial \nu$. The requirement for mid-side connexions turns out to be unfortunate because, as is later shown and explained both by Allman (1976) and by Bartholomew (1976), their introduction into Allman's finite element with the linearly varying trial functions in $\overline{N}_{\beta i}$ leads to a rank deficient stiffness matrix. It is too complicated to apply Allman's and Bartholomew's arguments to shell finite elements and so it was decided to conduct numerical experiments with trial functions in U_{Ci} as given by equations (4.36), (4.43) but using several different choices for the trial functions in $\overline{N}_{\beta i}$. (Rank deficiency with a slightly different aspect is

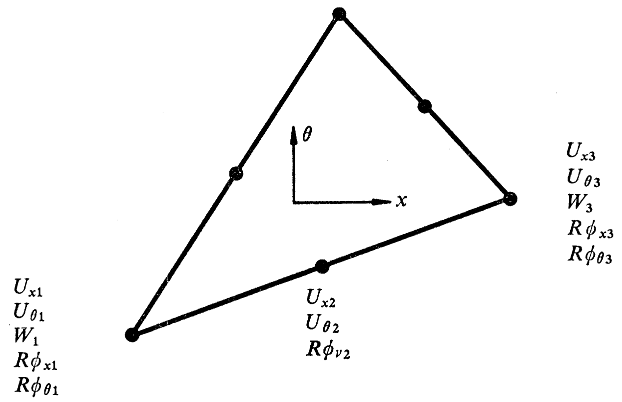

(*a*) 24 connexion quantities used for element development

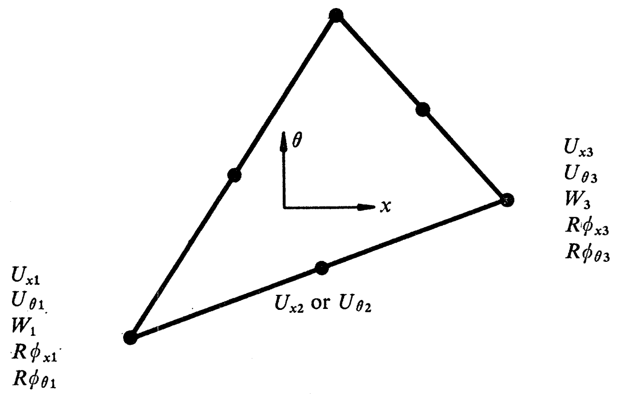

(*b*) 18 connexion quantities in final version

Figure 6. Nodal connexion quantities for triangular finite element in a circular cylinder.

experienced by Pian & Mau (1972) in an assumed stress hybrid model for planar continua using a quadrilateral finite element which has only corner nodes; they follow Fraeijs de Veubeke (1965) in referring to the phenomenon as 'kinematic deformation modes'. Pian & Mau, incidentally, accept the rank deficiency in their element stiffness matrix but ensure an adequate arrangement of finite elements, in combination with kinematic constraints on the structure boundary, to provide a rank sufficient global stiffness matrix.)

PHILOSOPHICAL TRANSACTIONS OF THE ROYAL SOCIETY A MATHEMATICAL, PHYSICAL & ENGINEERING SCIENCES

Now, the choice of the finite and usually rather small number of trial functions in $\overline{N}_{\beta i}$ is by no means arbitrary if convergence to the correct solution is to be secured in the limit of the finite element representation. It is required that some of the strain and curvature changes in the associated $\bar{\varepsilon}_{\beta i}$ be integrable and that they directly recover at least the sensitive inextensional solutions and two of the particularized strains† as are already recoverable by the trial function in U_{Ci} for the kinematic conditions at the element boundary. (Note that Allman's (1970) application of the assumed stress hybrid model recovers neither states of constant curvature change nor

TABLE 5. RANK OF 24 × 24 STIFFNESS MATRIX k_i FOR ASSUMED STRESS HYBRID TRIANGULAR FINITE ELEMENT USING TRIAL FUNCTIONS $\overline{N}_{\beta i}$ CALCULATED FROM COMPLETE POLYNOMIALS OF VARIOUS DEGREE FOR THE STRESS FUNCTIONS χ_x, χ_θ AND ψ IN CIRCULAR CYLINDRICAL SHELLS

degree of complete polynomial in χ, θ			rank of element stiffness matrix	number of stress fields
χ_x	χ_θ	ψ		
2	—	—	4	5
3	—	—	5	9
4	—	—	5	14
5	—	—	5	20
—	2	—	4	5
—	3	—	5	9
—	4	—	5	14
—	5	—	5	20
—	—	2	6	6
—	—	3	10	10
—	—	4	12	15
2	2	—	8	10
3	3	—	10	18
2	2	1	11	13
2	2	3	14	20
2	2	4	16	25
3	3	2	14	24
3	3	3	16	28
3	3	4	18	33

Note: a rank of 18 is required for a 24 × 24 stiffness matrix.

the correct stress couples when the thickness and/or material properties of the finite element are allowed to vary.) These requirements are satisfied for circular cylindrical shells with uniform wall thickness and uniform material properties when the trial functions in $\overline{N}_{\beta i}$ are calculated from complete polynomials of at least second degree in the surface coordinates x, θ for the stress functions χ_x and χ_θ and of at least first degree for the stress function ψ (see equations (4.13)).

In the present consideration of the assumed stress hybrid model, the triangularly shaped finite element has the 24 connexion quantities as shown in figure 6*a*. A rank of 18 is thus required for the 24 × 24 element stiffness matrix, namely, 24 displacement connexion quantities less the 6 rigid body freedoms. Values of this rank from experiments on various trial functions in $\overline{N}_{\beta i}$, calculated from complete polynomials in x, θ for the stress functions χ_x, χ_θ and ψ, are listed in table 5. Under

† Note that the stress resultants and stress couples in $\overline{N}_{\beta i}$ must satisfy the partial differential equations of homogeneous equilibrium, see equations (2.43) and (2.66). Under these conditions it is possible to secure only two particularized responses in the stress resultants N_{11}, N_{22}, $\overline{N}_{12}$ because of the essential relation $N_{11}/R_1 + N_{22}/R_2 = 0$ (i.e. $N_{22} = 0$ for cylinders). These remarks are the static-geometric equivalents of those given in the Introduction concerning the basic state (II) of static response.

these circumstances, it is seen that to achieve the desired rank of 18 requires at least 33 stress fields as are derived from the stress functions

$$\left.\begin{aligned}\chi_x &= \beta_1 x+\beta_2\theta+\beta_3 x^2+\beta_4 x\theta+\beta_5\theta^2+\beta_6 x^3+\beta_7 x^2\theta+\beta_8 x\theta^2+\beta_9\theta^3,\\ \chi_\theta &= \beta_{10} x+\beta_{11}\theta+\beta_{12} x^2+\beta_{13} x\theta+\beta_{14}\theta^2+\beta_{15} x^3+\beta_{16} x^2\theta+\beta_{17} x\theta^2+\beta_{18}\theta^3,\\ \psi &= \beta_{19}+\beta_{20} x+\beta_{21}\theta+\beta_{22} x^2+\beta_{23} x\theta+\beta_{24}\theta^2+\beta_{25} x^3+\beta_{26} x^2\theta+\beta_{27} x\theta^2\\ &\quad +\beta_{28}\theta^3+\beta_{29} x^4+\beta_{30} x^3\theta+\beta_{31} x^2\theta^2+\beta_{32} x\theta^3+\beta_{33}\theta^4,\end{aligned}\right\} \tag{4.55}$$

where $\beta_1, \beta_2, \ldots$ are constants. Note that χ_x, χ_θ = constant both give zero stress fields, note also that these conclusions on rank are independent of the uniformity of material properties, thickness and geometric configuration of the triangular element.

This is too large a number of stress fields to be handled with ease in practical situations. From experience with Allman's plate bending finite element it is recognized that it is the presence of the mid-side connexion quantities which is responsible for the difficulty in achieving requisite rank. Unlike the ordinary plate bending problem, however, the mid-side connexion quantities cannot be so readily eliminated in shell finite elements because of the nature of the transcendental functions which describe the rigid body movement. Moreover, elimination of just the connexion quantity $R\phi_\nu$, see figure 6, does not secure worthwhile improvement; a conjecture, based upon the results given in table 5, is that as many as 25 stress fields would still be required to achieve rank 15 for the 21×21 stiffness matrix. These 25 stress fields are derived from stress functions

$$\left.\begin{aligned}\chi_x &= \beta_1 x+\beta_2\theta+\beta_3 x^2+\beta_4 x\theta+\beta_5\theta^2,\\ \chi_\theta &= \beta_6 x+\beta_7\theta+\beta_8 x^2+\beta_9 x\theta+\beta_{10}\theta^2,\\ \psi &= \beta_{11}+\beta_{12} x+\beta_{13}\theta+\beta_{14} x^2+\beta_{15} x\theta+\beta_{16}\theta^2+\beta_{17} x^3+\beta_{18} x^2\theta+\beta_{19} x\theta^2\\ &\quad +\beta_{20}\theta^3+\beta_{21} x^4+\beta_{22} x^3\theta+\beta_{23} x^2\theta^2+\beta_{24} x\theta^3+\beta_{25}\theta^4.\end{aligned}\right\} \tag{4.56}$$

Furthermore, element flexibility matrices, as calculated from stress functions like those given in equations (4.55) and (4.56), exhibit an even more marked propensity towards ill-conditioning than was encountered in the stiffness matrix k_i of the rectangular element (see equation (4.50) and compare the condition numbers listed in tables 2 and 6).

The conclusion is that the assumed stress hybrid finite element model does not provide a practical means of solving the present shell problem. Hence the motivation to evolve a more versatile variational principle, see equations (2.67) and (2.73), where the trial functions in $\overline{N}_{\beta i}$ for stress resultants and stress couples may be supplemented with trial functions in $U_{\alpha i}$ for displacements. Amongst other advantages, requisite rank in the element stiffness matrix k_i is then achievable through the simplest possible trial functions. In the present problem of the circular cylindrical shell with walls which have uniform thickness and uniform material properties, the new variational principle permits the development of an efficient triangularly shaped finite element where the stress resultants and stress couples are only linearly varying in the surface coordinates. However, let us first investigate the elimination of mid-side connexion quantities.

4.4. *Elimination of mid-side connexion quantities*

The rank deficiency which is encountered in the derived stiffness matrix from the assumed stress hybrid model is associated with the presence of mid-side connexion quantities in U_{Ci} (see figures 3 and 6). Let us now examine whether it is feasible to modify the interpolation formulae of equations (4.36) and (4.43) so as to eliminate these quantities. The elimination is to be arranged so as not to disturb the capability to recover the particularized strains, sensitive inextensional solutions and arbitrary rigid body movements.

The following difference relations may be derived from the interpolation formulae of equations (4.36),

$$\left.\begin{aligned} \tfrac{1}{2}U_{x1} - U_{x2} + \tfrac{1}{2}U_{x3} &= \alpha_3 s_3^2 - \alpha_{13}(1-\cos\theta_3),\\ \tfrac{1}{2}U_{\theta 1} - U_{\theta 2} + \tfrac{1}{2}U_{\theta 3} &= \alpha_6 s_3^2 - \alpha_{10}(1-\cos\theta_3) + \alpha_{13}x_3\sin\theta_3,\\ -\tfrac{1}{2}(W_1 - W_3) &= \alpha_8 s_3 + \alpha_{10}\sin\theta_3 - \alpha_{13}x_3\cos\theta_3,\\ \frac{1}{2}\left(\frac{\partial W_1}{\partial s} + \frac{\partial W_3}{\partial s}\right) &= \alpha_8 + \alpha_{10}\cos\theta_3\cos\gamma\\ &\qquad + \alpha_{13}(\cos\theta_3\sin\gamma + x_3\sin\theta_3\cos\gamma),\\ \tfrac{1}{2}R\phi_{\nu 1} - R\phi_{\nu 2} + \tfrac{1}{2}R\phi_{\nu 3} &= -\alpha_{13}(1-\cos\theta_3)\cos\gamma + \alpha_6 s_3^2\sin\gamma, \end{aligned}\right\} \tag{4.57}$$

where, see figure 3, $U_{x1}, \ldots, \partial W_1/\partial s, \ldots$ refer to the values of $U_x, \ldots \partial W/\partial s, \ldots$ at node 1, s_3 refers to the value of the surface coordinate s at node 3 and

$$x_3 = -s_3\sin\gamma, \quad \theta_3 = s_3\cos\gamma. \tag{4.58}$$

Note also that from equations (2.17) and (2.27)

$$\partial W/\partial s = R\phi_x\sin\gamma - R\phi_\theta\cos\gamma + U_\theta\cos\gamma, \tag{4.59}$$

while from equations (2.34)

$$R\phi_\nu = R\phi_x\cos\gamma + R\phi_\theta\sin\gamma. \tag{4.60}$$

The simultaneous equations (4.57) permit the five constants α_3, α_6, α_8, α_{10} and α_{13} to be expressed in terms of five combinations of quantities which are simply related to the actual connexion quantities. However, the constants α_{10} and α_{13} relate directly to the displacement as a rigid body and cannot therefore be selected as candidates for elimination. The constant α_8 is also unsuitable because its elimination relates only to connexion quantities at end points, i.e. at nodes 1 and 3. Now, equations (4.57) may be solved to give

$$\tfrac{1}{2}R\phi_{\nu 1} - R\phi_{\nu 2} + \tfrac{1}{2}R\phi_{\nu 3} - (\tfrac{1}{2}U_{x1} - U_{x2} + \tfrac{1}{2}U_{x3})\cos\gamma = s_3^2(\alpha_6\sin\gamma - \alpha_3\cos\gamma) \tag{4.61}$$

so that if we put

$$\alpha_6\sin\gamma - \alpha_3\cos\gamma = 0 \tag{4.62}$$

then the mid-side connexion quantity $R\phi_{\nu 2}$ may be eliminated by expressing it in terms of the remaining quantities in equation (4.61). The equations (4.45) show that the relation

$$D_3 - A_3\cos\gamma = 0 \tag{4.63}$$

is equivalent to equation (4.62).

A further mid-side connexion quantity may be eliminated if, instead of equation (4.62), we put

$$\alpha_3 = \alpha_6 = 0; \tag{4.64}$$

reference to the equations (4.36) shows that this substitution still does not disturb the direct recovery of the three particularized strains of equations (3.58), the two most sensitive inextensional solutions of equations (4.27) (i.e. the terms which involve the constants c_2' and c_5') or the rigid body movements of equations (4.25). Thus, after substituting from equation (4.64), the equations (4.57) may be solved to give

$$\tfrac{1}{2}R\phi_{\nu 1}-R\phi_{\nu 2}+\tfrac{1}{2}R\phi_{\nu 3}-(\tfrac{1}{2}U_{x1}-U_{x2}+\tfrac{1}{2}U_{x3})\cos\gamma = 0 \tag{4.65}$$

cf. equations (4.61) and (4.62), together with

$$\frac{1}{2}\left\{-W_1+W_3-s_3\left(\frac{\partial W_1}{\partial s}+\frac{\partial W_3}{\partial s}\right)\right\}f_1(\theta_3) + (\tfrac{1}{2}U_{\theta 1}-U_{\theta 2}+\tfrac{1}{2}U_{\theta 3})f_2(\theta_3)-(\tfrac{1}{2}U_{x1}-U_{x2}+\tfrac{1}{2}U_{x3})\,x_3 = 0, \tag{4.66}$$

where

$$\left.\begin{aligned} f_1(\theta_3) &= \frac{(1-\cos\theta_3)^2}{\sin\theta_3(\theta_3-\sin\theta_3)} = \frac{3F_2^2(s_3,\gamma)}{2F_1(s_3,\gamma)\,F_3(s_3,\gamma)},\\ f_2(\theta_3) &= \frac{(\sin\theta_3-\theta_3\cos\theta_3)(1-\cos\theta_3)}{\sin\theta_3(\theta_3-\sin\theta_3)} = \frac{F_2(s_3,\gamma)\,G_3(s_3,\gamma)\cos\gamma}{F_1(s_3,\gamma)\,F_3(s_3,\gamma)}.\end{aligned}\right\} \tag{4.67}$$

Equations (4.42) show that in the limit as $\theta_3 \to 0$, i.e. as $\gamma \to \tfrac{1}{2}\pi$,

$$\lim_{\theta_3\to 0} f_1(\theta_3) = \tfrac{3}{2}, \quad \lim_{\theta_3\to 0} f_2(\theta_3) \to \theta_3 = 0. \tag{4.68}$$

Equation (4.65) allows the mid-side connexion quantity $R\phi_{\nu 2}$ to be eliminated by expressing it in terms of other connexion quantities, while equation (4.66) allows the subsequent elimination of either $U_{\theta 2}$ or U_{x2} depending upon whether, say, $|\theta_3| \geqslant$ or $< |x_3|$. If equations (4.64) are substituted into the rearranged interpolation formulae as presented in equations (4.43), then the following relations hold

$$D_3 = A_3\cos\gamma, \quad C_4 = \tfrac{1}{3}(A_3\sin\gamma+B_3\cos^3\gamma), \quad \Delta_2 = A_3. \tag{4.69}$$

The above elimination procedures preclude recovery of the two least sensitive inextensional solutions in equations (4.27), namely those terms which involve the coefficients c_1' and c_4'. The recovery of all four inextensional solutions may, however, be achieved if only one mid-side connexion quantity is eliminated on the basis that the strain ϵ_{ss} is constrained to remain constant along the geodesic line, see equation (4.38), thus

$$\frac{\partial}{\partial s}(R\epsilon_s) = 0 = -2\alpha_3\sin\gamma+2\alpha_6\cos\gamma+\alpha_8\cos^2\gamma, \tag{4.70}$$

rather than being allowed to vary in some constrained linearly varying manner. The equations (4.57) can now be resolved to provide a relationship like equations (4.65), (4.66) although the new relation takes on a much more complicated form. The relation

$$-2A_3\sin\gamma+2B_3\cos\gamma+C_2\cos^2\gamma = 0 \tag{4.71}$$

is equivalent to equation (4.70). It is to be remarked, however, that there is no certainty that this particular elimination is effective in resolving the rank difficulties discussed in §4.3.

Equations (4.46) show, in the special instance where the side coincides with a generator, i.e. where $\gamma = \tfrac{1}{2}\pi, \tfrac{3}{2}\pi$, that it is legitimate to eliminate all three mid-side connexion quantities U_{x2}, $U_{\theta 2}$, $R\phi_{\nu 2}$. Practical application is, however, really restricted to the lines of curvature finite element developed in §4.2. Equations (4.47) confirm that $U_{\theta 2}$, but not U_{x2}, can be eliminated in the special case where the side coincides with a circumference, i.e. where $\gamma = 0, \pi$.

PHILOSOPHICAL TRANSACTIONS OF THE ROYAL SOCIETY A MATHEMATICAL, PHYSICAL & ENGINEERING SCIENCES

4.5. *Triangular finite element using new variational principle*

A more versatile variational principle was introduced in §2.4 in anticipation of difficulties to be encountered with Pian's assumed stress hybrid finite element model. The new variational principle requires trial functions in

(i) U_{Ci} which interpolate the kinematic conditions along the boundary C_i of the ith finite element;

(ii) $\bar{N}_{\beta i}$ which partially describe the stress resultants and stress couples over the surface A_i of the element;

(iii) $U_{\alpha i}$ which partially describe the displacements over A_i.

The trial functions in $\bar{N}_{\beta i}$ and $U_{\alpha i}$ supplement each other to provide completeness in the strain energy $\frac{1}{2}\iint(\bar{N}^{\mathrm{T}}_{\alpha i}+\bar{N}^{\mathrm{T}}_{\beta i})\,(\bar{\varepsilon}_{\alpha i}+\bar{\varepsilon}_{\beta i})\,\mathrm{d}A_i$. The kinematic subsidiary conditions on the trial functions in $U_{\alpha i}$ are that they are linearly related in some (best) way with the trial functions in U_{Ci}, e.g. through

$$\left.\begin{aligned} U_{\alpha Ci} &= U_{Ci} \quad \text{at points on } C_i,\dagger \\ U_{Ci} &= U^* \quad \text{where } U^* \text{ is prescribed,}\end{aligned}\right\} \tag{2.65 bis}$$

where $U_{\alpha Ci}$ is expressed in terms of $U_{\alpha i}$ by equations like (4.23) and (4.24). Subsidiary conditions on the trial functions in $\bar{N}_{\beta i}$ are such that they satisfy the differential equations (2.66) of homogeneous equilibrium over A_i.

The variational principle separates naturally into two successively applied principles. The first operates at element level and only the trial functions in $\bar{N}_{\beta i}$ are subject to arbitrary variation

$$\iint \delta\bar{N}^{\mathrm{T}}_{\beta i}\,\bar{\varepsilon}_{\beta i}\,\mathrm{d}A_i - \int \delta\bar{N}_{\beta Ci}(U_{Ci}-U_{\alpha Ci})\,\mathrm{d}C_i = 0, \tag{2.67 bis}$$

it relates $\bar{N}_{\beta i}$ with U_{Ci}. The second principle applies at global level where the trial functions in U_{Ci} are subject to arbitrary variation,

$$\sum_i \left\{\iint (\bar{N}^{\mathrm{T}}_{\alpha i}+\bar{N}^{\mathrm{T}}_{\beta i}-\bar{N}^{\mathrm{T}}_{pi})\,(\delta\bar{\varepsilon}_{\alpha i}+\delta\bar{\varepsilon}_{\beta i})\,\mathrm{d}A_i + \int N^{\mathrm{T}}_{pCi}\,\delta U_{Ci}\,\mathrm{d}C_i - \int_{N^*_C} N^{*\mathrm{T}}_C\,\delta U_{Ci}\,\mathrm{d}C_i\right\} = 0; \tag{2.73 bis}$$

the column matrix $\bar{N}_{pi}$ which deals with the distributed surface load p^* is readily calculated from equations (3.45) and (3.46).

This variational principle is now employed to develop a triangularly shaped finite element for a circular cylindrical shell with a wall of uniform thickness and uniform material properties. Initially, it is convenient to assume that the triangle has a full complement of 24 connexion quantities as depicted in figure 6*a*. The trial functions in U_{Ci}, which interpolate the kinematic conditions along C_i, are then suitably expressed by equations (4.43) and the 13 constants $A_1, A_2, \ldots$ are readily determined in terms of the 13 connexion quantities along each side

The trial functions in $\bar{N}_{\beta i}$ are selected in accordance with similar criteria as laid down in §4.3 for the assumed stress hybrid model, namely they are calculated from complete surface polynomials of x and θ for the stress functions χ_x, χ_θ, ψ. Because these trial functions are to be supplemented by trial functions in $U_{\alpha i}$, attention may be confined to polynomials of minimum degree, thus

$$\left.\begin{aligned} \chi_x &= \beta_1 x+\beta_2\theta+\beta_3 x^2+\beta_4 x\theta+\beta_5\theta^2, \\ \chi_\theta &= \beta_6 x+\beta_7\theta+\beta_8 x^2+\beta_9 x\theta+\beta_{10}\theta^2, \\ \psi &= \beta_{11}+\beta_{12}x+\beta_{13}\theta,\end{aligned}\right\} \tag{4.72}$$

† See footnote on p. 130.

where $\beta_1, \beta_2, \ldots$ are constants. These give 13 stress fields which are linear in x and θ (cf. the fourth degree polynomial stress fields of the 33 stress functions in equations (4.55)). A 13×13 element flexibility matrix H_i is then derived by substituting into the strain energy integral $\frac{1}{2}\iint \bar{N}^{\mathrm{T}}_{\beta i}\, \bar{\varepsilon}_{\beta i}\, \mathrm{d}A_i$, see equation (2.67), after making use of the constitutive relations (2.48). It is recalled that in §4.2 it is suggested that Turing's (1948) M-condition number be used to measure the conditioning of a matrix. A comparison of M-condition numbers in table 6 for the 13×13 matrix H_i, with those in table 2 for the comparatively larger 26×26 reduced stiffness matrix k_i of the compatible lines of curvature rectangular element, indicates that the problems of matrix conditioning remain severe and highlights the continuing need for care in the numerical work. Assuming for the moment that $U_{\alpha i} = 0$, the table 5 shows that the 13 trial functions in $\bar{N}_{\beta i}$ when taken in conjunction with the U_{Ci} of equations (4.43) yield a 24×24 element stiffness matrix which has rank 11.

Table 6. Typical values of the M-condition number for the element flexibility and stiffness matrices of the triangular finite element for circular cylindrical shells

		flexibility matrix H_i (13×13)		stiffness matrix k_i (12×12)	
R/h	k	M-condition number	average M-condition number	M-condition number	average M-condition number
52.7	0.30×10^{-4}	0.5×10^{8}	0.9×10^{1}	0.2×10^{7}	0.9×10^{1}
320.0	0.81×10^{-6}	0.2×10^{10}	0.9×10^{1}	0.9×10^{8}	0.9×10^{1}

All these triangles are right angled triangles with the smaller sides of size 0.26 and $\frac{1}{8}\pi$. The reduced size of the stiffness matrix is quoted where rigid body freedoms are constrained.

The primary rôle of the displacement trial functions in $U_{\alpha i}$ is to augment the rank of the element stiffness matrix. Thus if attention is confined just to those $U_{\alpha i}$ which give rise to linearly varying stress fields then the rank can be augmented at most from 11 to 16 in correspondence with the 5 surface force distributions p^*_{x0}, $p^*_{\theta 0}$, p^*_0, xp^*_1, θp^*_2 of equations (4.29) and (4.30). Accordingly, consider the following trial functions in $U_{\alpha i}$

$$\left.\begin{aligned} U_x + \partial W/\partial x &= \alpha_1 x + \alpha_2 \theta + \alpha_3 x^2 + \alpha_4 x\theta + \alpha_5 \theta^2 + (\alpha_{14}), \\ U_\theta - \partial W/\partial \theta &= \alpha_6 x + \alpha_7 \theta + \alpha_8 x^2 + \alpha_9 x\theta + \alpha_{10} \theta^2 + (\alpha_{15}), \\ W &= \alpha_{11} + \alpha_{12} x + \alpha_{13}\theta + (\alpha_{16} F_2 + \alpha_{17} F_3 + \alpha_{18} x F_1 + \alpha_{19} x F_2), \end{aligned}\right\} \tag{4.73}$$

where $\alpha_1, \alpha_2, \ldots$ are constants. The six terms in parentheses, $\alpha_{14}, \alpha_{15}, \ldots, \alpha_{19}$, contain expressions which describe the rigid body movements, see equations (4.25), these terms do not contribute novel stress distributions. The functions F_1, F_2, F_3 are defined by

$$\left.\begin{aligned} F_1 &= F_1(\theta, 0) = \sin\theta, \\ F_2 &= F_2(\theta, 0) = 2(1-\cos\theta), \\ F_3 &= F_3(\theta, 0) = 6(\theta - \sin\theta), \end{aligned}\right\} \tag{4.74}$$

see equations (4.41); evaluation of these functions is accomplished accurately by using equations (4.39).

The 19 trial functions in $U_{\alpha i}$ may be related to the 24 connexion quantities in U_{Ci} through the kinematic subsidiary conditions given in equations (2.65). The number of possible equalities needs, however, to be reduced to 19 by temporarily removing 5 connexion quantities (other than mid-side connexion quantities) so that the resulting 19×19 matrix is susceptible to inversion.† Note that the boundary distribution $U_{\alpha Ci}$ is here directly recoverable by the trial functions in U_{Ci}, cf. equations (4.43) and (4.73). The choice of trial functions in $U_{\alpha i}$ need not, however, be so strictly inhibited.‡

The 24 by 24 element stiffness matrix k_i may now be derived by substituting into the strain energy integral $\frac{1}{2}\iint(\bar{N}^{\mathrm{T}}_{\alpha i}+\bar{N}^{\mathrm{T}}_{\beta i})\,(\bar{\varepsilon}_{\alpha i}+\bar{\varepsilon}_{\beta i})\,\mathrm{d}A_i$, equation (2.73), and making use of the constitutive relations (2.48) together with the fact that $\bar{N}_{\beta i}$ is already known in terms of U_{Ci} and hence of the element connexion quantities. It is remarked that the numerical work involved in calculating both the element flexibility matrix H_i and the element stiffness matrix k_i is relatively simple because only linearly varying stress fields are involved.

The rank of this 24×24 matrix k_i is 16, it is therefore deficient. The remedy, of course, is to reduce the size of k_i by eliminating mid-side connexion quantities as described in §4.4. Although an elimination of just three mid-side connexion quantities is sufficient to restore the correct rank, one may as well adopt the philosophy that as many of these quantities as possible (i.e. 6) should be eliminated because this results in no further degradation of the recovery capabilities of the trial functions. When this is done, the element stiffness matrix k_i is reduced to a size of 18×18 and has rank sufficiency of 12; the 18 connexion quantities which remain are

$$\left.\begin{array}{cccccc}
U_{x1}, & U_{x2}\text{ or }U_{\theta 2}, & U_{x3}, & U_{x4}\text{ or }U_{\theta 4}, & U_{x5}, & U_{x6}\text{ or }U_{\theta 6},\\
U_{\theta 1}, & & U_{\theta 3}, & & U_{\theta 5}, & \\
W_1, & & W_3, & & W_5, & \\
R\phi_{x1}, & & R\phi_{x3}, & & R\phi_{x5}, & \\
R\phi_{\theta 1}, & & R\phi_{\theta 3}, & & R\phi_{\theta 5}, &
\end{array}\right\} \tag{4.75}$$

as illustrated in figure 6*b*. The choice between U_{x2} or $U_{\theta 2}$, etc. is dependent upon the orientation of the particular side of the triangle, see equation (4.63) *et seq*. Table 6 shows that the M-condition number for this k_i is slightly improved over that for the element flexibility matrix H_i.

To summarize, this triangularly shaped finite element for circular cylindrical shells having walls of uniform thickness and uniform material properties directly recovers (I) the three particularized strains; (II) the two most sensitive inextensional solutions; (III) the six different modes of rigid body movement.

The same example problem of a pinched cylinder, as treated in §4.2, is solved with this triangular finite element. Numerical results are listed in table 7 for the radial deflexion W underneath each of the concentrated loads and in table 8 for the stress couple M_θ mid-way between the concentrated loads. All these results are specific to an elimination procedure for the mid-side connexion quantities which is based upon equation (4.64). This particular elimination procedure, however, prejudices the direct recovery of two of the four inextensional solutions. In consequence, these numerical results reflect a finite element which is slightly overstiff in bending, cf. the known

† First select the two vertices which belong to the side of the triangle which most nearly coincides with a generator. Remove $R\phi_\theta$ from the one vertex which provides the intersection with the side most nearly coinciding with a circumference, then remove $R\phi_x$, $R\phi_\theta$ from the other vertex. Lastly, remove the connexion quantities W from all but one of the three vertices of the triangle.

‡ For example, we may complete the surface (pseudo) cubic by adding the terms $\alpha_{20}x^2+\alpha_{21}x^3+\alpha_{22}x^2\theta$ to the expression for W in equation (4.73).

values from inextensional theory and with those obtained from the lines of curvature compatible rectangular finite element described in §4.2; it is likely that an elimination procedure which is based upon equation (4.70) would provide considerably more accurate results in this instance. Note that in table 7, although the magnitude of the radial deflexion W underneath each concentrated load is less than the comparative result from the compatible rectangular finite element, the underlying variational principle does not now provide a bound.

In other numerical examples, it is found that although the membrane action solutions which belong to the coefficients c_1'' and c_4'' in equations (4.30) and (4.34) cannot be directly recovered they are, indeed approximated quite accurately with a relatively coarse mesh. The overall conclusion is that this triangular finite element shows considerable promise in its application to many different kinds of practical problems where both the stresses and displacements are smoothly varying over the shell surface and where edge effects are of small consequence.

Table 7. Radial deflexion W underneath each of the concentrated loads in the pinched circular cylindrical shell for the triangular finite element

mesh size (see figure 5)	thick walled cylinder $R/h = 52.7$ $10^2 W/P$	thin walled cylinder $R/h = 320.0$ W/P
2 by 2	−0.0796	−0.1782
4 by 4	−0.1012	−0.2254
6 by 6	−0.1052	−0.2341
3 by 8	—	−0.2360
inextensional shell theory	−0.1084	−0.2428

Table 8. Stress couple M_θ mid-way between concentrated loads in the pinched circular cylindrical shell for the triangular finite element

mesh size (see figure 5)	M_θ/P thick walled cylinder $R/h = 52.7$	M_θ/P thin walled cylinder $R/h = 320.0$
2 by 2	0.0631/0.0631	0.0631/0.0631
4 by 4	0.0808/0.0808	0.0804/0.0804
6 by 6	0.0841/0.0841	0.0837/0.0837
3 by 8	—	0.0844/0.0844

Inextensional shell theory gives $M_\theta^{(\text{inext.})}/P = 0.0870$. Note that M_θ is multi-valued on inter-element boundaries.

5. Conclusions

Under the precept that the practical and efficient numerical analysis of shells is far from a reality, the finite element method is re-examined and contributions are given towards the solution of a special class of shell which has a developable middle surface.

As a preliminary, working formulae are assembled for a valid first approximation theory most suitable for finite element analysis of linear small deflexion behaviour of arbitrary shells. This makes reference convenient, unambiguous and consistent. The outline derivation is presented in lines of curvature coordinates, with subsequent transformations along arbitrary orthogonal directions to facilitate the introduction of geodesic coordinates. A further preliminary introduces a variational principle which is more versatile than that used in the well known assumed stress hybrid finite element model. The new principle makes use of assumed displacements which are supplemented with assumed stresses; its main purpose is to overcome problems of excessive rank deficiency which occur in the derived element stiffness matrix of the assumed stress hybrid finite element model.

Continuing in the general context, it is recalled that the finite element method is a piecewise application of the Rayleigh–Ritz variational process and, as such, requires trial functions. Difficulties are experienced, however, in deriving a set of satisfactory piecewise trial functions for shells and these difficulties are unlike any which have been encountered in analysis in the plane. The guidance of sufficiency conditions is usually sought because they provide assurance of convergence in the limit of the finite element representation. However, existing sufficiency conditions, directly extrapolated from those for planar continua, are not really applicable to shells and therefore provide inadequate guidance. The paper contends that practical conditions for convergence in the finite element analysis of shells require the trial functions to have capability to reproduce, in a general but piecewise smoothly varying way, each of four basic states of static response. These states are essentially

(I) membrane actions where the stresses from bending vanish;

(II) inextensional deformations where the middle surface of the shell remains unstretched;

(III) rigid body movements which contribute nothing to the stresses or strains;

(IV) simple edge effects where the stress/strain intensities from stretching and bending are essentially of the same order of magnitude and decay rapidly with distance away from the edge; the simple edge effect varies smoothly along the edge.

The above mentioned working formulae are specialized for shells with developable middle surface and, preparatory for finite element analysis, general solution forms are derived for inextensional deformations as well as for membrane actions and rigid body movements. It is shown how to derive the 'most sensitive' inextensional solutions from the general solution forms for the rigid body movements. (Sensitive solutions are the smoothest distributions of displacements which produce inextensional deformation; many finite element analyses produce extraordinarily inaccurate results when they are set the task of recovering these simple and basic deformations.) All these general solution forms are, incidentally, readily available only for certain shell shapes such as the developable surface which, fortunately, includes the most commonly occurring shapes used in technology. The objective is moderated, however, so as to exclude questions of edge effect and this inevitably restrains the useful application of the finite elements which are developed in the sequel. Edge effects in finite element analysis will have to form the subject of further and special investigation.

Specific application of the formulae is then made in the development of finite elements for circular cylindrical shells. Central to the finite element development is the interpolation of kinematic continuity conditions along an arbitrary geodesic line. The interpolation is carried out so that it is pseudo-quadratic for the insurface displacements and pseudo-cubic for the out of surface displacement.

This interpolation is first used in the guise of Hermitian interpolation to develop a lines of curvature rectangular finite element, which is distinguished from all other known shell finite elements because it directly recovers (I) essential membrane actions; (II) sensitive inextensional solutions; (III) arbitrary rigid body movements, and satisfies all inter-element continuities as are demanded by the underlying principle of minimum total potential energy. Numerical application is given to an example problem which is often used to test shell finite elements, this concerns a circular cylinder which is pinched by two concentrated radial loads. The results are very satisfactory and the deflexion underneath the load is calculated, for the first time, as a lower bound. It is emphasized that in all numerical work on shells, it is necessary to take great care because of the inevitable loss of (at least four) significant figures which occurs because of the considerable differences in orders of magnitude in the stretching and bending contributions to the stiffness matrix.

It is recognized that useful application of the rectangular finite element is limited to special problems where the boundary contours of the shell coincide with the lines of curvature. Consequently, attention is next given to the development of a more practically useful finite element which is triangularly shaped with each side coinciding with a geodesic line. The possibility of development by using the well known assumed stress hybrid finite element model, is first discussed. The conclusion, however, is that this does not provide a practicable means of solving this shell problem because the presence of mid-side connexion quantities leads to unacceptable difficulty in acquiring requisite rank sufficiency in the derived element stiffness matrix. Recourse is thus made to the more versatile variational principle, earlier introduced, so as to develop a satisfactory finite element where the stress resultants and stress couples are only linearly varying in the surface coordinates. This finite element also performs satisfactorily with regard to the aforementioned basic states (I), (II) and (III) of static response; it is anticipated that it will find widespread application. Satisfactory numerical results are obtained in its use to solve the same test problem of the pinched cylinder.

List of principal symbols

All symbols are defined when first introduced.

Two right handed orthogonal curvilinear coordinate systems are used on the shell reference surface, namely lines of curvature coordinates ξ_1, ξ_2 and arbitrary coordinates ν, σ. The lines σ = constant are used also to define the boundary C of the shell and/or the boundary C_i of the ith finite element. Special notation is used for circular cylinders, see equations (4.1) *et seq.*

The following superscripts are generally used

(inext.)	inextensional action
(memb.)	membrane action
(r.b.)	rigid body movement
*	prescribed quantity

The following subscripts are generally used

C	action at the boundary
i	ith finite element
α	actions derived from trial functions in the displacements
β	actions derived from trial functions in the stress resultants and stress couples

A	area
D	flexural rigidity, defined in equation (2.49)
$\boldsymbol{e}_1$, $\boldsymbol{e}_2$, $\boldsymbol{e}_3$	unit vectors in the z_1, z_2, z_3 rectangular Cartesian coordinate system
E	Young modulus
h	wall thickness
k	small parameter defined in equation (2.50)
$M_{11}, M_{22}, M_{12} = M_{21}$	stress couples
$M_{\nu\nu}$, $M_{\nu\sigma}$	stress couples

$N_{11}, N_{22}, N_{12}, N_{21}$	stress resultants
$N_{\nu\nu}, N_{\nu\sigma}$	stress resultants
$\bar{N}_{12}$	modified shear stress resultant defined in equation (2.45)
O	'a term of order most...'
p_1^*, p_2^*, p^*	distributed surface forces acting in the ξ_1, ξ_2, z directions
Q_1, Q_2	shear stress resultants acting in z direction
Q_ν	shear stress resultant acting in z direction
$\boldsymbol{r}$	radius vector of an arbitrary point on the shell reference surface
R_1, R_2	principal radii of curvature in the ξ_1, ξ_2 directions
$R_\nu, R_\sigma, R_{\nu\sigma}$	radii of curvature defined in equations (2.30)
$\boldsymbol{t}_1, \boldsymbol{t}_2, \boldsymbol{n}$	unit vectors in the ξ_1, ξ_2, z directions
$\boldsymbol{t}_\nu, \boldsymbol{t}_\sigma, \boldsymbol{n}$	unit vectors in the ν, σ, z directions
$\boldsymbol{U}$	displacement vector of a point lying on the shell reference surface, defined in equations (2.15), (2.31)
U_1, U_2, W	components of displacement acting in the ξ_1, ξ_2, z directions
U_ν, U_σ, W	components of displacement acting in the ν, σ, z directions
V_ν	Kirchhoff stress resultant acting in the z direction
z	coordinate normal to the shell surface
z_1, z_2, z_3	rectangular Cartesian coordinates
α_1, α_2	coefficients of the first fundamental form for ξ_1, ξ_2 coordinates
$\alpha_\nu, \alpha_\sigma$	coefficients of the first fundamental form for ν, σ coordinates
γ	included angle between vectors $\boldsymbol{t}_\nu$ and $\boldsymbol{t}_1$
$\epsilon_{11}, \epsilon_{22}, \epsilon_{12} = \epsilon_{21}$	components of strain
$\epsilon_{\nu\nu}, \epsilon_{\sigma\sigma}, \epsilon_{\sigma\nu} = \epsilon_{\nu\sigma}$	components of strain
$\kappa_{11}, \kappa_{22}, \kappa_{12}, \kappa_{21}$	components of curvature change
$\kappa_{\nu\nu}, \kappa_{\sigma\sigma}, \kappa_{\nu\sigma}, \kappa_{\sigma\nu}$	components of curvature change
$\bar{\kappa}_{12}, \bar{\kappa}_{\nu\sigma}$	modified changes of twist defined in equations (2.21) and (2.38)
ν	Poisson ratio
ν, σ	arbitrary orthogonal curvilinear coordinates on shell reference surface (the symbol ν is used also to denote the Poisson ratio)
ξ_1, ξ_2	lines of curvature curvilinear coordinates on shell surface
ρ_1, ρ_2, ρ_n	coefficients defined in equation (2.14)
ϕ_1, ϕ_2, ϕ_n	components of rotation
$\phi_\nu, \phi_\sigma, \phi_n$	components of rotation
$\boldsymbol{\Phi}$	rotation vector of a point lying on the shell reference surface, defined in equations (2.16), (2.33)
χ_1, χ_2, ψ	stress functions

A bold faced character denotes a matrix and the symbol T denotes that the transpose is to be taken

$$\mathbf{N} = (N_{11}\, N_{22}\, N_{12}\, N_{21}\, M_{11}\, M_{22}\, M_{12}\, M_{21})^{\mathrm{T}}$$
$$\bar{\mathbf{N}} = (N_{11}\, N_{22}\, \bar{N}_{12}\, M_{11}\, M_{22}\, 2M_{12})^{\mathrm{T}}$$
$$\bar{\mathbf{N}}_p = (N_{11p}\, N_{22p}\, \bar{N}_{12p}\, M_{11p}\, M_{22p}\, 2M_{12p})^{\mathrm{T}}$$
$$\mathbf{N}_C = (N_{\nu\nu}\, N_{\nu\sigma}\, M_{\nu\nu}\, V_\nu)^{\mathrm{T}}$$
$$\mathbf{N}_{pC} = (N_{\nu\nu p}\, N_{\nu\sigma p}\, M_{\nu\nu p}\, V_{\nu p})^{\mathrm{T}}$$

PHILOSOPHICAL TRANSACTIONS OF THE ROYAL SOCIETY A MATHEMATICAL, PHYSICAL & ENGINEERING SCIENCES

$N_C^* = (N_{\nu\nu}^* \, N_{\nu\sigma}^* \, M_{\nu\nu}^* \, V_\nu^*)^{\mathrm{T}}$

$N_C' = (N_{\nu\nu} \, N_{\nu\sigma} \, M_{\nu\nu} \, M_{\nu\sigma} \, Q_\nu)^{\mathrm{T}}$

$p^* = (p_1^* \, p_2^* \, p^*)^{\mathrm{T}}$

$U = (U_1 \, U_2 \, W)^{\mathrm{T}}$

$U_C = (U_\nu \, U_\sigma \, \phi_\nu \, W)^{\mathrm{T}}$

$U_C^* = (U_\nu^* \, U_\sigma^* \, \phi_\nu^* \, W^*)^{\mathrm{T}}$

$U_C' = (U_\nu \, U_\sigma \, \phi_\nu \, \phi_\sigma \, W)^{\mathrm{T}}$

$\boldsymbol{\varepsilon} = (\epsilon_{11} \, \epsilon_{22} \, \epsilon_{12} \, \epsilon_{21} \, \kappa_{11} \, \kappa_{22} \, \kappa_{12} \, \kappa_{21})^{\mathrm{T}}$

$\bar{\boldsymbol{\varepsilon}} = (\epsilon_{11} \, \epsilon_{22} \, 2\epsilon_{12} \, \kappa_{11} \, \kappa_{22} \, \bar{\kappa}_{12})^{\mathrm{T}}$

References

Ahlin, A. C. 1964 A bivariate generalisation of Hermite's interpolation formula. *Math. Comp.* **18**, 264.

Allman, D. J. 1970 Triangular finite elements for plate bending with constant and linearly varying bending moments. In *Proc. IUTAM Symposium on High Speed Computing of Elastic Structures*, University of Liège, 105.

Allman, D. J. 1976 A simple cubic displacement element for plate bending. *Int. J. num. Methods Engng* (to appear).

Ashwell, D. J. & Sabir, A. B. 1972 A new cylindrical shell finite element based on simple independent strain functions. *Int. J. Mech. Sci.* **14**, 171.

Bartholomew, P. 1976 A comment on hybrid finite elements. *Int. J. num. Methods Engng* (to appear).

Bogner, F. K., Fox, R. L. & Schmitt, L. A. 1966 The generation of interelement compatible stiffness and mass matrices by the use of interpolation formulas. In *Proc. Conf. on Matrix Methods in Structural Mechanics*. Wright-Patterson Air Force Base, Ohio, AFFDL-TR-66-80, 397.

Budiansky, B. & Sanders, J. L. 1963 On the 'best' first-order linear shell theory. In *Progress in Appl. Mechs. The Prager Anniversary Volume*, p. 129. London: Macmillan.

Cantin, G. 1970 Rigid body motions in curved finite elements. *Am. Inst. Aviation astronaut. J.* **8**, 1252.

Cantin, G. & Clough, R. W. 1968 A curved, cylindrical shell, finite element. *Am. Inst. Aviation astronaut. J.* **6**, 1057.

Clough, R. W. & Johnson, C. P. 1968 A finite element approximation for the analysis of thin shells. *Int. J. Solids Structures*, **4**, 43.

Dawe, D. J. 1971 Curved finite elements in the analysis of shell structures by the finite element method. In *Proc. 1st Int. Conf. on Structural Mechs. in Reactor Technology, Berlin*, **5J**, 17.

Donnell, L. H. 1933 Stability of thin-walled tubes under torsion. *NACA Tech. Rep.* 479.

Fraeijs de Veubeke, B. 1965 Displacement and equilibrium models in the finite element method. In *Stress Analysis* (ed. O. C. Zienkiewicz & G. S. Hollister), p. 145. New York: Wiley.

Fried, I. 1971 Basic computational problems in the finite element analysis of shells. *Int. J. Solids Structures* **7**, 1705.

Gallagher, R. H. 1969 Analysis of plate and shell structures. In *Symposium on Finite Element Methods in Civil Engng*. Vanderbilt University, Nashville, U.S.A.

Gallagher, R. H. 1974 General thin shell analysis. In *Proc. Conf. on Finite Elements for Thin Shells and Curved Members. University College, Cardiff, U.K.*

Gol'denveizer, A. L. 1961 *Theory of elastic thin shells.* Pergamon.

Hellinger, E. 1914 Der allgemeine Ansatz der Mechanik der Kontinua. In *Encyclopädie der Mathematischen Wissenschaften* **4**, 602.

Koiter, W. T. 1960 A consistent first approximation in the general theory of thin elastic shells. In *Theory of thin elastic shells*. First IUTAM Symposium (ed. W. T. Koiter), p. 12. Amsterdam: North-Holland Publishing Co.

Koiter, W. T. 1968 Summary of equations for modified, simplest possible accurate linear theory of thin circular cylindrical shells. Internal Report of Laboratory of Engng Mechs., Dept. of Mechanical Engng, Delft.

Love, A. E. H. 1890 The small free vibrations and deformation of a thin elastic shell. *Phil. Trans. R. Soc. Lond.* **A179**, 491.

Love, A. E. H. 1927 *Mathematical theory of elasticity*, 4th ed. Cambridge University Press.

Marguerre, K. 1938 Zur Theorie der gekrümmten Platte grosser Formänderung. In *Proc. 5th Int. Congress Appl. Mechs.*, p. 93. Cambridge, Mass.

Melosh, R. J. 1963 Basis for derivation of matrices for the direct stiffness method. *Am. Inst. Aviation astronaut. J.* **1**, 1631.

Merrifield, B. C. 1976 A computer program for the finite element analysis of circular cylindrical shells. Unpublished Report, R.A.E. Farnborough, U.K.

Morley, L. S. D. 1959 An improvement on Donnell's approximation for thin-walled circular cylinders. *Q. Jl mech. appl. Math.* **12**, 89.

Morley, L. S. D. 1972 Polynomial stress states in first approximation theory of circular cylindrical shells. *Q. Jl mech. app. Math.* **25**, 13.

Morley, L. S. D. 1973 Finite element solution of boundary-value problems with non-removable singularities. *Phil. Trans. R. Soc. Lond.* A **275**, 463.

Morley, L. S. D. & Merrifield, B. C. 1974 Polynomial comparison solutions in the Sanders–Koiter theory of circular cylindrical shells. In *Proc. Conf. on Finite Elements for Thin Shells and Curved Members, University College, Cardiff, U.K.*

Morris, A. J. 1974 A summary of appropriate governing equations and functionals in the finite element analysis of thin shells. In *Proc. Conf. on Finite Elements for Thin Shells and Curved Members, University College, Cardiff, U.K.*

Pian, T. H. H. 1964 Derivation of element stiffness matrices by assumed stress distributions. *Am. Inst. Aviation astronaut. J.* **2**, 1333.

Pian, T. H. H. & Mau, S. T. 1972 Some recent studies in assumed stress hybrid models. In *Advances in computational methods in structural mechanics and design. 2nd U.S. Japan Seminar on matrix methods of structural analysis and design* (ed. J. T. Oden, R. W. Clough & Y. Yamamoto), p. 87. Huntsville Press, University of Alabama.

Pian, T. H. H. & Tong, P. 1969 Basis of finite element methods for solid continua. *Int. J. num. Methods Engng.* **1**, 3.

Rayleigh, Lord 1881 On the infinitesimal bending of surfaces of revolution. *Lond. Math. Soc. Proc.* **13**, 4.

Reissner, E. 1941 A new derivation of the equations for the deformation of elastic shells. *Am. J. Math.* **63**, 177.

Reissner, E. 1950 On a variational theorem in elasticity. *J. math. Phys.* **29**, 90.

Sanders, J. L. 1959 An improved first-aproximation theory for thin shells. *NASA Report* 24.

Simmonds, J. G. 1966 A set of simple, accurate equations for circular cylindrical elastic shells. *Int. J. Solids Structures* **2**, 525.

Strang, G. & Fix, G. J. 1973 *An analysis of the finite element method.* Prentice-Hall.

Tong, P. 1970 New displacement hybrid finite element model for solid continua. *Int. J. num. Methods Engng* **2**, 78.

Tong, P. & Pian, T. H. H. 1967 The convergence of finite element methods in solving linear elastic problems. *Int. J. Solids Structures* **3**, 865.

Turing, A. M. 1948 Rounding-off errors in matrix processes. *Q. Jl Mech. app. Math.* **1**, 287.

Vlasov. V. Z. 1958 *Allgemeine Schalentheorie und ihre Anwendung in der Tcehnik.* Berlin: Akademie-Verlag. (Translated from the 1949 Russian ed.)

Washizu, K. 1968 *Variational methods in elasticity and plasticity.* Pergamon.

Zienkiewicz, O. C., Taylor, R. L. & Too, J. M. 1971 Reduced integration technique in general analysis of plates and shells. *Int. J. num. Methods Engng* **3**, 275.